FINAL REPORT
SRB ASCENT AERODYNAMIC HEATING DESIGN CRITERIA REDUCTION STUDY
VOLUME I

January 18, 1989

Prepared by:

W.K. Crain
C.L. Frost
C.D. Engel

REMTECH, Inc.

Contract:

NAS8-35322

For:

George C. Marshall Space Flight Center
Marshall Space Flight Center, Alabama 35812

FOREWORD

This final report documents the SRB thermal environment generation work performed under the TPS Reduction Study (NAS8-35322). The work was performed for the Thermal Environments Branch (ED-33) of the George C. Marshall Space Flight Center (MSFC).

During the course of the work significant results and progress were documented under monthly progress reports (RPR 090-01 through -65) submitted each month. The purpose of this report is to summarize the thermal environment generation methodology, time wise environments, wind tunnel/flight test data base used in the study, and to present a comparison with the Rockwell IVBC-3 and 1980 Ascent Design environments. The report is presented in two Volumes; Volume I contains the methodology and environment summaries. Volume II contains the tabulated data base, timewise tabulated environments and timewise plotted environments comparing the REMTECH results to the Rockwell RI-IVBC-3 results.

Contents

List of Figures

List of Tables

NOMENCLATURE

CTM	Thermal mismatch correction factor defined by Fig. 16
f_3, f_4	Flight Factor at $M_\infty = 3$, 4 respectively, $f_3, f_4 = \frac{Hi/Hu_{flight}}{Hi/Hu_{wind\ tunnel}}$
h	Heat transfer coefficient with boundary layer temperature discontinuity (Eq. 6.1)
H	Heat transfer coefficient, BTU/FT^2 Sec °R $\frac{\dot{q}}{TR-TW}$, $\frac{\dot{q}}{HR-HW}$
h_{iso}	Heat transfer coefficient without boundary layer temperature discontinuity, (Eq. 6.1)
Hi/Hu	Interference to undisturbed heat transfer amplification factor
HR	Recovery enthalpy, BTU/lbm °R
L	Boundary layer running length to the upstream edge of the boundary layer temperature discontinuity, FT (see Fig. 15)
M	Mach number
MULT 3, MULT 4	Same as f_3, f_4
Pi/Pu	Interference to body alone undisturbed pressure ratio
$\dot{q}$	Heating rate, BTU/FT^{2}Sec
Q_{LOAD}	Integrated heat load, BTU/FT^2
T	Temperature -°F, °R
TR	Recovery Temperature, °R
To	Freestream total temperature, °R
T_o	Stream reference temperature in the thermal mismatch correction equation (Eq. 6.1)
TW	Wall temperature, °R
TW_1	TPS temperature, °R (see Fig. 15 and Eq. 6.1)

TW_2	Calorimeter temperature, °R (see Fig. 15 and Eq. 6.1)
W	Boundary layer running length to the back edge of the calorimeter, FT (see Fig. 15)
X_B	SRB axial coordinate measured along center line from vehicle nose tip, FT

Subscripts

cw	Cold wall - refers to the reference state of 0 deg. F
Hw	Hot wall - refers to actual wall temperature at which measurement was made
i	Interference
L	Integrated load
Max	Peak value along the ascent trajectory
u	Undisturbed
∞	Freestream conditions

Greek

α	SRB angle of attack in the body axis system, nominal design trajectory, deg.
α_{eff}	Effective angle of attack defined by Eq. 3.1
α^-	Angle of attack with negative dispersions, deg.
α^+	Angle of attack with positive dispersions, deg.
β	SRB angle of sideslip in the body axis system, nominal design trajectory, deg.
β^-	Angle of sideslip with negative dispersions
β^+	Angle of sideslip with positive dispersions, deg.
Δ_α	Angle of attack dispersions, deg.
Δ_β	Angle of sideslip dispersions, deg.
θ_β	SRB Circumferential coordinate, deg.

Section 1
INTRODUCTION

The objective of this study was to produce an independent set of SRB convective ascent design environments which would serve as a check on the Rockwell IVBC-3 environments (Ref. [1]) used to design the ascent phase of flight. In addition, the study provided support for lowering the design environments such that TPS, based on conservative estimates, could be removed leading to a reduction in SRB refurbishment time and cost. Ascent convective heating rates and loads were generated at locations in the SRB where lowering the thermal environment would impact the TPS design.

Body points where the environments were generated were selected based on several factors, the more important of these being:

(a) Areas where the thickest and/or most expensive TPS was applied

(b) The severity of the ascent environment compared to the plume heating or reentry environment

(c) Areas where wind tunnel data were available for environment definition

The aeroheating data base used consisted of the wind tunnel results IH-97 (Ref. [2]) from the most geometrically up to date model (60 - OTS), and current flight test data from STS 1-3, 5, 6. Wind tunnel results from IH-47, 72, 85 and IH-11 (Ref. [3]-[6]) were used at locations not covered by the IH-97 data.

This report documents the ascent thermal environments, the wind tunnel/flight test data base used as well as the trajectory and environment generation methodology. Methodology, as well as, environment summaries compared to the 1980 Design and Rockwell IVBC-3 (October 1987) Design environments are presented in Volume I. The wind tunnel/flight test data base as well as time wise environments for each body point are presented in tabular and plotted form in Volume II.

Section 2
VEHICLE DESCRIPTION AND BODY POINT DEFINITION

2.1 SRB DESCRIPTION

A pictorial description of the Solid Rocket Booster depicting the major external components is shown in Fig. 1, (Ref. [7]). Of the two SRBs used on the STS launch system (Fig. 2), all hardware and data in this report are referenced to the left SRB. Major components consist of the nose cap and forward frustum (X_B = 200 - 395), forward skirt (X_B = 395 - 600), SRM motor case (X_B = 600 - 1300), aft motor case (X_B = 1300 - 1839), aft skirt (X_B = 1839 - 1930.4). Major protuberances consist of the systems tunnel (X_B = 443.62 - 1837), range safety antenna (X_B = 495.8), SRB/ET forward attach hardware (X_B = 401 - 515), SRB/ET attach ring (X_B = 1511), aft motor case stiffners (X_B = 1613.5, 1657.5, 1733.56, 1777.58), kick ring (X_B = 1839.8), rooster tail (X_B = 1839) and aft separation motors (X_B = 1860.7). The SRB coordinate system (X_B, θ_B) used in this report is defined in Fig. 3.

2.2 BODY POINT DEFINITION

Body point locations where ascent environments were calculated are shown in Fig. 4, and are presented according to zone.

Zone	Component	X_B inches
2	Corresponds to the nose cone	200 - 395
3	Corresponds to the forward skirt	395 - 600
4	Corresponds to the motor case	600 - 1300
5	Corresponds to the motor case in vicinity of attach ring	1300 - 1600
6	Corresponds to the aft motor case	1600 - 1839
7	Corresponds to the aft skirt	1839 - 1930.64

The 7000 and 8000 series body point numbers refer to the DFI (Developmental Flight Instrumentation) locations present in the IH-97 wind tunnel test (Ref. [2])

and the STS 1-3, 5, 6 series flight tests. The body points along with the X_B, θ_B location, corresponding RI IVBC-3 body point number are presented in tabular form in Table 1.

The body point locations were chosen based on the following criteria:

(a) Areas where the thickest and/or most expensive TPS was applied

(b) The severity of the ascent environment compared to the plume heating or reentry environment

(c) Areas where wind tunnel data were available for environment definition

After all these locations were correlated with areas of important heating and availability of test data, the body point locations were selected.

Section 3
METHODOLOGY

The procedure used to calculate the thermal environment for any particular surface location (body point) on the SRB first calculates the clean skin-body alone heating distribution at the flight condition. The undisturbed heating is then amplified with interference factors that provide the effects of protuberances and/or the mated (ET, Orbiter) configuration. The interference heating was obtained from the experimental wind tunnel and flight test data base.

The calculation technique that was selected requires a table of interference heating factors (Hi/Hu) for each body point as a function of α (-5, 0, 5 deg.) and β (-9, -5, -3, 0, 3, 5, 9 deg.) at two Mach numbers (M = 3.00 and 4.00). At each time point in the trajectory, the limits of α and β are calculated from the design trajectory. A fine matrix of (α, β) is formed and interference factor data (Hi/Hu) are calculated at each (α, β) combination. In addition, the undisturbed body alone heating rate is calculated as a function of effective angle of attack, where α effective is:

$$\alpha_{\text{eff}} = -\alpha_n \cos\theta_b + \beta_n \sin\theta_b \tag{3.1}$$

$\theta_B =$ SRB circumferential angle to the body point in question, deg.

Interference heating (q_{i_n}) at each time point is then calculated for each (α, β) by:

$$q_{i_n} = [(q_{u_n}) \cdot (hi/hu)_n] \text{ , BTU/FT}^2\text{Sec} \tag{3.2}$$

and the maximum value of q_i over the (α, β) matrix used. A schematic of this methodology is shown in Fig. 5. Variation of the interference factors (Hi/Hu) with Mach number is assumed linear in the log - log plane between M = 3.00 and 4.00. In addition, Hi/Hu is assumed 1.00 at M = 1.00 and a linear log - log relationship used from M = 1.00 to 3.00. To obtain interference factors at flight conditions for M > 4.00, Hi/Hu was assumed constant at the M = 4.00 value. This was

adopted so that comparison between Rockwell and REMTECH could be made since Rockwell does not extrapolate their Hi/Hu data past M = 4.00.

The undisturbed heating distribution was calculated using the REMTECH modified version of the MINIVER Code (Ref. [8]). Options used for the undisturbed methodology are summarized in Fig. 6. Basically an 18 deg. cone shock was used on the fore-cone and aft skirt. Pressures were generated using the tangent cone technique while heat transfer was generated using the Spalding-Chi correlations with a Von Karman Reynolds analogy.

The actual calculation procedure for generating the thermal environments along with codes used and input/output information is shown in Fig. 7. A description of the sequence is as follows:

The MINSLA code developed for use on the External Tank was modified for the SRB (MINSRB) to produce the undisturbed environment. The SRB was divided into axial body cuts and these locations input for calculation of the undisturbed environment. Each trajectory produced an output tape corresponding to the eight wind directions.

The MINSRB output tapes were fed to an interpolation routine, INTERP, which accepts input body point information and interpolates to obtain the undisturbed environment at the body point. INTERP produces eight tapes as output.

The undisturbed environments from INTERP along with trajectory information were fed to the RESADM code one trajectory at a time. The primary environment calculations are performed in RESADM according to the procedure described in Fig. 7 This procedure was repeated for each time in flight. The RESADM code output the environments on tape for each trajectory.

The output tapes from RESADM were fed to the DESSRB code. This code took in the data from all eight trajectories and selected the design trajectory for each body point. The trajectory which produced the highest heating load was chosen as the design environment for that body point. In subsequent studies it was found that the use of the eight trajectories, corresponding to the eight head winds, was not necessary and the most severe condition could be represented by one trajectory. At this point, the Light Weight Tank Design Trajectory was adopted as it represented the worst case. It is based on a right quartering headwind, and all the final environments were generated using this trajectory. Consequently, the use of DESSRB was no longer needed and RESADM was used to generate the environments and produce the environment file.

Section 4
TRAJECTORY

The trajectory used to generate the final environments was the 1980 BRM 3A 3σ Dispersed Light Weight Tank Design Trajectory. It is based on a Western Test Range December launch, incorporating right quartering head winds, with α and β dispersions. Data for the trajectory are presented in Table 2 in the form of time, altitude, α and β enveloped, ambient pressure, density and velocity. Since the SRBs are symmetrical in the yaw plane about the external tank, the loads seen by the right SRB at β^- are the same as those seen by the left SRB at β^+. Consequently, the β envelope for (β^-) was "mirror imaged" about $\beta = 0$ degrees to produce the β^+ envelope, i.e.,

$$\beta^+ = -\beta^- \tag{4.1}$$

Nominal trajectory α and β values were combined with the $\Delta\ \alpha$ and $\Delta\ \beta$ dispersions to produce the worst case envelopes as follows:

$$\alpha^+ = \alpha + \Delta\alpha^+ \tag{4.2}$$
$$\alpha^- = \alpha - \Delta\alpha^- \tag{4.3}$$
$$\beta^- = \beta - \Delta\beta \tag{4.4}$$
$$\beta^+ = -\beta^- \tag{4.5}$$

A plot of the ascent α and β envelopes comparing the REMTECH and RI IVBC-3 data is presented in Fig. 8. Except for the discrepancy at t = 20 and 40 - 50 seconds in the α envelope, comparative envelopes were used for environment calculation. To demonstrate that the calculated environments were within the trajectory envelopes, data from Body Point 7414 is presented as a representative case also in the figure. The environment for BP 7414 is seen to track the α, β boundaries demonstrating that the values used were within the maximum/minimum limits.

Comparisons of trajectory, altitude, and velocity for Rockwell IVBC-3 and REMTECH are shown in Fig. 9.

The Vandenburg Reference atmosphere was used to calculate the final ascent environments. The Vandenburg Hot Day profile was originally used by REMTECH but was changed such that direct comparisons with the Rockwell IVBC-3 environments could be made. Properties of these two atmospheres are presented in Table 3. A plot of the corresponding temperature profiles is shown in Fig. 10. The Vandenburg Hot Day profile produces about a 7 percent increase in integrated heat load. This is mainly due to the temperature difference at altitudes less than 40 KFT. This is shown in Fig. 11 which is a time wise plot of heating rate and integrated heat load for one of the SRB nose cone body points.

Section 5
WIND TUNNEL DATA BASE

The procedure to calculate a thermal environment for any particular surface location (body point) on the SRB was described in Section 2.1 where it was noted that the basic procedure was to first calculate the environment as if the SRB was unmated and to amplify this undisturbed environment with an amplification factor that provides the effects of protuberances and/or the mated (ET, Orbiter) configuration. The calculation technique that was selected requires a table of amplification factors (Hi/Hu) for each body point from the wind tunnel data base. This table consists of amplification factor as a function of α (-5, 0, +5 deg.) and β (-9, -5, -3, 0, 3, 5, 9 deg.) for two Mach Numbers (3 and 4). The wind tunnel derived amplification factors may be further adjusted from the analysis of the flight data base as discussed in the next Section (6.3). This section will only address the derivation of the wind tunnel amplification factors. Interference heating data were obtained from IH-97 wind tunnel data, (Ref. [2]) where available. IH-47, 72, 85, and 11 data (Refs. [3]-[6]) were used where IH-97 data base did not exist. Results from the IH-97 test were acquired on the most up to date wind tunnel model geometry.

The wind tunnel data were nondimensionalized by undisturbed heat transfer coefficients calculated on the clean unmated SRB. These were generated using the MINIVER code (Ref. [8]) run at the wind tunnel conditions. As previously stated, the undisturbed methodology uses a tangent-cone approximation to obtain the pressure distribution and a Spalding-Chi/von Kármán Reynolds analogy to generate the local heat transfer. Boundary layer running lengths were measured from the nose tip of the SRB.

Ratios of:

$$\frac{Hi}{Hu} = \frac{\dot{q}i}{\dot{q}u}\left[\frac{TR_{\text{clean}} - 460}{RTO - 460}\right] \tag{5.1}$$

were formed and referenced to cold wall temperature (TW = 460°R). The data were then put in tabular form with the corresponding α and β orientation.

At locations where the wind tunnel heating data were questionable, Hi/Hu values were generated from pressure data acquired on IH-11 (Ref. [6]) by the pressure

interaction relationship:

$$Hi/Hu = (Pi/Pu)^{0.85} \tag{5.2}$$

Before incorporating the Hi/Hu values into the data base, all results were referenced to the left hand SRB. Consequently the β values for data obtained on the right hand SRB were reversed.

A listing of the wind tunnel data base for each body point is given in Table 1, of Volume II. The table gives the body point number, X_B, θ_B location, α, β and the corresponding interference to undisturbed (Hi/Hu) cold wall heat transfer coefficient ratio at Mach 3 and Mach 4. Included in the table is the flight factor for Mach 3 and 4 also. (The origin and application of this factor is discussed in detail in Section 6.3. The data base is divided into zones corresponding to the body point grouping on the SRB listed in the table defining the body points (Table 1).

Section 6
FLIGHT DATA

Flight hot wall heating rates were measured by DFI Calorimeters on the right and left hand SRB for STS 1-4, 5, 6. These data were converted to cold wall heat transfer coefficient, corrected for thermal mismatch where applicable, and applied as a multiplier to adjust the wind tunnel data base to a level more commensurate with flight. Calorimeter locations are shown in Fig. 4 for the right and left hand ascent calorimeters and in Fig. 13 for the reentry calorimeters. They correspond to the 7000 and 8000 series body point numbers listed in the table of body points (Table 1).

Gage data at locations on the acreage ahead of the attach ring were corrected for thermal mismatch between the gage wall temperature and the hot boundary layer. Data from the gages on the forward face of the attach ring and/or aft of the attach ring were used as is. The following sections describe flight calorimeter measurement correction, handling, and application to generating the enclosed designed environments.

6.1 THERMAL MISMATCH CORRECTIONS

Flight calorimeter measurements on the SRB contain significant errors due to the fact that the TPS surface is at a much higher temperature than the calorimeter surface. An example of this is shown in Fig. 14 for Body Point 7432 (STS-2) on the SRB nose cone. At $M_\infty \sim 3.5$ the boundary layer temperature is ~300°F higher than the calorimeter. The consequence of this is higher indicated heat flux than actually exists by the calorimeter. Methods of accounting for this discontinuity have been derived by Rubesin (Ref. [9]) and the subsequent work of Reynolds, Kays and Kline (Ref. [10]). They relate the film coefficient with temperature discontinuity (h) to that with no temperature discontinuity (h_{iso}). Westkeamper (Ref. [11]) integrated these results into a form where the effective total h can be calculated over an entire region of temperature discontinuity (such as exists in the case of a calorimeter):

$$\frac{h}{h_{iso}} = F\left(\frac{L}{W}\right) + H'\left(\frac{L}{W}\right)\left[\frac{TW2 - TW1}{TW2 - T_0}\right] \tag{6.1}$$

where

$$H'\left(\frac{L}{W}\right) = \frac{5}{4}\,\frac{(L/W)^{0.8}}{(1-L/W)}\left[\left(\frac{W}{L}\right)^{0.9} - 1\right]^{8/9} \tag{6.2}$$

and

$$F\left(\frac{L}{W}\right) = \frac{5}{4}\left[\frac{2}{1+L/W}\right]^{1/5}\left[\frac{1-(L/W)}{1-L/W}\right]^{4/5} \tag{6.3}$$

Values of L and W are based on boundary layer running length. A graphical definition of the variables used in the equation as well as numerical values of H'(L/W) versus L/W are given in Fig. 15, (Ref. [12]).

Westkeamper's method was applied to the SRB flight calorimeter data to produce a corrected heating rate and film coefficient for each gage and time point during the ascent flight. These data along with the initial wall temperature were input to a one-dimensional model of the SRB calorimeter and a new wall temperature generated using the EXITS code (Ref. [13]). This wall temperature was used interactively then to generate the appropriate value of heat transfer correction factor. A stepwise description of this procedure is shown in Fig. 16. The corrected flight heating rates were then converted to Hi/Hu form by nondimensionalizing the corrected heat transfer coefficient by the undisturbed MINIVER calculation run at the flight trajectory conditions. $F\left(\frac{L}{W}\right)$ was assumed ≈ 1.00 for this analysis.

An example of the effect of the correction on the cold wall design heating rate is shown in Fig. 17. These results pertain to Body Point 7430 on the SRB nose cone.

Thermal mismatch corrections were generated for the following gage flight measurements.

GAGE	χ_B	θ_B	STS 1	STS 2	STS 3	STS 5	STS 6
7429	300.0	180	X	X			
7431	388.0	45	X	X			
7432	388.0	60	X	X			
7413	313.0	72	X	X			
7427	214.0	0	X	X			
7446	286.0	54	X				
7412	287.0	74	X	X			
7660	↓	90			X	X	X
7428	300.0	352	X	X	X	X	X
7658	↓						
7444	419.0	46	X	X			
7446	286.0	54		X			
7430	388.0	0		X	X	X	X
7661	280.0	270			X	X	X
7657	373.1	90			X	X	X
7659	284.9	20			X	X	X
7655	448.0	73			X	X	X
7653	459.6	0			X	X	X
7654	462.0	100			X	X	X

6.2 ATTACH RING/ AFT MOTOR CASE AND/ AFT SKIRT DATA

Flight hot wall heating rate data from the attach ring and aft skirt were reduced to heat transfer coefficient using the Martin calculated calorimeter wall temperature and the trajectory recovery enthalpy

$$Hi_{HW} = \frac{\dot{q}_{HW}}{H_R - 0.24T_W}, \text{ BTU/FT}^2\text{Sec}^\circ R \tag{6.4}$$

Cold wall (TW = 460°R) heat transfer coefficient was then calculated by

$$Hi_{CW} = Hi_{HW} * \frac{H_R - 0.24T_W}{H_R - (0.24)(460)}, \text{ BTU/FT}^2\text{Sec}^\circ R \tag{6.5}$$

Cold wall heating rates were calculated by the relation:

$$\dot{q}_{cw} = H_{i_{cw}} * (H_R - 110.4)\ , \text{BTU/FT}^2\text{Sec} \tag{6.6}$$

Interference heating was then converted to the (Hi/Hu) amplification factor form by nondimensionalizing Hi by the undisturbed clean-skin MINIVER heating calculation along the flight trajectory.

6.3 FLIGHT DATA APPLICATION

Flight test data from STS 1-3, 5, and 6 were used to generate scale factors between wind tunnel and flight. The scale factor:

$$f = \frac{(Hi/Hu)_{\text{flight}}}{(Hi/Hu)_{\text{wind tunnel}}} \tag{6.7}$$

was applied as a direct multiplier on the wind tunnel data.

$$\dot{q}_{cw} = (Hi/Hu)_{\text{wind tunnel}} \times f \times \dot{q}_{\text{undisturbed}} \tag{6.8}$$

to adjust the wind tunnel data level to that commensurate with flight measurements.

Flight data in the form of cold wall corrected heat transfer coefficient was nondimensionalized by the undisturbed heating calculated from MINIVER (Ref. [8]) and put in the form Hi/Hu versus time. The Hi/Hu data for each gage were then plotted on semilog paper versus Mach number for each flight. A linear fit was applied to the data and a value of Hi/Hu corresponding to M = 3.00 and 4.00 read from the curve fit. An example of this procedure is shown in Fig. 18 for Gage 7414. Values of Hi/Hu at M = 4.00 were obtained by linear extrapolation since SRB separation usually occurs at M < 4.00. These values of Hi/Hu were then plotted on the Hi/Hu versus β wind tunnel data base, Fig. 19. A flight factor for each individual flight was calculated by dividing the flight Hi/Hu by the wind tunnel Hi/Hu at the same β:

$$f_{3,4} = \frac{(Hi/Hu)_{\text{flight}}\ \alpha,\beta}{(Hi/Hu)_{\text{wind tunnel}}\ \alpha,\beta} \tag{6.9}$$

To get the corresponding angle of attack between wind tunnel and flight, the wind tunnel data base was interpolated between α's. An average flight factor at M = 3.00 (f_3) and M = 4.00 (f_4) was calculated for each gage by averaging over all

available flights for the particular gage in question. This factor (f_3, f_4) was then used as a direct multiplier on the wind tunnel data base on input to the trajectory program. A summary of flight factors for all Shuttle DFI (Developmental Flight Instrumentation) instrumented points - the 7000 and 8000 series body points - is presented in Table 4. These points correspond to body points with both wind tunnel and flight measurements.

Flight factors for body points which did not have corresponding flight measurements were obtained by either direct comparison with an analogous point where flight data existed or by globally plotting all DFI flight factors in a particular region versus θ_B. A fairing was applied to the M = 3.00 data and M = 4.00 data. The fairings were then used to define flight factors at locations not supported by flight data. An example of this is shown in Fig. 20 for the SRB nose cone.

In general, the magnitude of the flight factors ranged from $\approx$ 1.00 to 1.50 (Table 4, Fig. 20). This says that the wind tunnel data base and model geometry did fairly good jobs of duplicating flight. There are a few outliers where the flight factors were in the 2.5 to 3.00 range. They were, however, in the minority. This also says that the Hi/Hu approach does a fairly good job in accounting for Reynolds number effects even in the presence of protuberances.

Flight factors (f_3, f_4) for each SRB body point are listed in the wind tunnel data base (Volume II) as MULT 3 and MULT 4 for each body point.

Section 7
ASCENT ENVIRONMENTS

7.1 GENERAL COMMENTS

As previously stated the objective of this study was to produce an independent set of SRB environments which would serve as a check on the Rockwell IVBC-3 Design environments. In addition, they would also provide support for lowering the design from the conservative 1980 Design set.

Rockwell generated environments at approximately 740 body points, many of these being acreage locations. The REMTECH set of body points, while fewer in number, were located in areas where the more severe environments would occur and/or areas with the most potential for impact on the TPS design. Many of the Rockwell environments were cleared by analogy with the closest REMTECH body point and/or consistency within the Rockwell local set of body point environments, themselves. This is especially true of the forward skirt acreage, forward and aft motor case acreage, and aft skirt acreage body points. Rockwell environments in areas of the more severe environments were cleared by direct comparison with corresponding REMTECH points.

As much as possible, similar methodologies were used so that the environments would be comparable. To accommodate this, REMTECH changed the Hi/Hu - Mach numbers extrapolation methodology such that Hi/Hu was kept constant for $M \geq 4.00$. In addition, the reference atmosphere was changed from the Vandenburg "Hot" Day to the Vandenburg "Reference" Atmosphere.

7.2 ENVIRONMENT SUMMARIES

A summary of the design environments generated in this study is presented in Table 5. The data are in the form of maximum heating rate ($\dot{q}_{Max}$) and integrated heat load (Q_{LOAD}) along with the X_B and θ_B location for each body point. In addition to the REMTECH environments, corresponding Rockwell IVBC-3 and 1980 Design environment summaries are presented also. The data are presented by zone. While there is not a complete one to one correspondence in body point locations between Rockwell and REMTECH, they are close enough that the difference should be of no consequence.

Comparisons of the updated environment set (RI IVBC-3/REMTECH) with the 1980 Design show a definite justification for lowering the design requirements in areas such as the nose cone acreage, forward SRB/ET attach-bolt catcher area and the forward face of the attach ring. Comparative plots of $\dot{q}_{Max}$ and Q_{LOAD} for these areas are shown in Figs. 21 - 24 respectively. Other areas show a need to increase the design requirements such as on the nose cone - 90 deg. ray area where the SRB/ET reflected shock impinges on the SRB, and the forward face of the Systems Tunnel. See Figs. 25 and 26.

Concerning the updated environment calculations (Table 5), in general, corresponding environments between the Rockwell (IVBC-3) and REMTECH methods compared favorably with no impact on the IVBC-3 calculations. Areas where significant discrepancies and inconsistencies existed were reported in the monthly progress reports (Ref. [14]) as well as, IVBC-3 assessment reports (Refs. [15] and [16]) and adjustments made. Current design exceedences are indicated by the starred body point numbers in Table 5. An environment was judged to exceed the RI IVBC-3 environments if the calculated heating rate was > 2 BTU/FT^2 Sec and the integrated heat load was > 50 BTU/FT^2 Sec.

Of the environments generated, nine in Zone 2, three in Zone 6, two in Zone 5 and one in Zone 3 exceed the IVBC-3 calculated environments. Of these exceedences, most are viewed as not being critical as far as impacting TPS design. This is due to the fact that the design is driven by other dominant factors. For example, Zone 2 TPS is driven by the bolthead environments. Consequently, the differences for Body Points 1313, 1326 and 1449 are not critical. Areas aft of the attach ring i.e., Zone 6 and 7, are driven by plume impingement and reentry heating. The remaining areas where exceedences and or differences between the REMTECH and RI IVBC-3 environments exist and are considered important are Body Points 1326, 3226 and 7432 in Zone 2 (Fig. 21), Body Points 1045 and 7656 in Zone 3 (Fig. 23) and Body Points 54 and 55 (Fig. 24) in Zone 5. These areas are covered by a "best" estimate, however, a disparity between the two methods still exists. For the Zone 2 and 5 body points, data are to be obtained in the upcoming DFI flights which will provide confirming information, as in Zone 2, or information where data did not previously exist, as in Zone 5. These results should determine which environment designs the $\theta_B = 90$ deg. ray in Zone 2 and the Attach Ring in Zone 5.

Plots of design cold wall heating rate for each body point comparing RI IVBC-3 with REMTECH are presented under plotted data section of Volume II. These data are intended to give a visual trajectory comparison with pertinent comments concerning the status of each body point and any existing discrepancies between the two methods. The comments are made from a standpoint of impact on TPS

design. Where no comment exists it is implied that the agreement is acceptable. Integrated heat load for each method is also given.

7.3 TIMEWISE ENVIRONMENTS

Timewise ascent design environments generated in this study for the SRB are presented in Volume II. They are composed of ascent convective aerodynamic heating only, and do not contain plume convection or SSME/SRM radiation. They are arranged to correspond to the body point and wind tunnel data base tables in order of presentation and zone, and are identified by body point number, axial location (X_B) and circumferential location (θ_B). In addition to the heating rate (DESIGN HTG RATE), and integrated heat load (Q LOAD), other pertinent parameters listed are: cold wall heat transfer coefficient (FILM COEFF.), recovery enthalpy (RECOV. ENTH.), local undisturbed static pressure (UNDIST. PRESS.), interference to undisturbed heating factor (Hi/Hu), freestream Mach number (MACH No.), SRB angle of attack (ALPHA), angle of side slip (BETA), freestream unit Reynolds number (REINF.), altitude (ALT.) and freestream velocity (VEL.). The environments go from liftoff to SRB separation (t=126 seconds) for body points up to and on the forward face of the attach ring. Environments on the aft face of the attach ring, aft portion of Zone 5, as well as, Zone 6 and Zone 7 i.e., aft motor case and aft skirt, are terminated at t=96 seconds. This is due to plume recirculation which becomes dominant in these areas for t>96 seconds.

Section 8

CONCLUSIONS AND COMMENTS

Verification of the Rockwell generated RI IVBC-3 ascent design environments was made by independently calculating environments on the SRB. In general, the environments compared favorably with Rockwell. Areas where discrepancies occured were reported in the monthly progress reports and assessment reports and corrective action taken by either Rockwell or REMTECH. While the REMTECH calculated points were fewer in number than Rockwell, each Rockwell point was considered and cleared either by one to one comparison with REMTECH or by consistency within the local set of Rockwell points. Conclusions of the study are summarized below:

1. The wind tunnel data base represented the flight case fairly well at both M = 3.00 and 4.00.

2. Calculated environments between Rockwell and REMTECH compared favorably at most locations. There are 5 locations, however, where the differences are unresolved and will require results from the upcoming DFI flights to resolve the disparities.

3. Use of wind tunnel/flight correction factors at off DFI points appears to be very subjective and calls for much "engineering judgement."

4. Use of the thermal mismatch methodology especially in shock interference regions remains questionable. The magnitude of the correction (30 - 50 percent) seems quite high, especially in light of the fact that the corrections were developed for subsonic noninterfering flow fields. Basic research is needed to upgrade the methodology to supersonic and/or supersonic interference type flow fields before confidence in the application and magnitude of correction can be fully achieved.

5. In the absence of experimental data protuberance amplification factors were generated by the relationships developed from Refs. 17, 18: i.e.,

$$\left.\frac{hi}{hu}\right)_{\max} = 1 + C_1 \left(\frac{K}{\delta}\right)^{0.863}$$

where C_1 = constant dependent on the protuberance height
δ = boundary layer thickness
K = protuberance height

Examples of this for various K/δ are shown in Fig. 27 for large protuberances like the systems tunnel and small protuberances like the low profile sealant caps.

Application of this approach as with the off DFI flight factor determination requires much "engineering judgement" and shows a need for a concise set of 3 dimensional protuberance heating data on current flight shapes with corresponding methodology development.

Section 9

REFERENCES

[1] "Space Shuttle Flight Performance Data Book, Volume 1 - Ascent," SD73-SH-0178-IC (Revision 8), revised December 8, 1980.

[2] Crain, William K., and Nutt, Kenneth W., "NASA/Rockwell International IH-97 Space Shuttle Heating Test," AEDC-TSR-82-V37, December 1982.

[3] Nutt, K.W., "Results from the NASA/Rockwell International Space Shuttle Solid Rocket Heating Test (IH-47) Conducted in the AEDC-VKF Tunnel A," AEDC-DR-76-35, May 1976.

[4] Lemoine, P.L., and Marroquin, J., "Results of Heat Transfer Tests of a 0.0175 Scale Space Shuttle Integrated Vehicle Model 60-OTS in the AEDC-VKF Tunnel A (IH-72)," NASA-CR-160, 843, August 1981.

[5] Foust, J.W., "Test Results from the NASA/Rockwell International Space Shuttle Integrated Vehicle Test Using A 0.0175 - Scale Model (60-OTS) Conducted in the AEDC-VKF Tunnel A (IH-85)," NASA-CR-151, 800, April 1980.

[6] Carrol, P. R., "Wind Tunnel Tests of the 0.035-Scale Integrated Space Shuttle Vehicle Model 84-OTS in the NASA/Lewis 10 $\times$ 10^{-} Foot Supersonic Wind Tunnel (IH11)," Vol. 4, NASA-CR-160, 526, October, 1980.

[7] "Space Shuttle Pictorial Representations," NASA Report 10A00545, Revision F, April 1978.

[8] Engel, Carl D., and Praharaj, Sarat C., "MINIVER Upgrade for the AVID System, Volume 1 - LANMIN Users Manual," NASA CR 172212, August 1983.

[9] Rubesin, M.W., "The Effects of an Arbitrary Surface Temperature Variation Along a Flat Plate on the Convective Heat Transfer in an Incompressible Boundary Layer," NACA TN 2345, April 1951.

[10] Reynolds, W.C., Kays, W.M., and Kline, S.J., "Heat Transfer in the Turbulent Incompressible Boundary Layer. II-Step Wall Temperature Distribution," NASA Memo 12-2-58W, December 1958.

[11] Westkeamper, J.C., "On the Error in Plug-Type Calorimeters Caused by Surface Temperature Mismatch," Journal of Aerospace Sciences, November 1961, pp. 907-908.

[12] Crain, W.K., and Schmitz, C.P., "SRB Flight Thermal Mismatch Corrections and Tabulated Data," REMTECH Report RTN-090-2, January 1985.

[13] Pond, J.E., and Schmitz, C.P., "MINIVER Upgrade for the AVID System," NASA CR 172214, Volume III: "EXITS User's and Input Guide," August 1983.

[14] Crain, W.K., Frost, C.L., and Engel, C.D., "SRB Ascent Aerodynamic Heating Design Criteria Reduction Study," Monthly Progress Reports, RPR 090-01 - 090-66, July 1983 - January 1988.

[15] Crain, W.K., and Engel, C.D., "RI IVBC-3 Environment Assessment," RTN 090-03, February 1985.

[16] Engel, C.D., "Additional Body Point Definitions for the IVBC-3 SRB Ascent Aeroheating Environment," RTN 090-04, November 1985.

[17] Hung, F.T., "Three Dimensional Protuberance Interference Heating in High Speed Flow," AIAA-80-0289, January 1980.

[18] "SRB Ascent Aerodynamic Heating Design Criteria Reduction Study," REMTECH Progress Report 090-22, 10 April 1985.

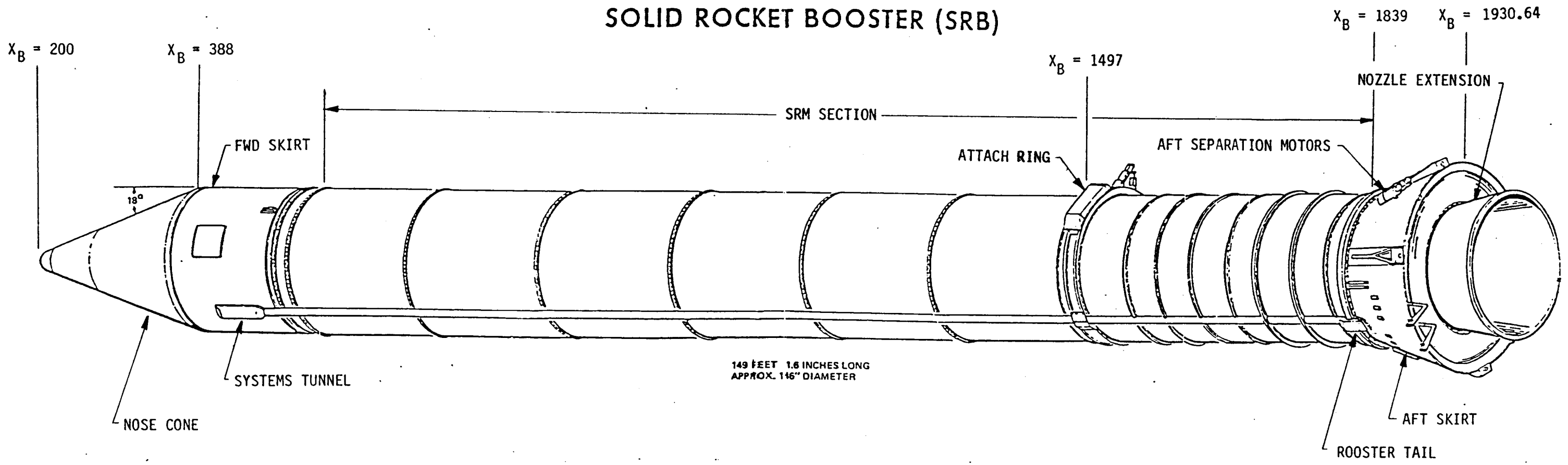

a) General Description

Fig. 1 Solid Rocket Booster (SRB) Description

FOLDOUT FRAME

FOLDOUT FRAME

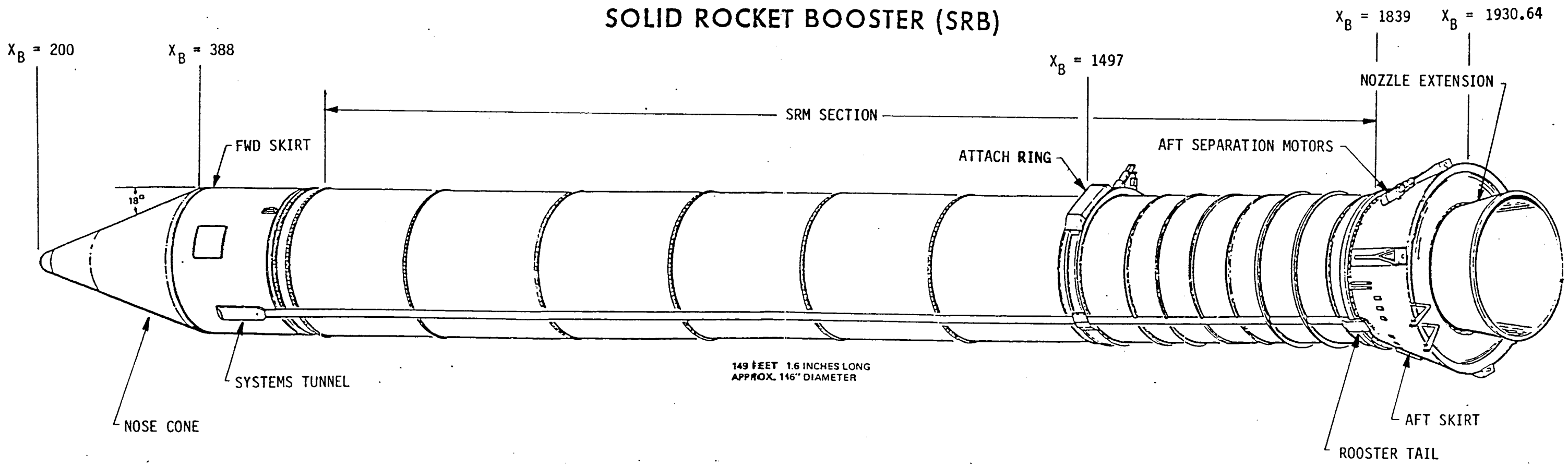

a) General Description

Fig. 1 Solid Rocket Booster (SRB) Description

FOLDOUT FRAME

FOLDOUT FRAME

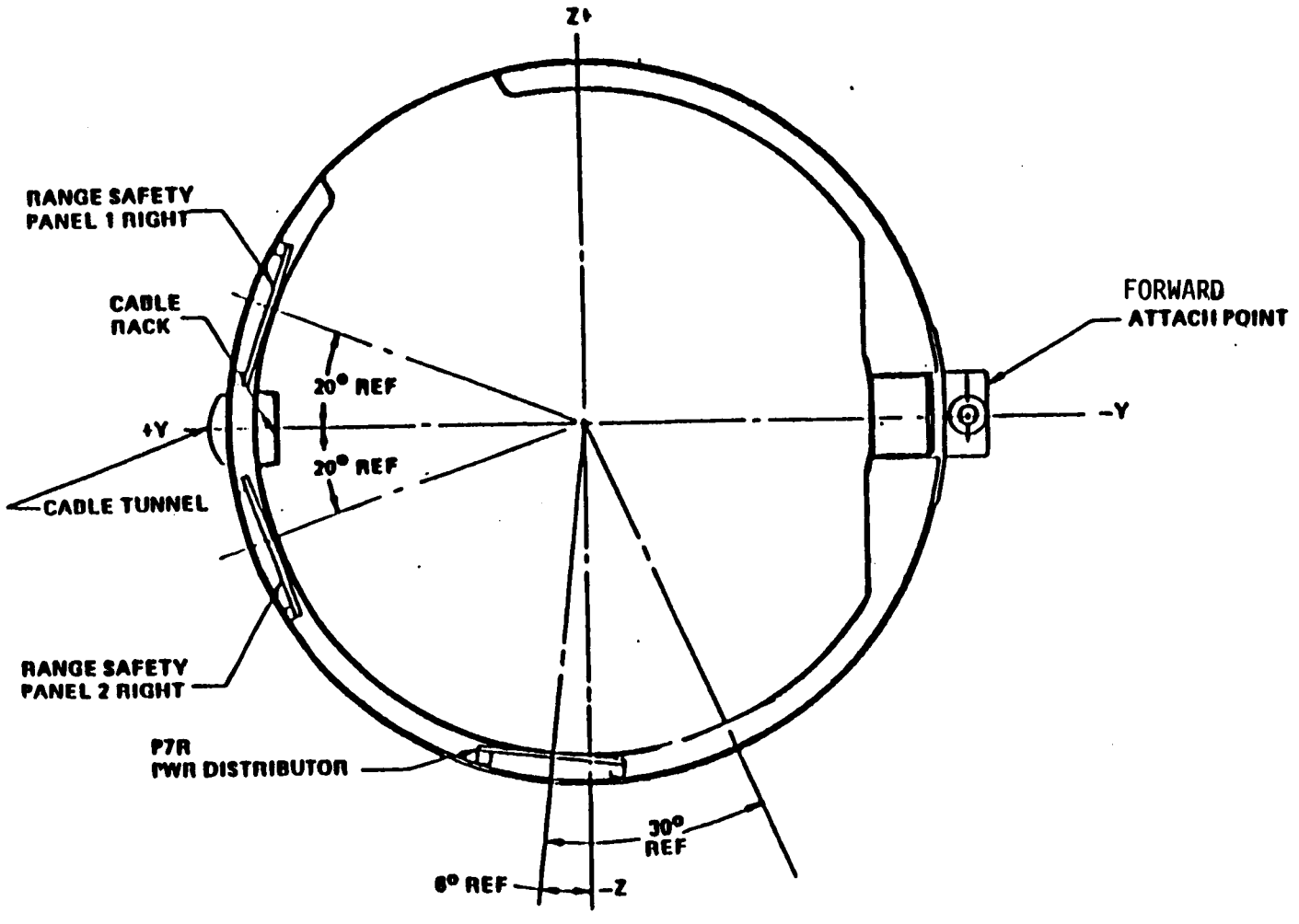

VIEW LOOKING AFT

b) SRB (Right) Ring at Sta. 445.50

Fig. 1 (Concluded)

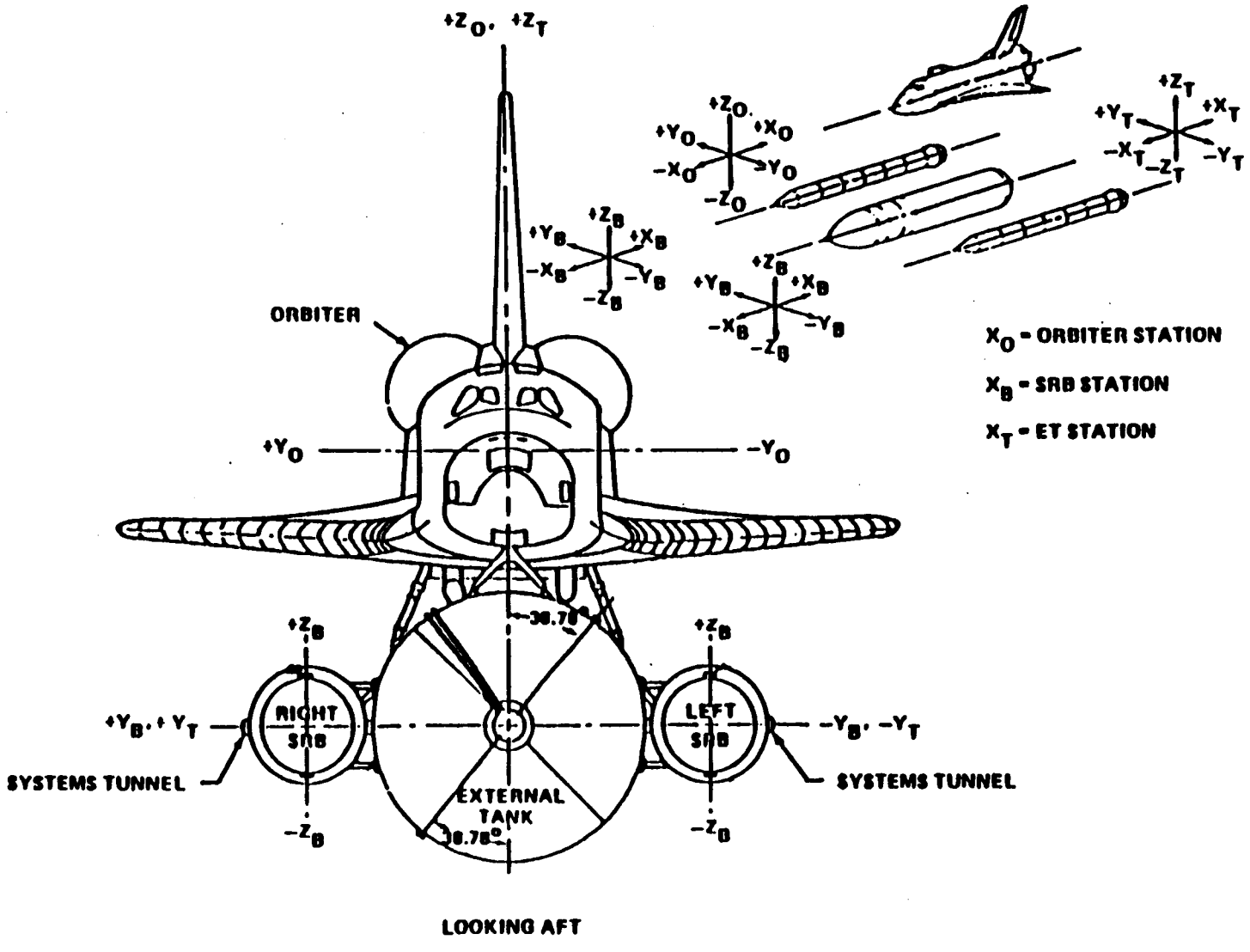

Fig. 2 Space Shuttle Launch Configuration

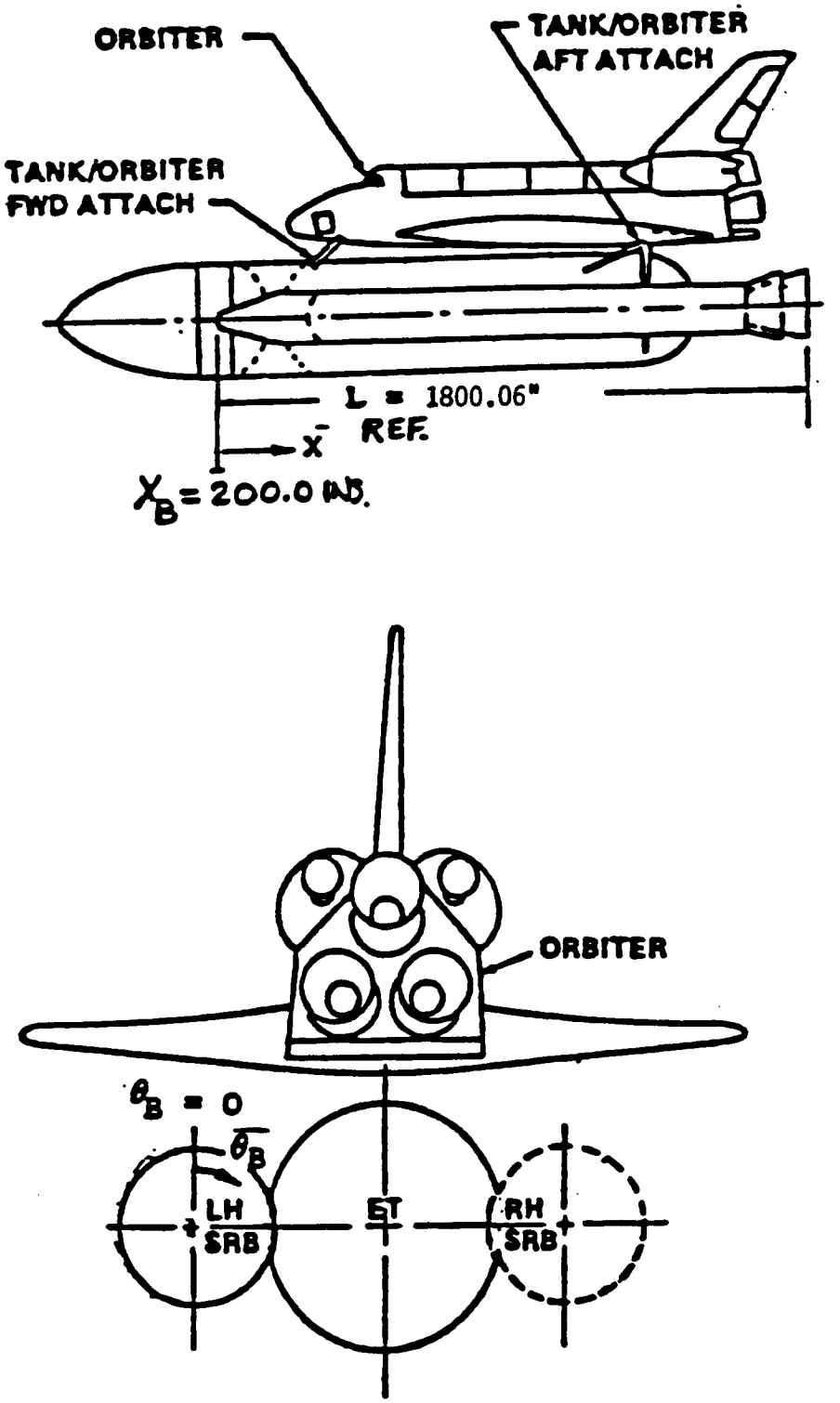

Fig. 3 SRB Coordinate System Definition

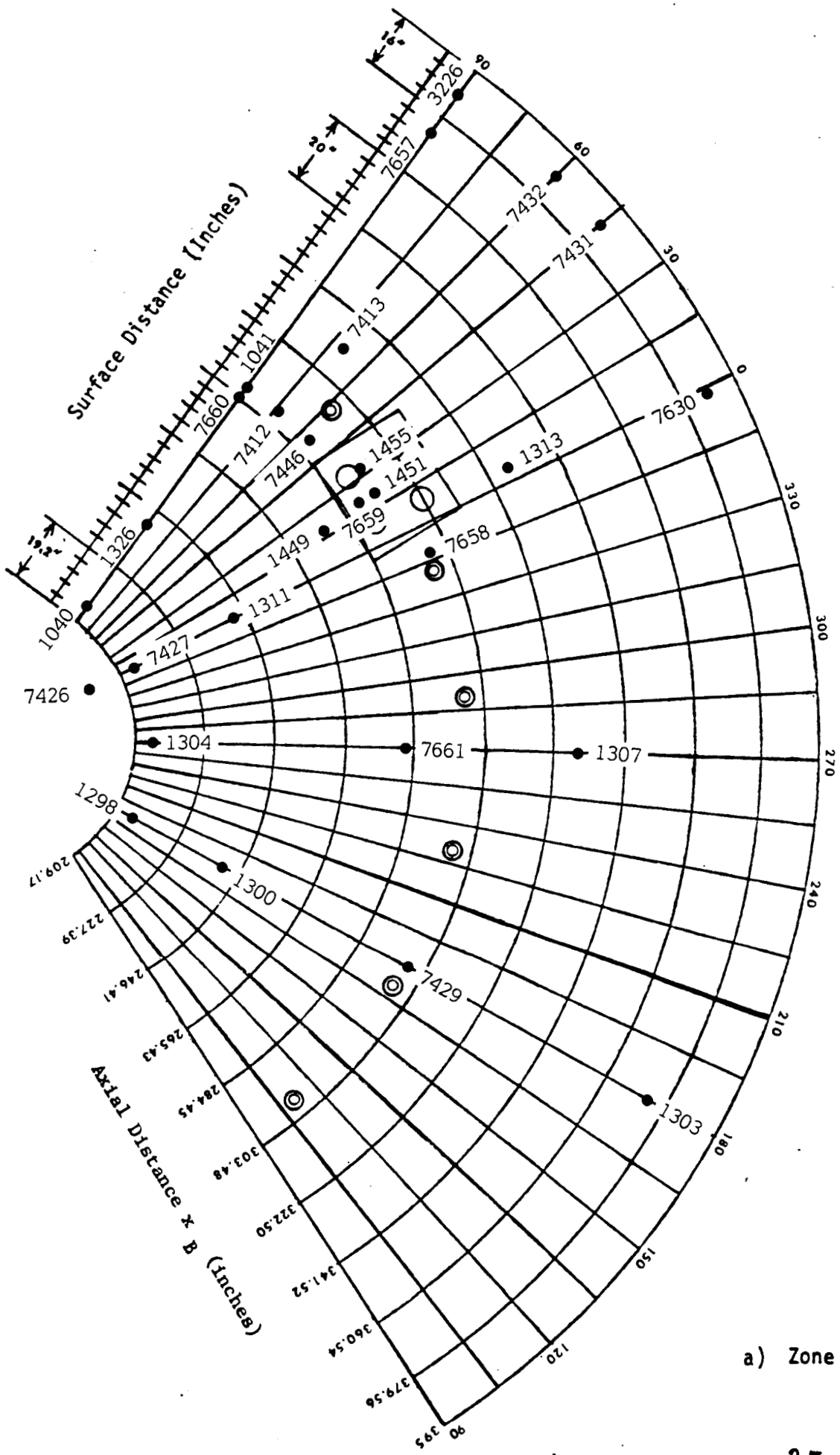

a) Zone 2

Fig. 4 SRB Body Point Locations

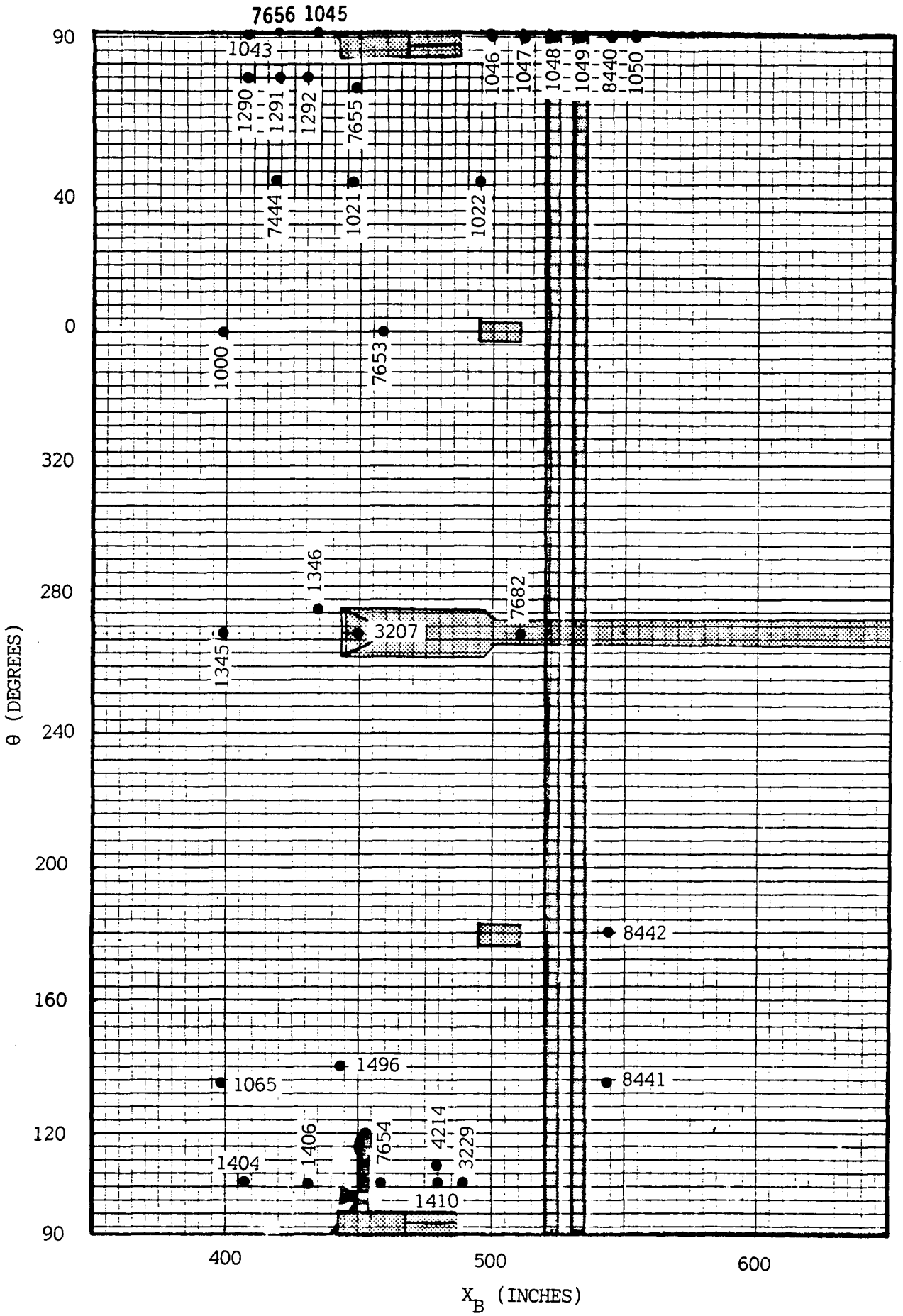

b) Zone 3
Fig. 4 (Continued)

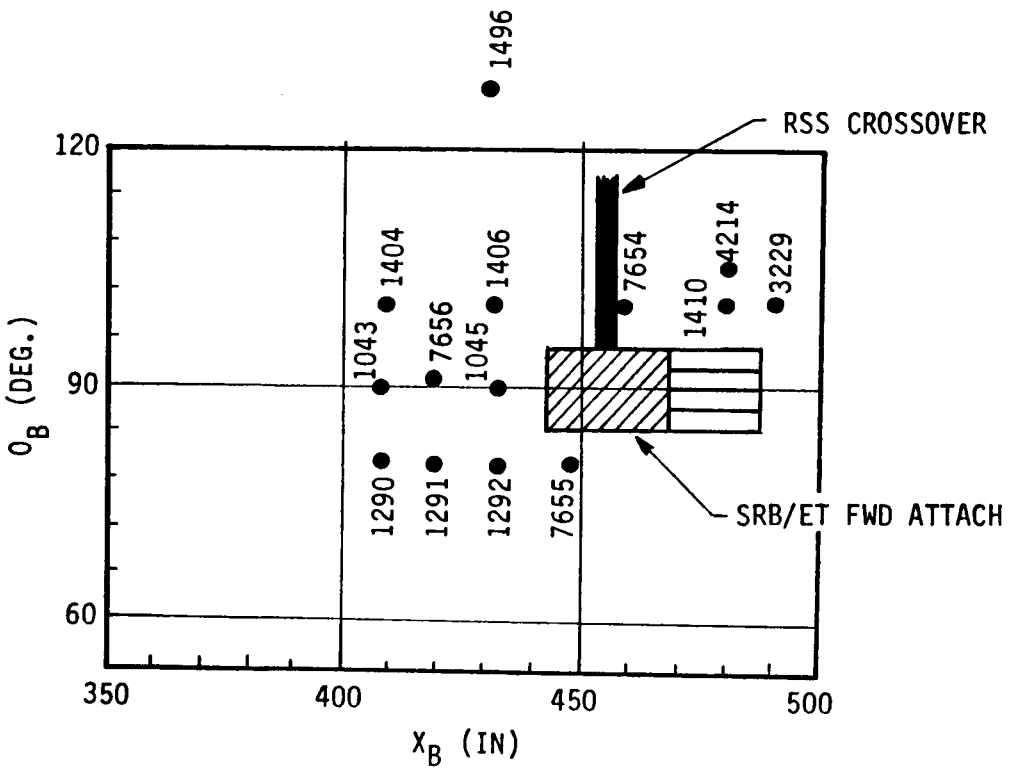

c) Zone 3 - FWD Attach Body Point Distribution

Fig. 4 (Continued)

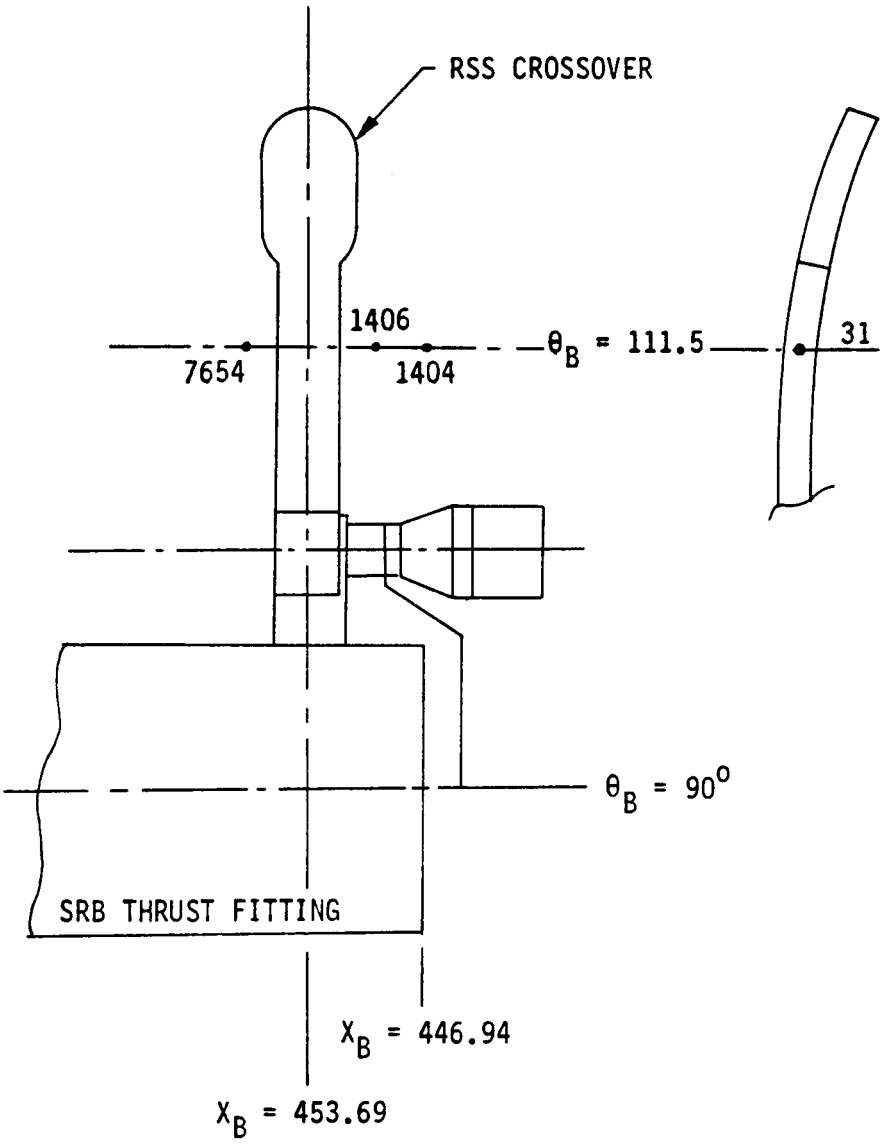

d) Zone 3 - RSS Crossover Cable Tray Body Point Distribution

Fig. 4 (Continued)

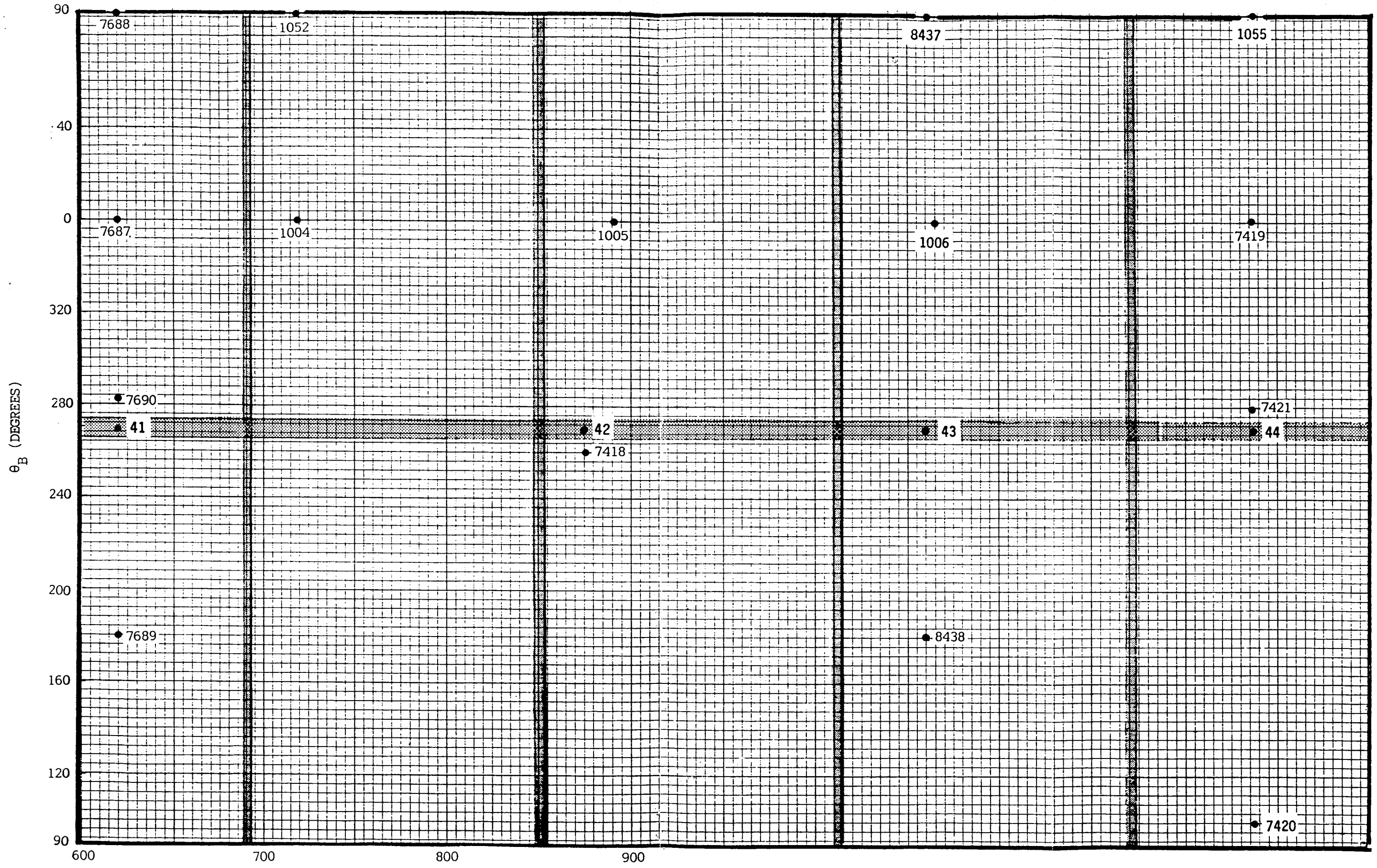

FOLDOUT FRAME

FOLDOUT FRAME

e) Zone 4

Fig. 4 (Continued)

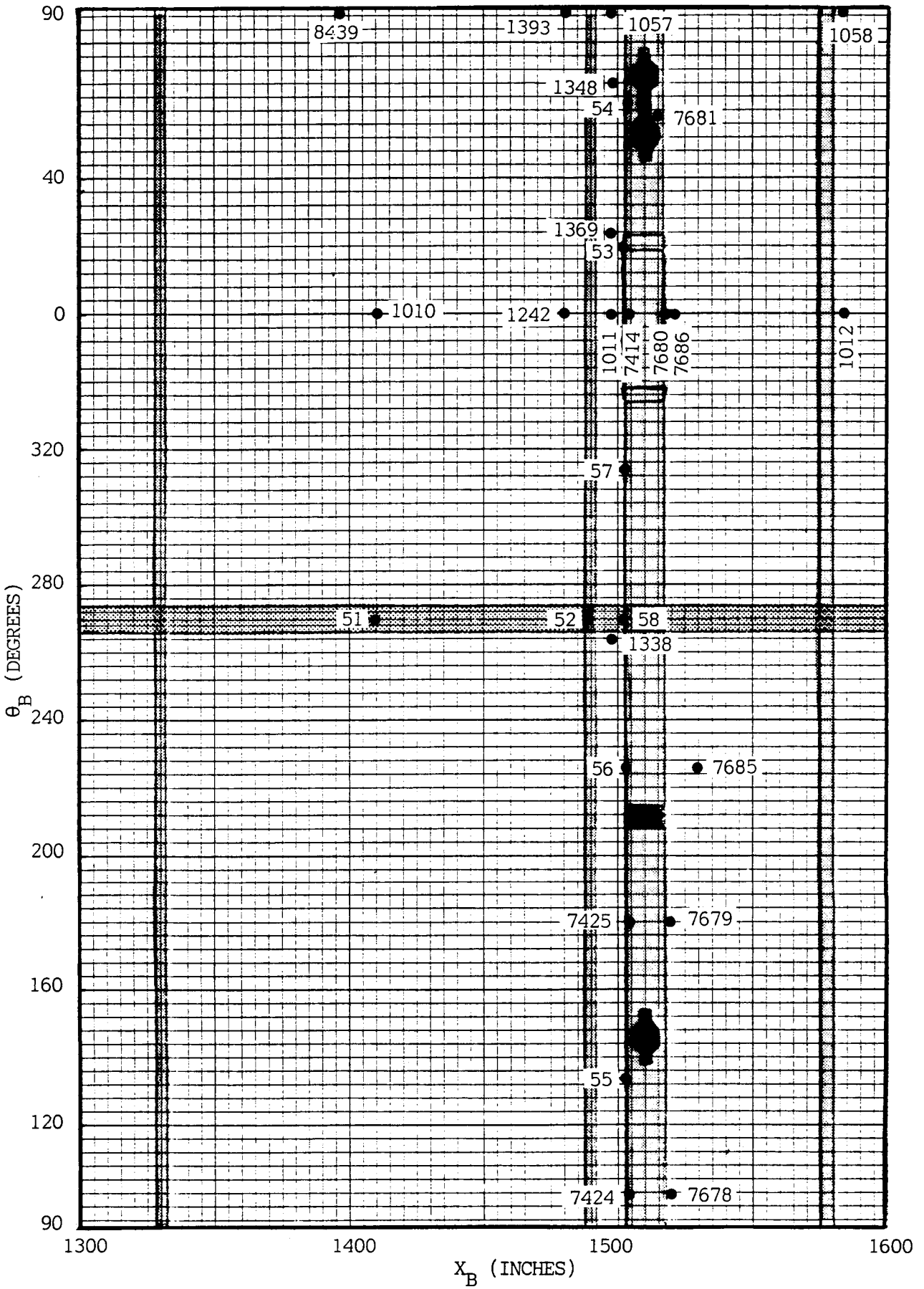

f) Zone 5

Fig. 4 (Continued)

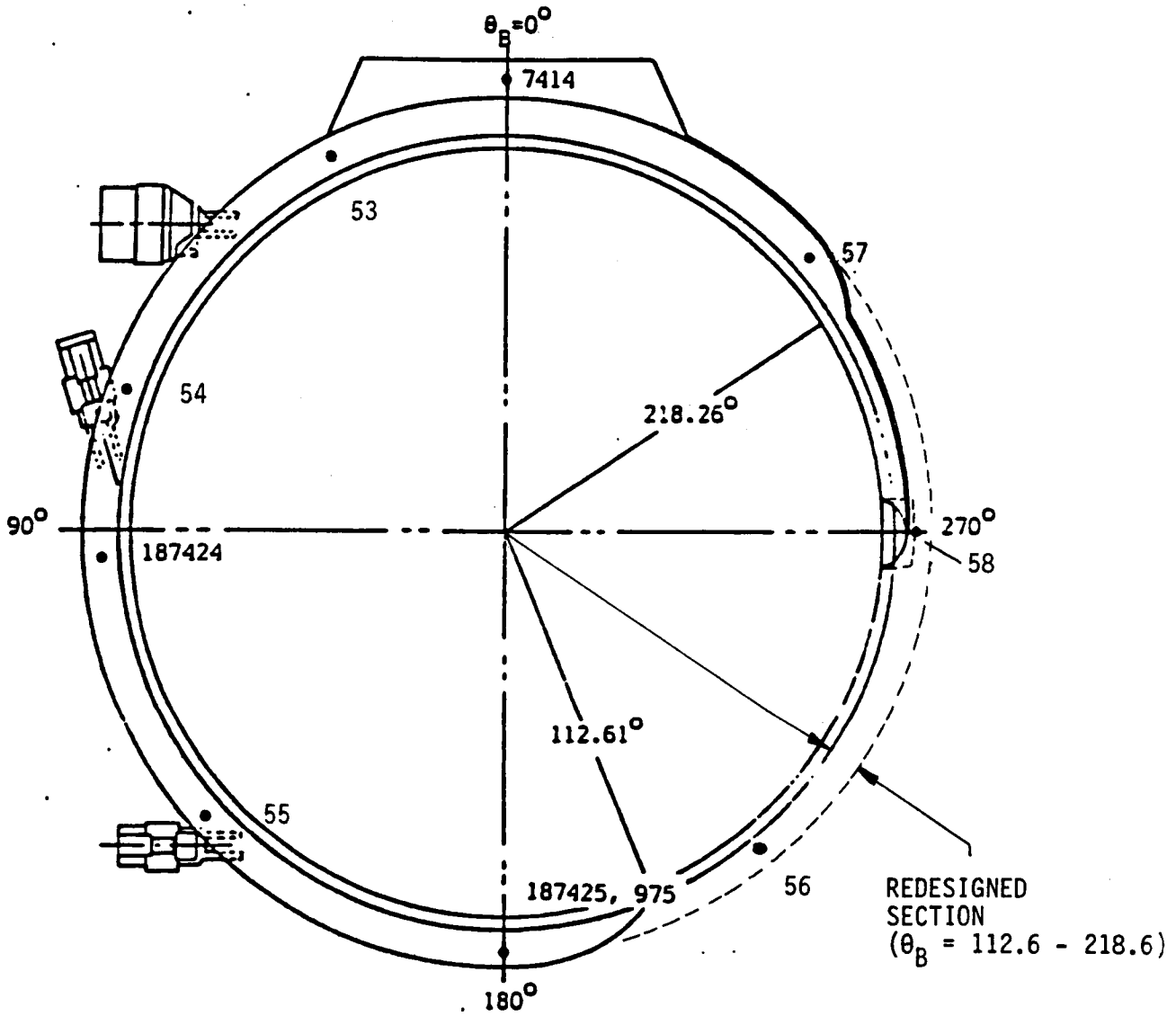

g) Zone 5

Fig. 4 (Continued)

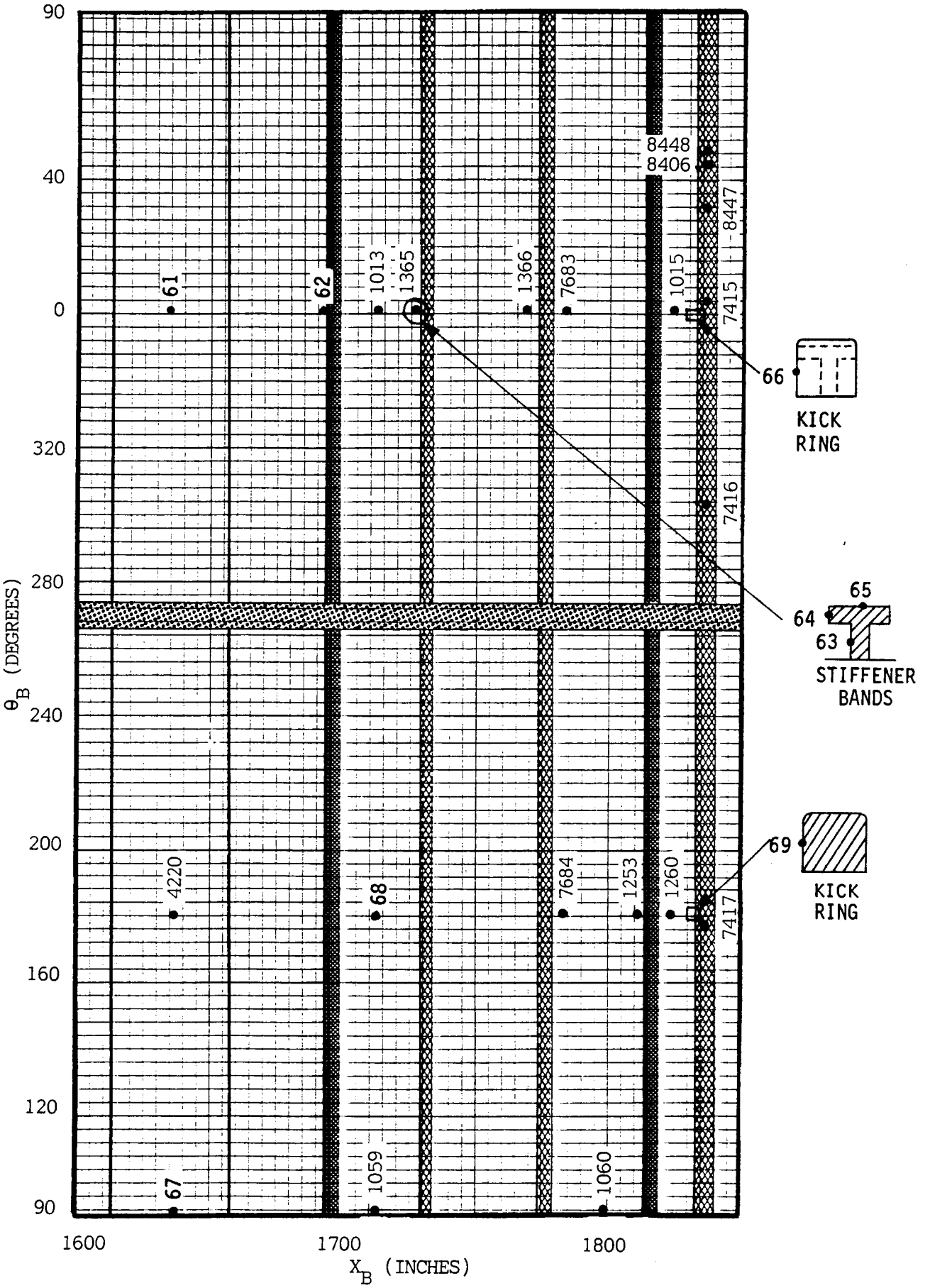

n) Zone 6
Fig.4 (Continued)

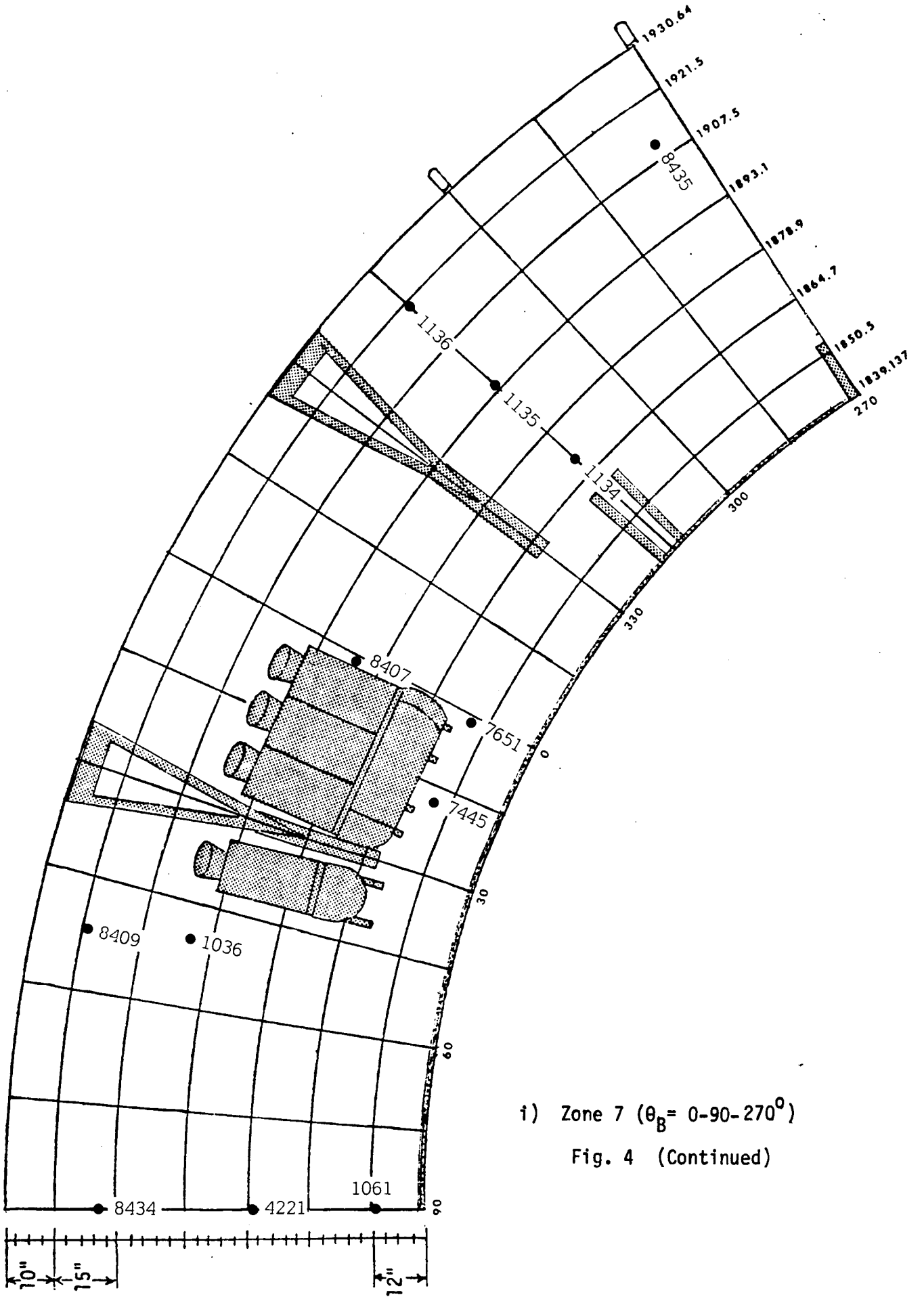

i) Zone 7 (θ_B= 0-90-270^0)

Fig. 4 (Continued)

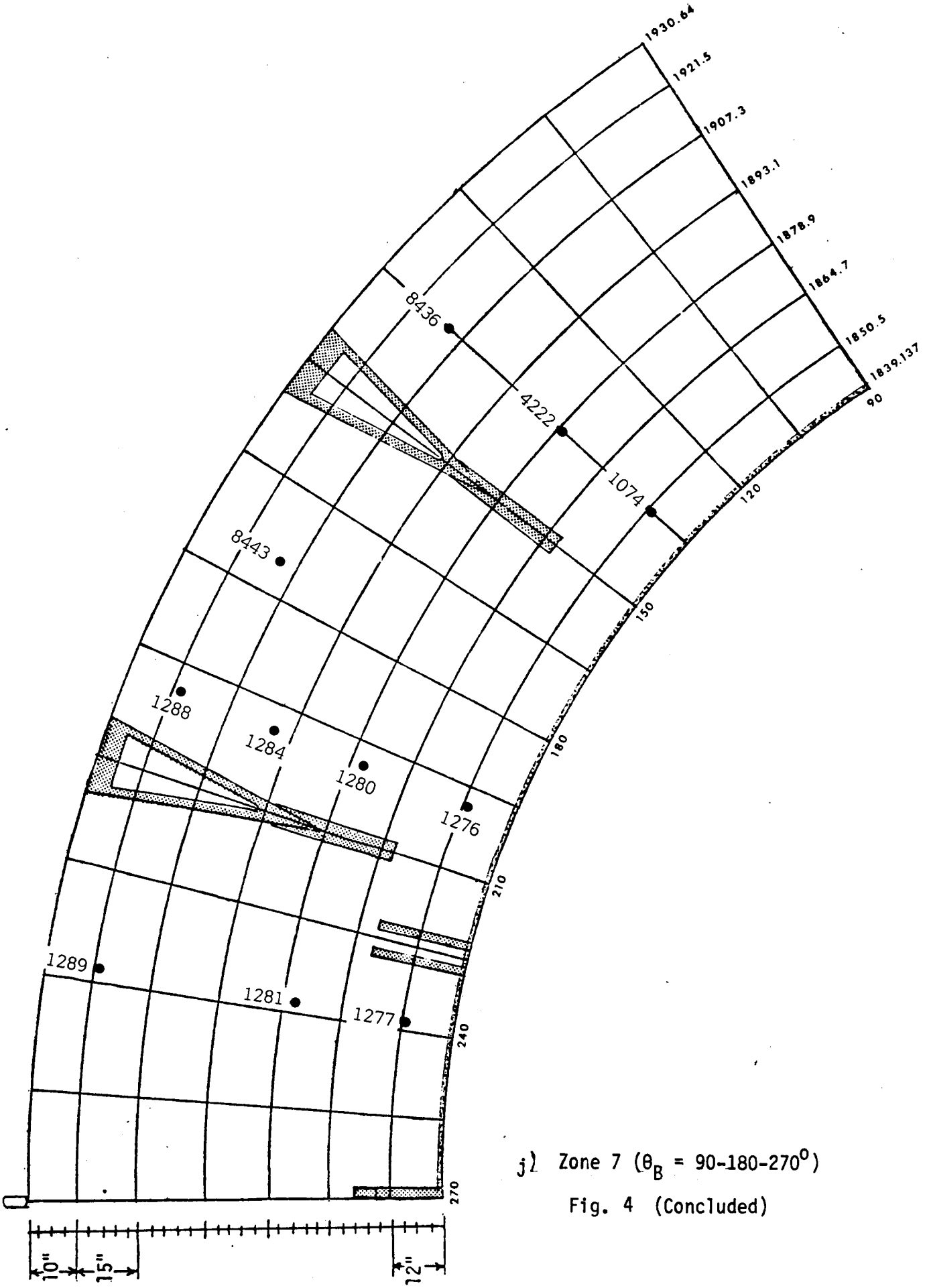

j) Zone 7 (θ_B = 90-180-270°)

Fig. 4 (Concluded)

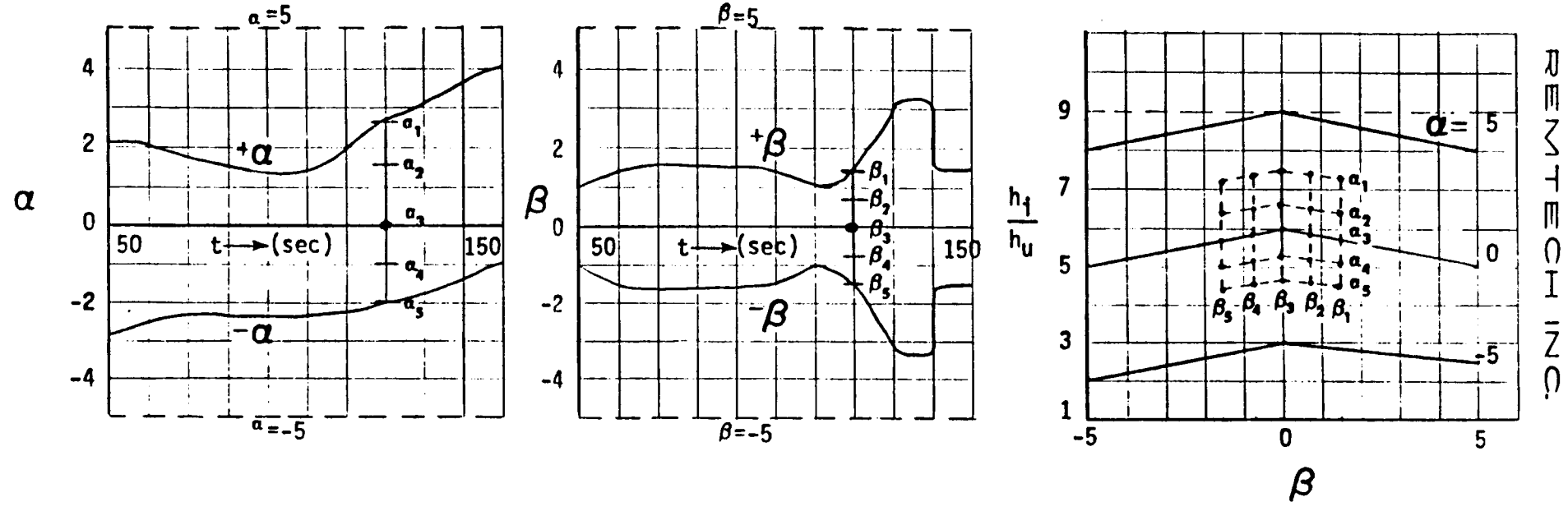

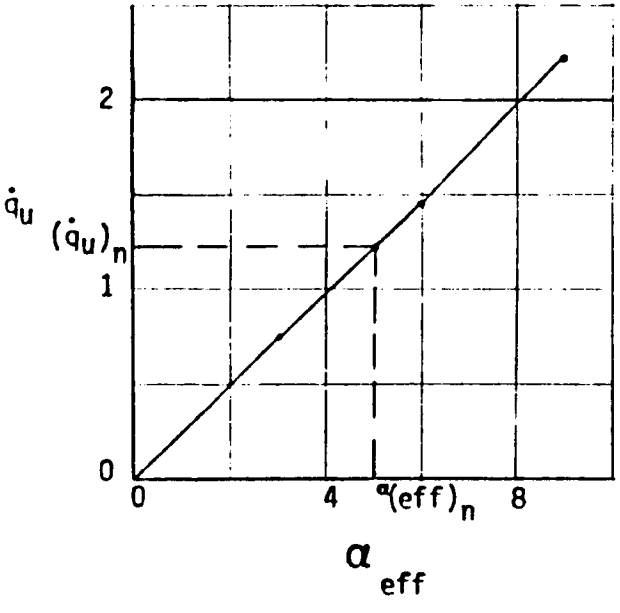

For any cut (α_n, β_n),

$(\alpha_{eff})_n = -\alpha_n \cos\theta_T + \beta_n \sin\theta_T$

$(\dot{q}_u)_n$ is obtained from $\dot{q}_u \underline{\text{vs}} \alpha_{eff}$ plot

Finally,

$$\dot{q}_{i_{BP}} \text{ @ any traj. time} = \left[\begin{matrix}\text{Max} \\ \text{over} \\ \text{N cuts}\end{matrix} \left\{(\dot{q}_u)_n \cdot (h_f/h_u)_n\right\}\right]$$

where

N = Total number of α, β cuts = m^2

m = Number of cuts in α or β

Fig. 5 Design Methodology for SRB Ascent

BODY / ITEMS	18° FORE-CONE	BARREL	18.67° AFT SKIRT
SHOCK	CONE	CONE	CONE (BODY ANGLE = 18°) CONE (BODY ANGLE = 18.67°)
PRESSURE	TANGENT - CONE (BODY ANGLE = 18°)	TANGENT -CONE (BODY ANGLE = 0°)	TANGENT CONE (BODY ANGLE = 0°) TANGENT CONE (BODY ANGLE = 18.67°)
HEAT TRANSFER	SPALDING-CHI	← SAME	← SAME
DIVERGENCE FACTOR	3: LAMINAR 2: TURBULENT	1: LAMINAR 1: TURBULENT	3: LAMINAR 2: TURBULENT
REYNOLDS ANALOGY	VON KARMAN	← SAME	← SAME
RUNNING LENGTH	MEASURED FROM THE NOSE	← SAME	← SAME
ROUGHNESS	NONE	← SAME	← SAME

Fig. 6 SRB Undisturbed Heating Methodology

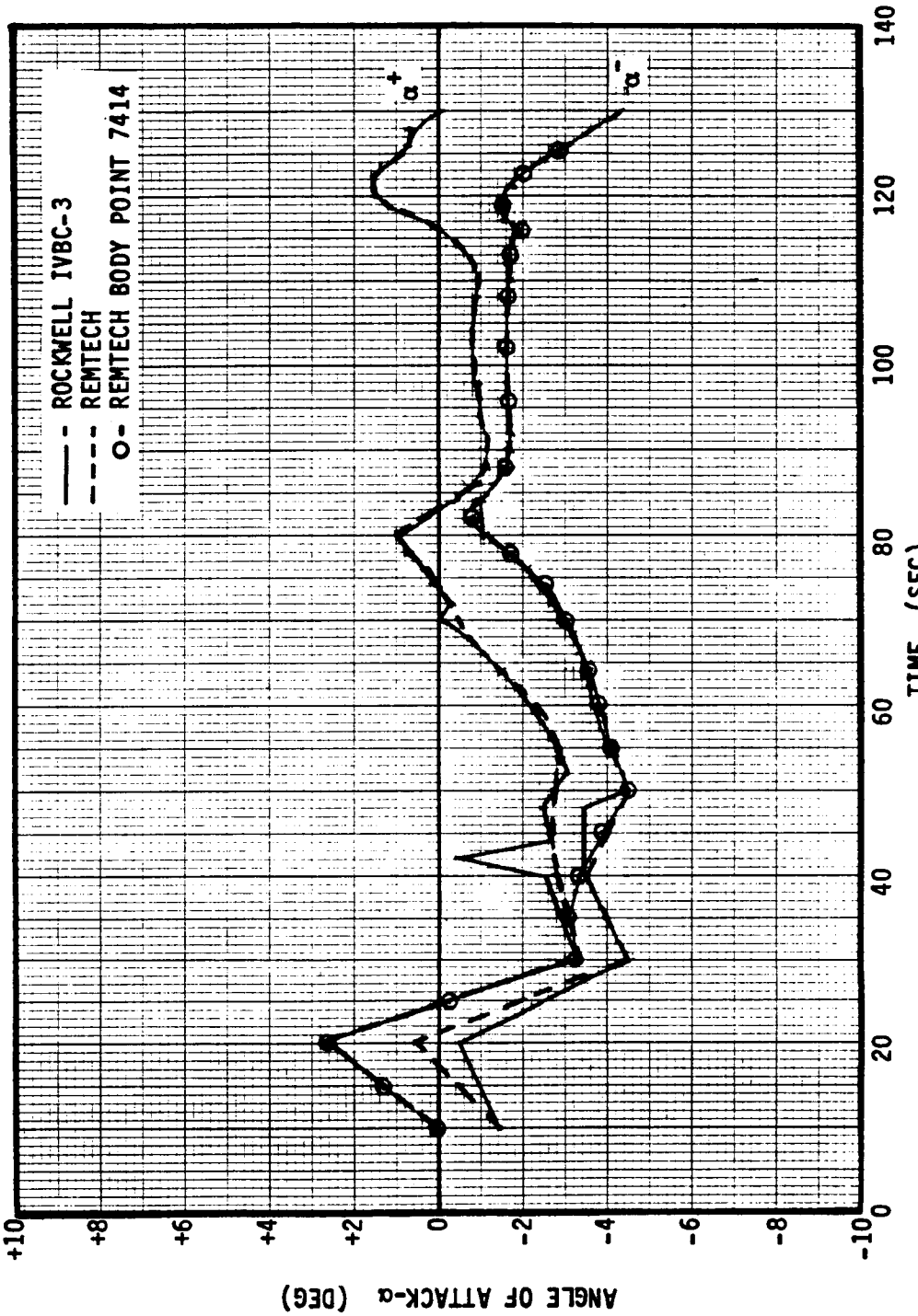

a) α Envelope

Fig. 8 αβ Envelope for the 1980 BRM 3A 3σ Dispersed LWT Trajectory

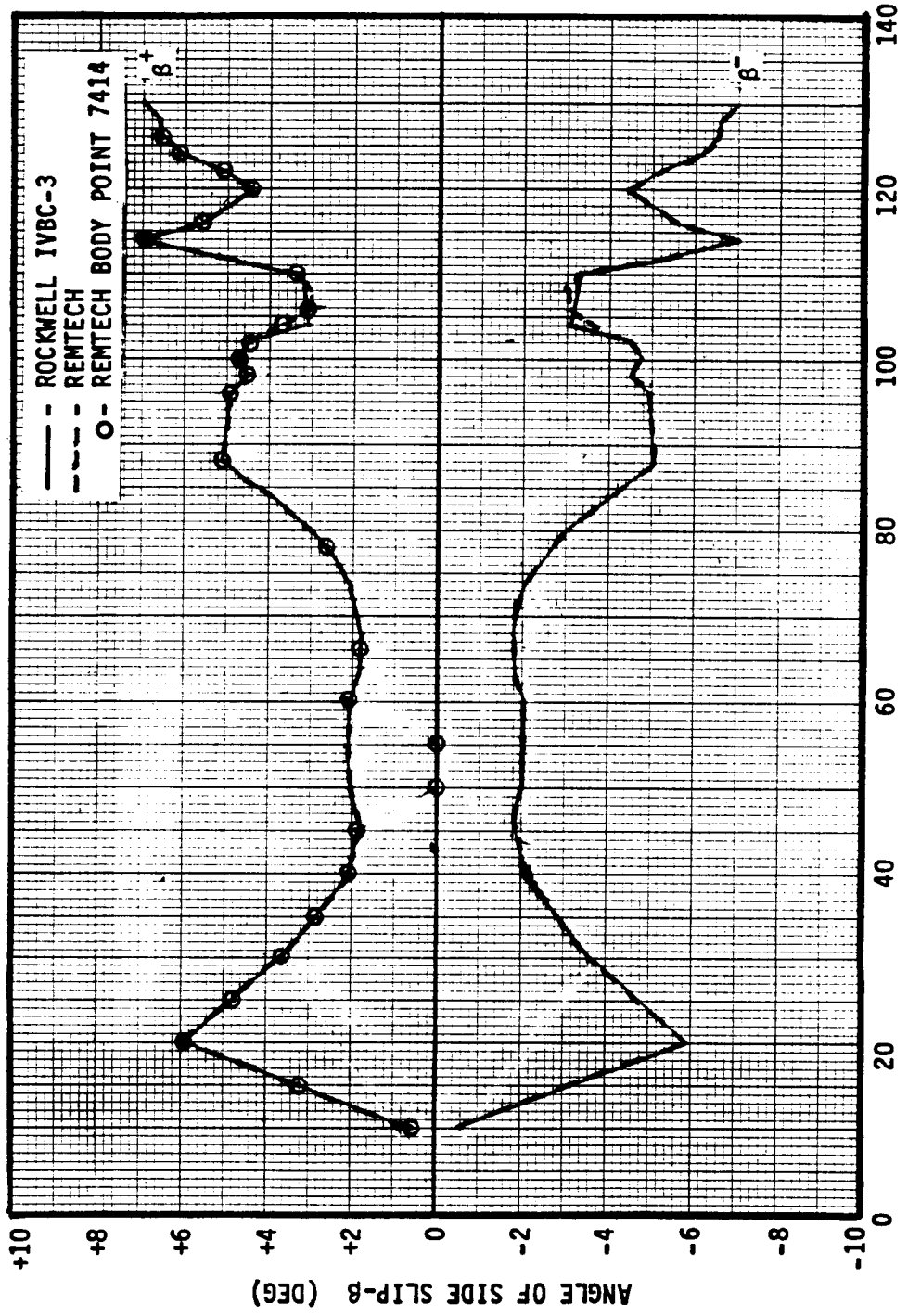

b) β Envelope

Fig. 8 (Concluded)

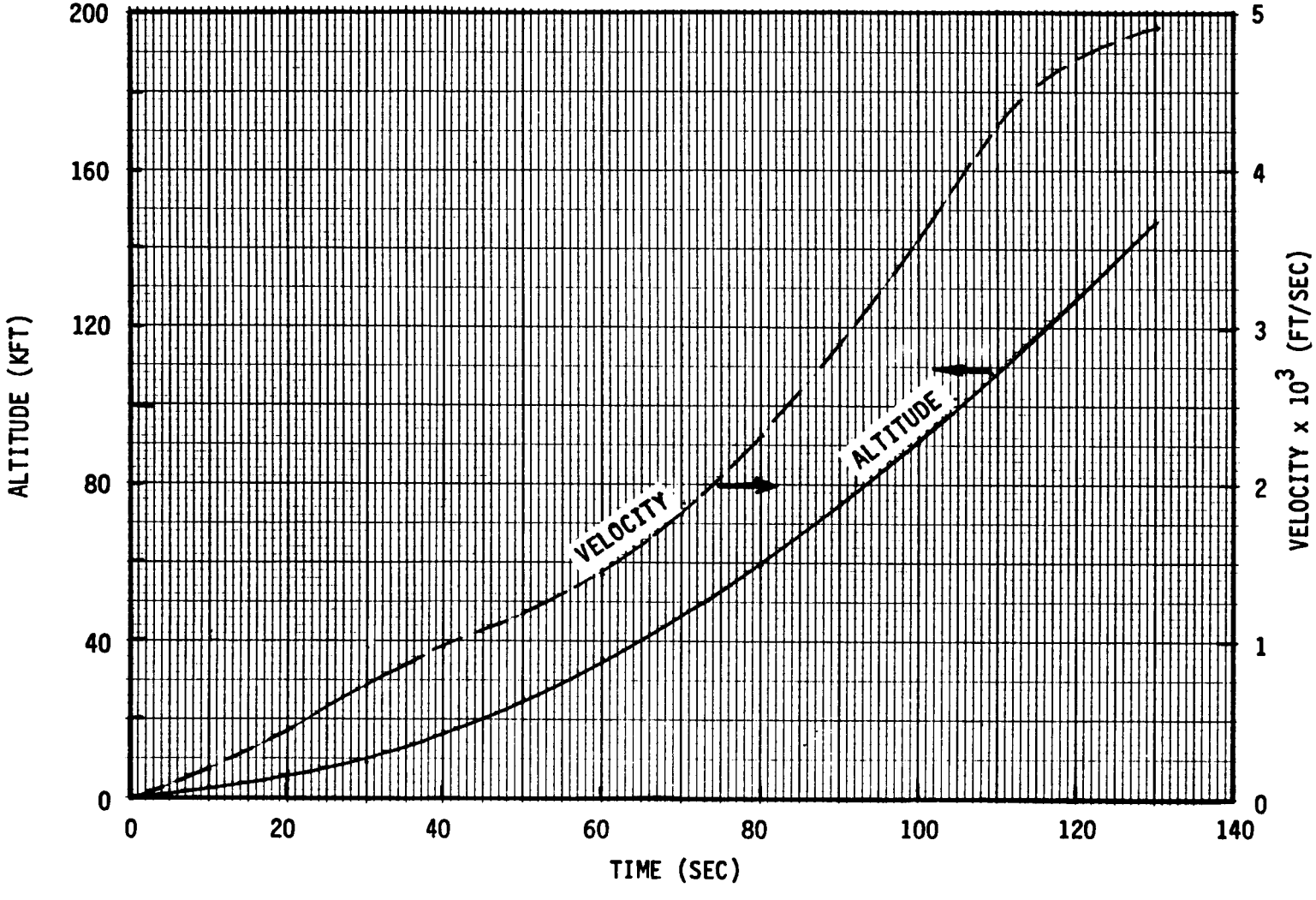

Fig. 9 Altitude/Velocity Profiles from the 1980 BRM 3A 3β Dispersed LWT Design Trajectory

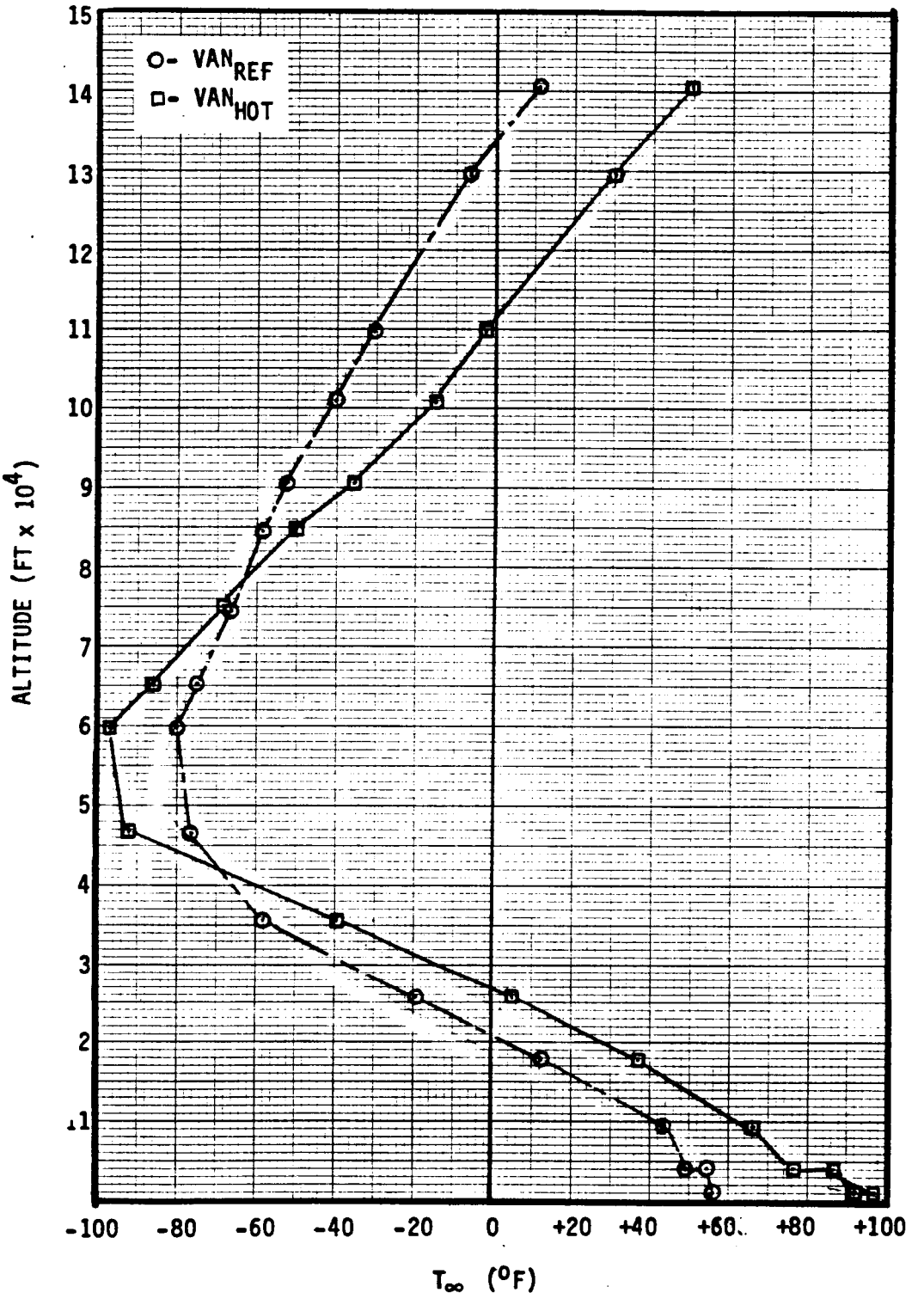

Fig. 10 Comparison between the Vandenburg Hot and Vandenburg Reference Atmospheres

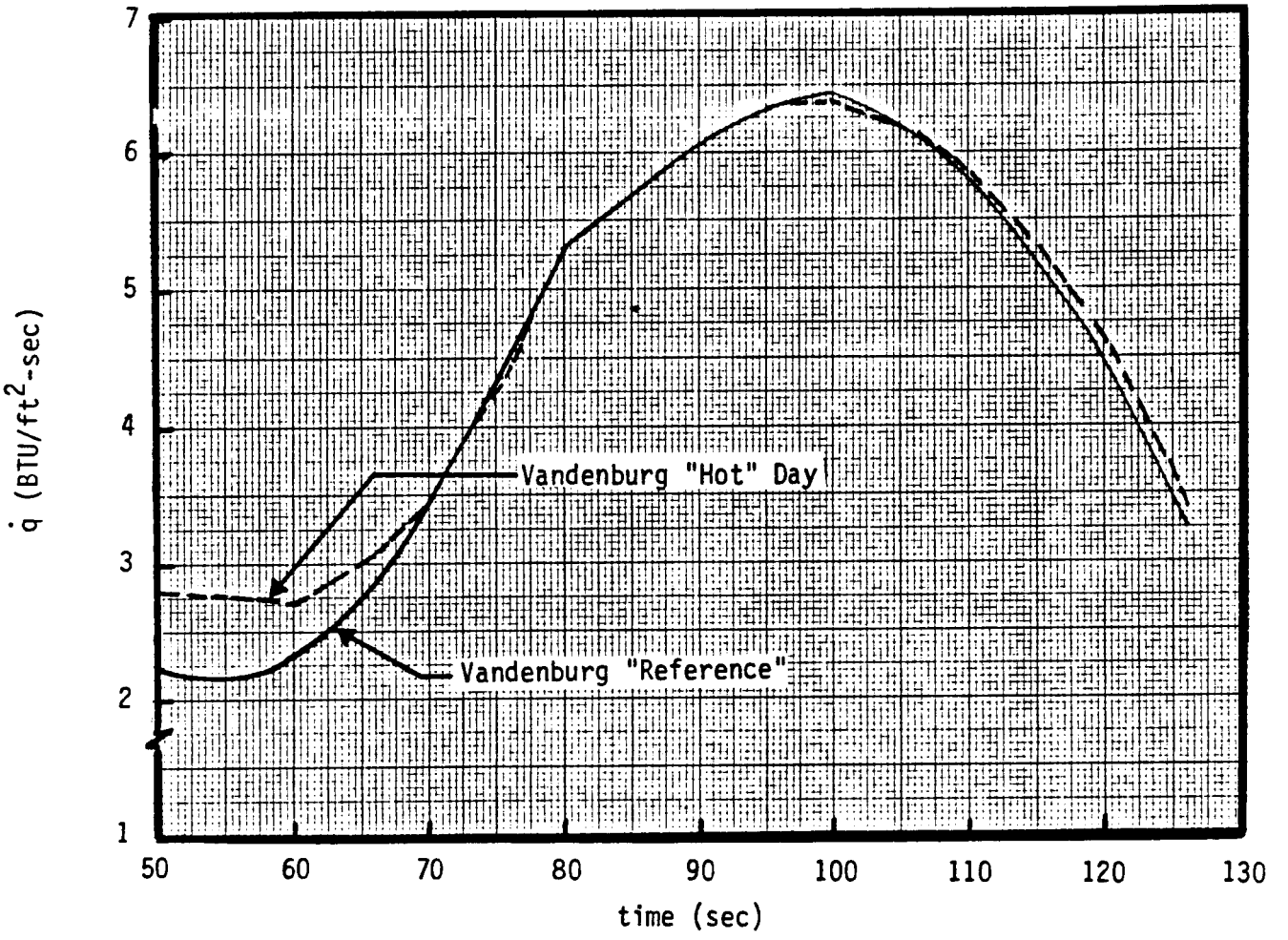

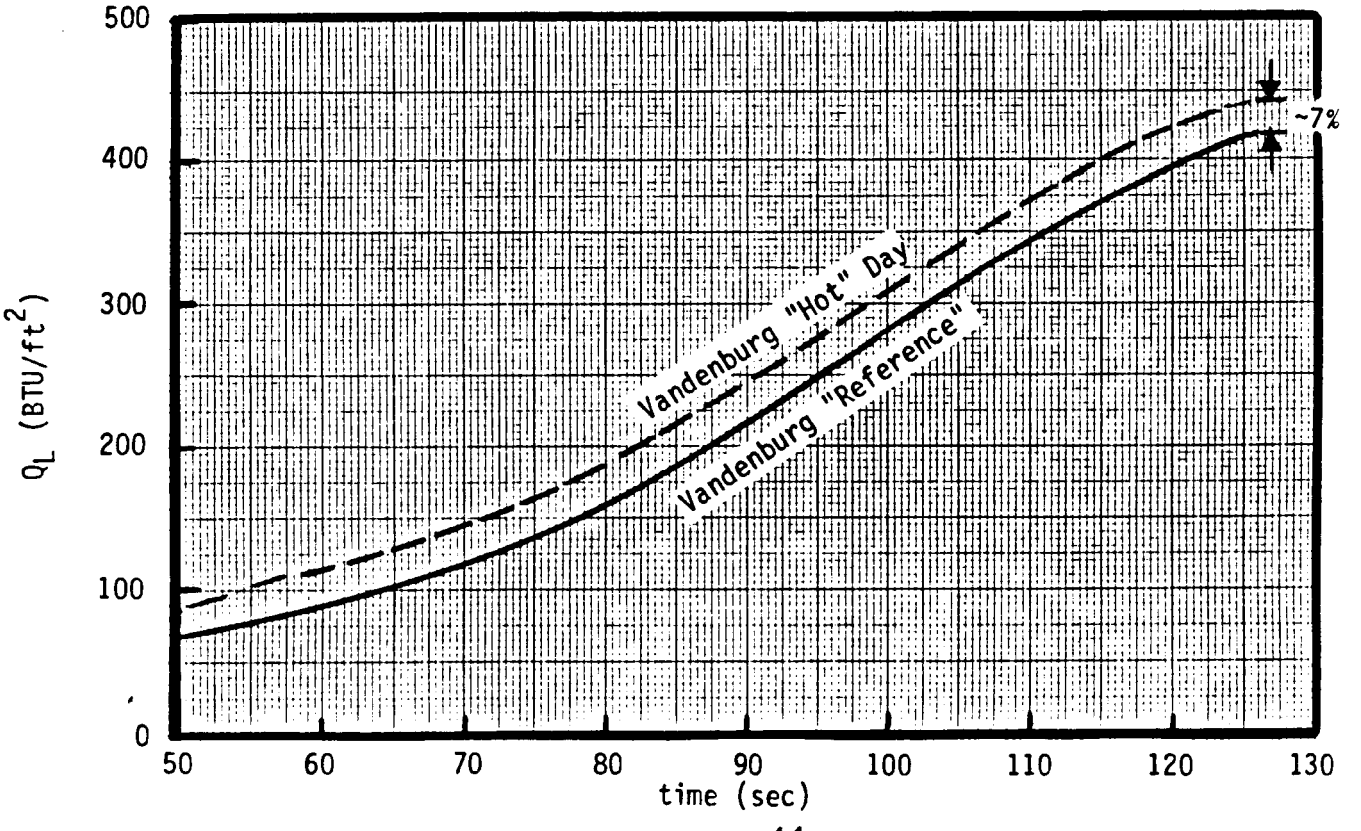

Fig. 11 Effect of Temperature Profiles on SRB Nose Cone Environments

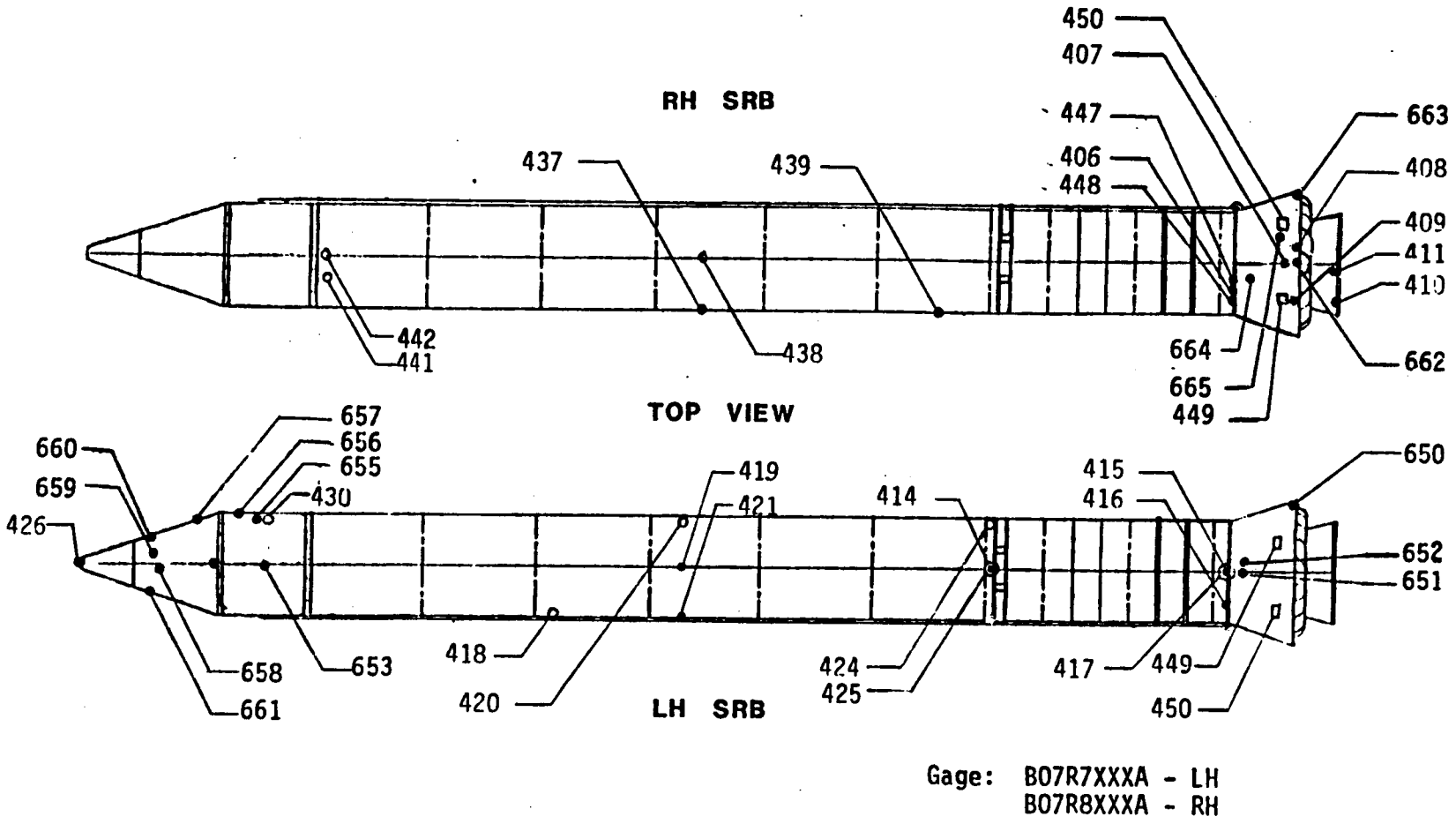

Fig. 12 SRB Ascent Calorimeter Locations

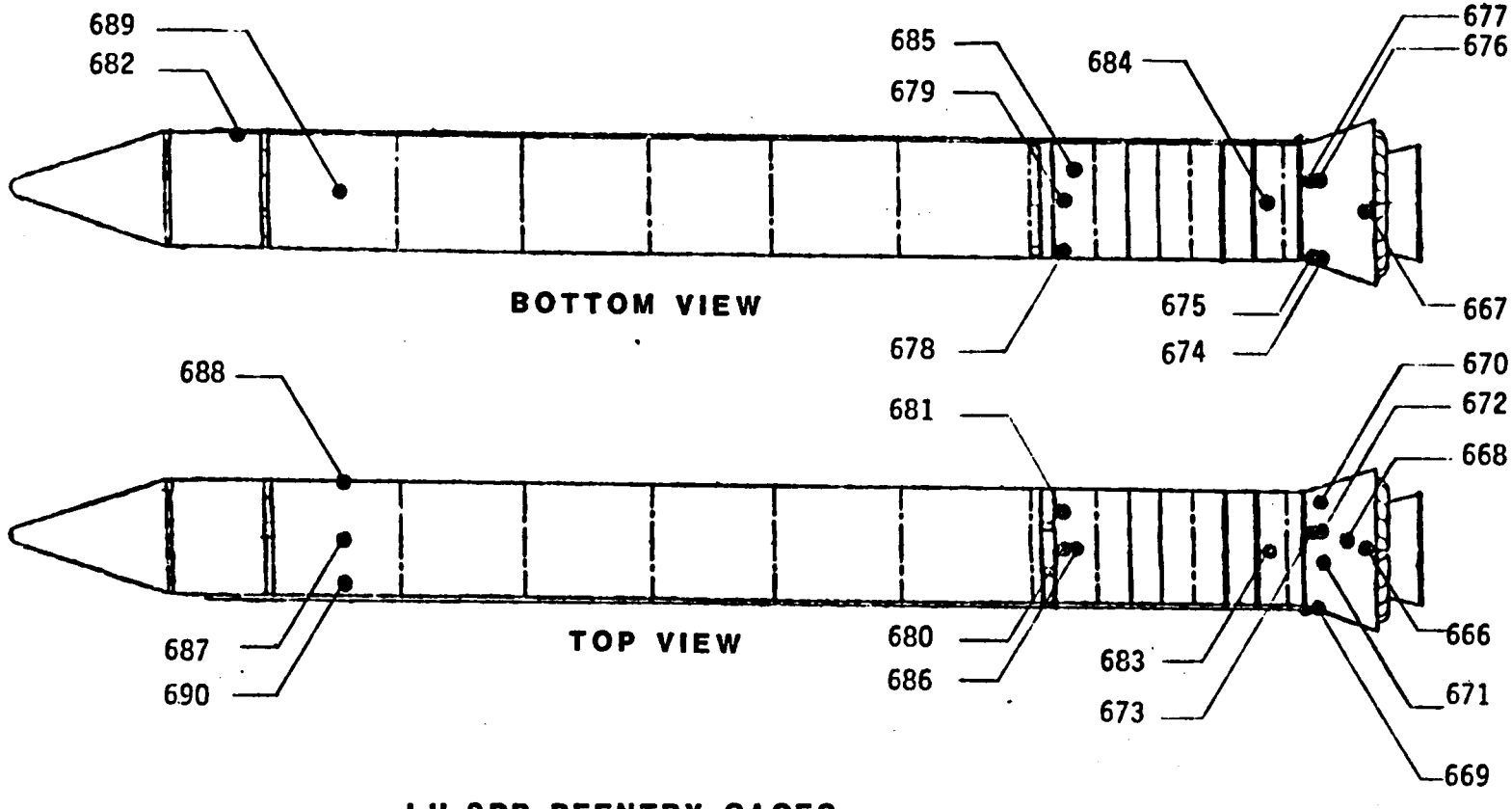

Fig. 13 SRB Reentry Calorimeter Locations

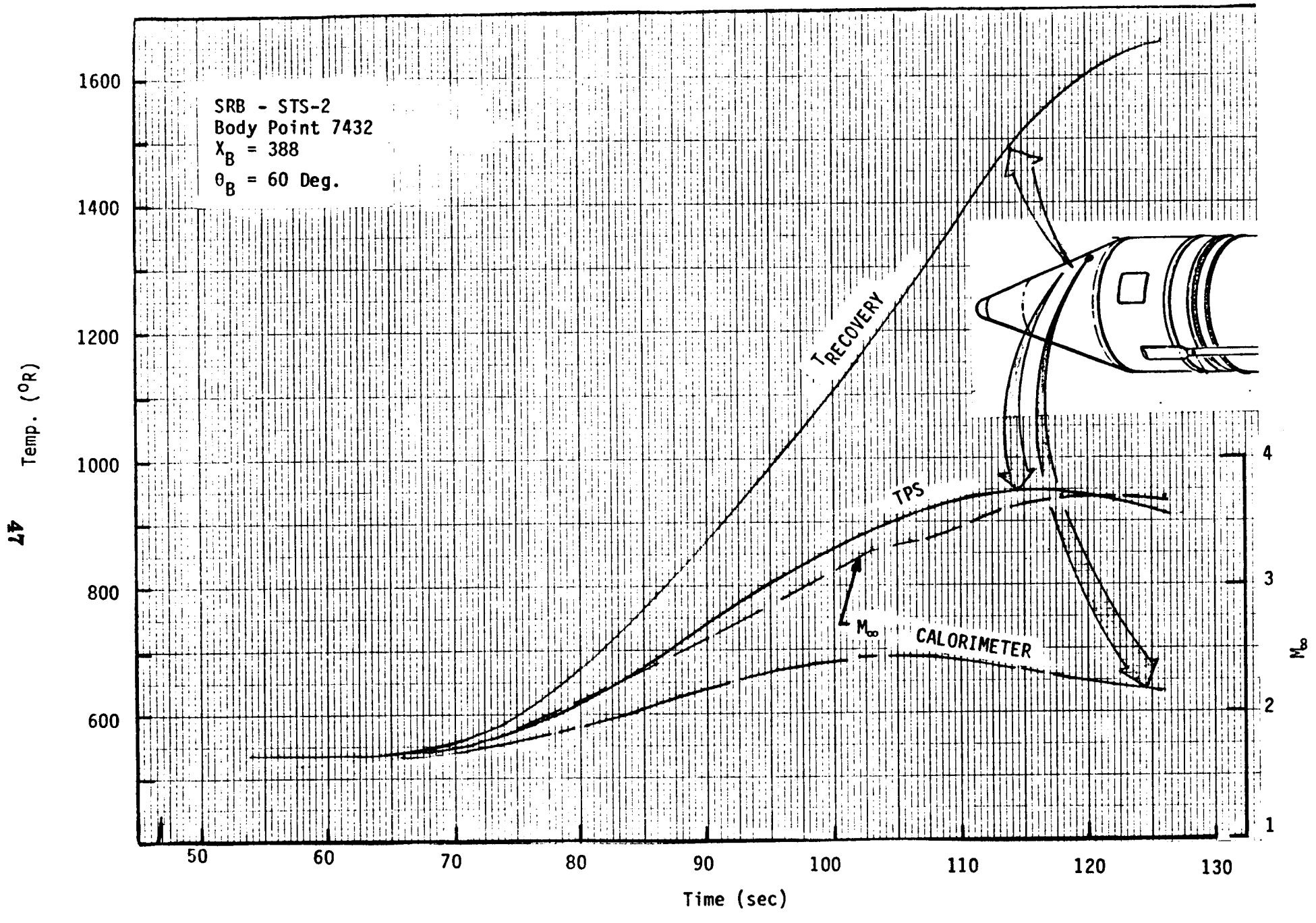

(a) SRB

Fig. 14 Typical SRB TPS/Calorimeter Temperature Differences

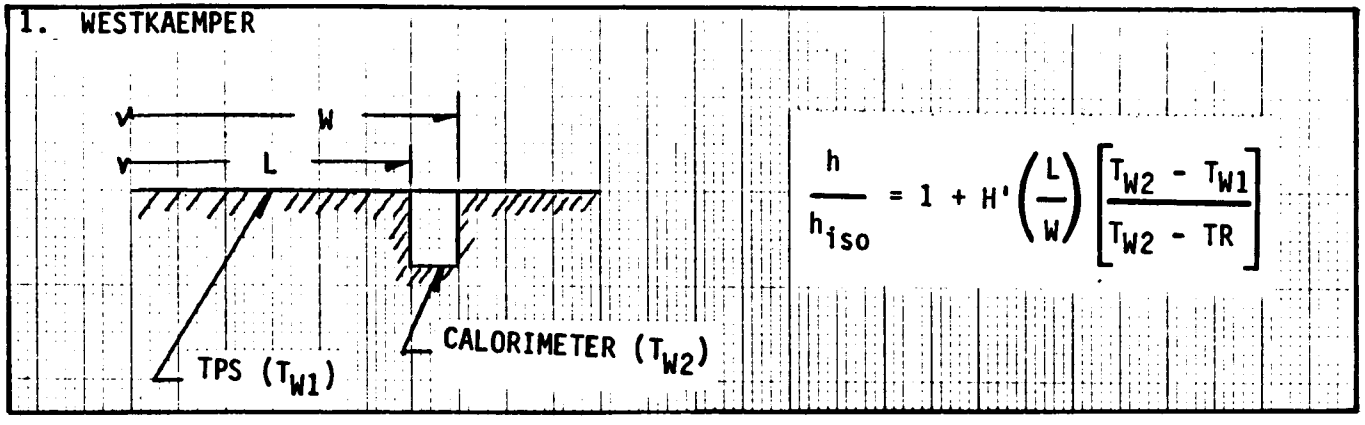

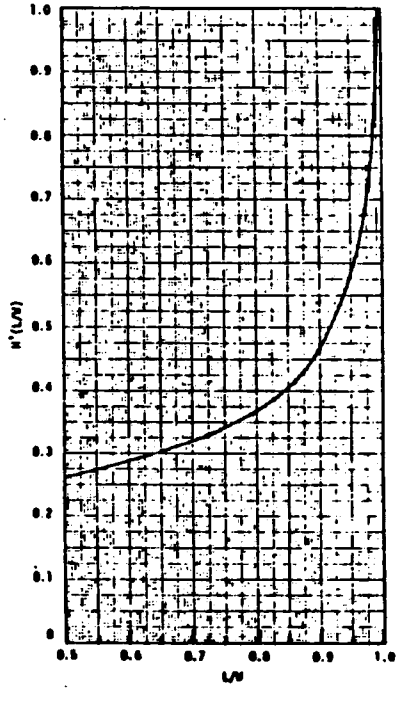

Numerical Values Of
$H'(L/W)$ - Westkaemper

Fig. 15 Definition of Variables for Temperature Discontiniuty Correction

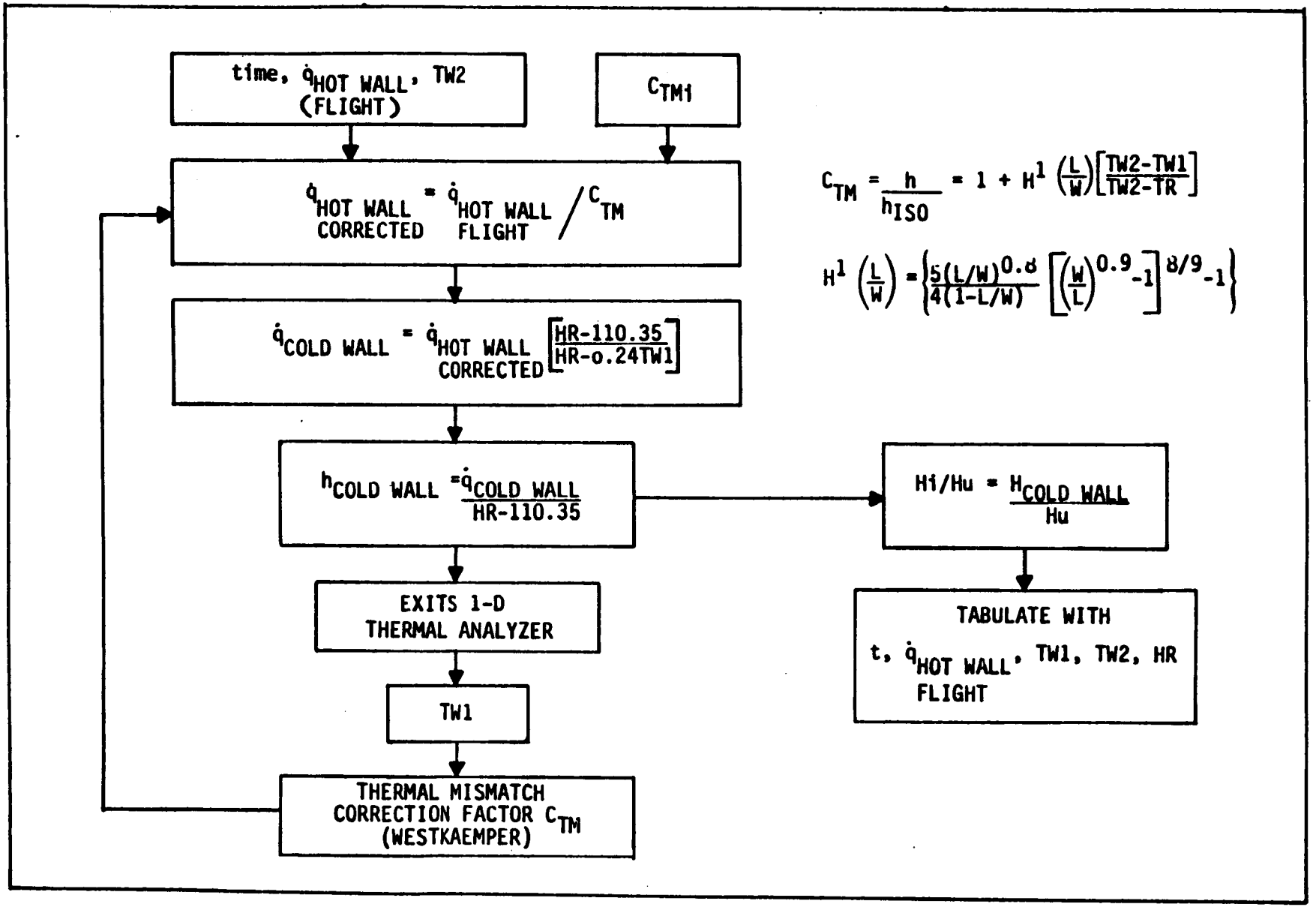

Fig. 16 Thermal Mismatch Correction Methodology

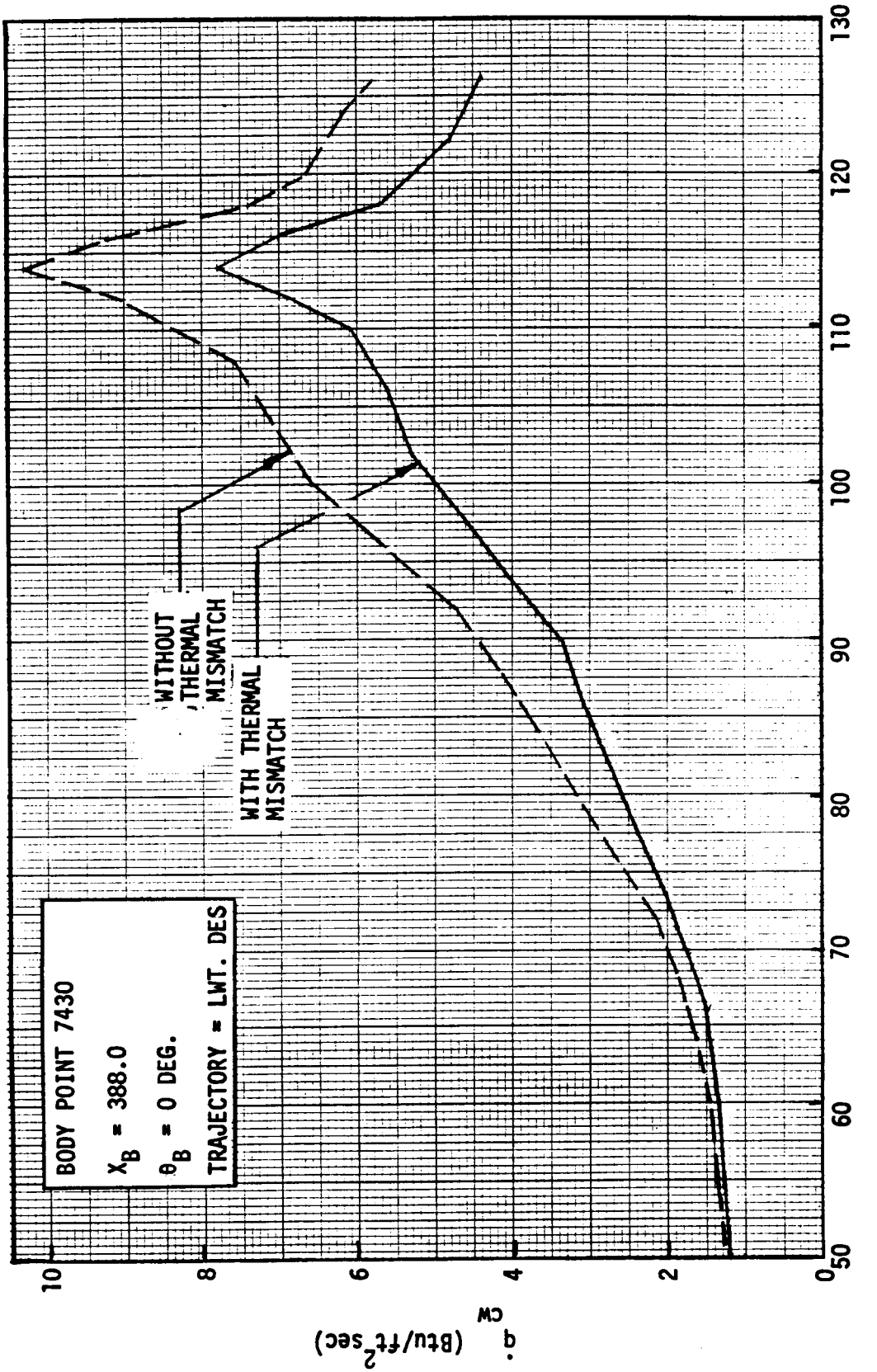

Fig. 17 Effect Of Thermal Mismatch Correction On Cold Wall Heating

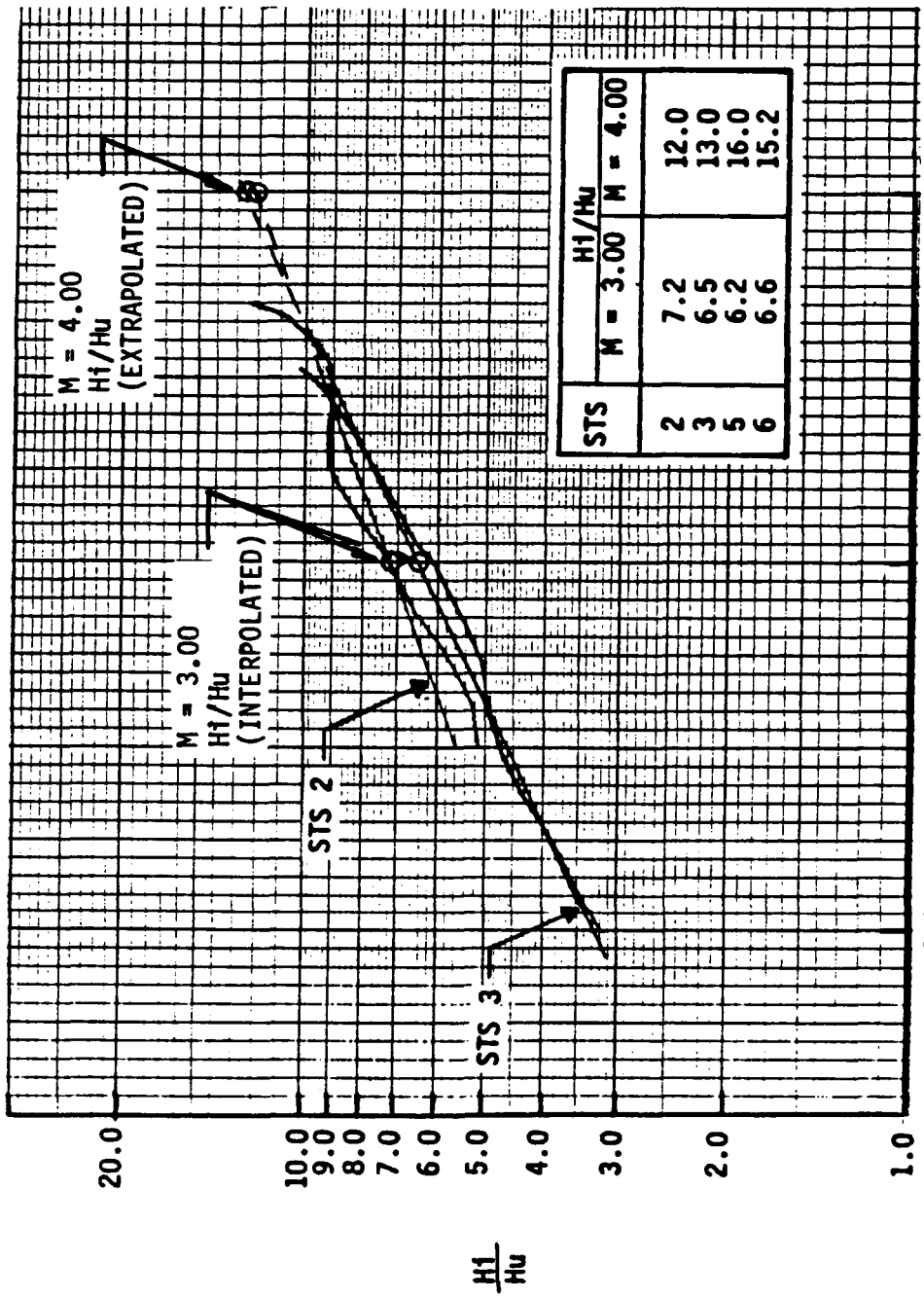

Fig. 18 Flight Hi/Hu Determination at M_∞ = 3 and 4 for BP 7414

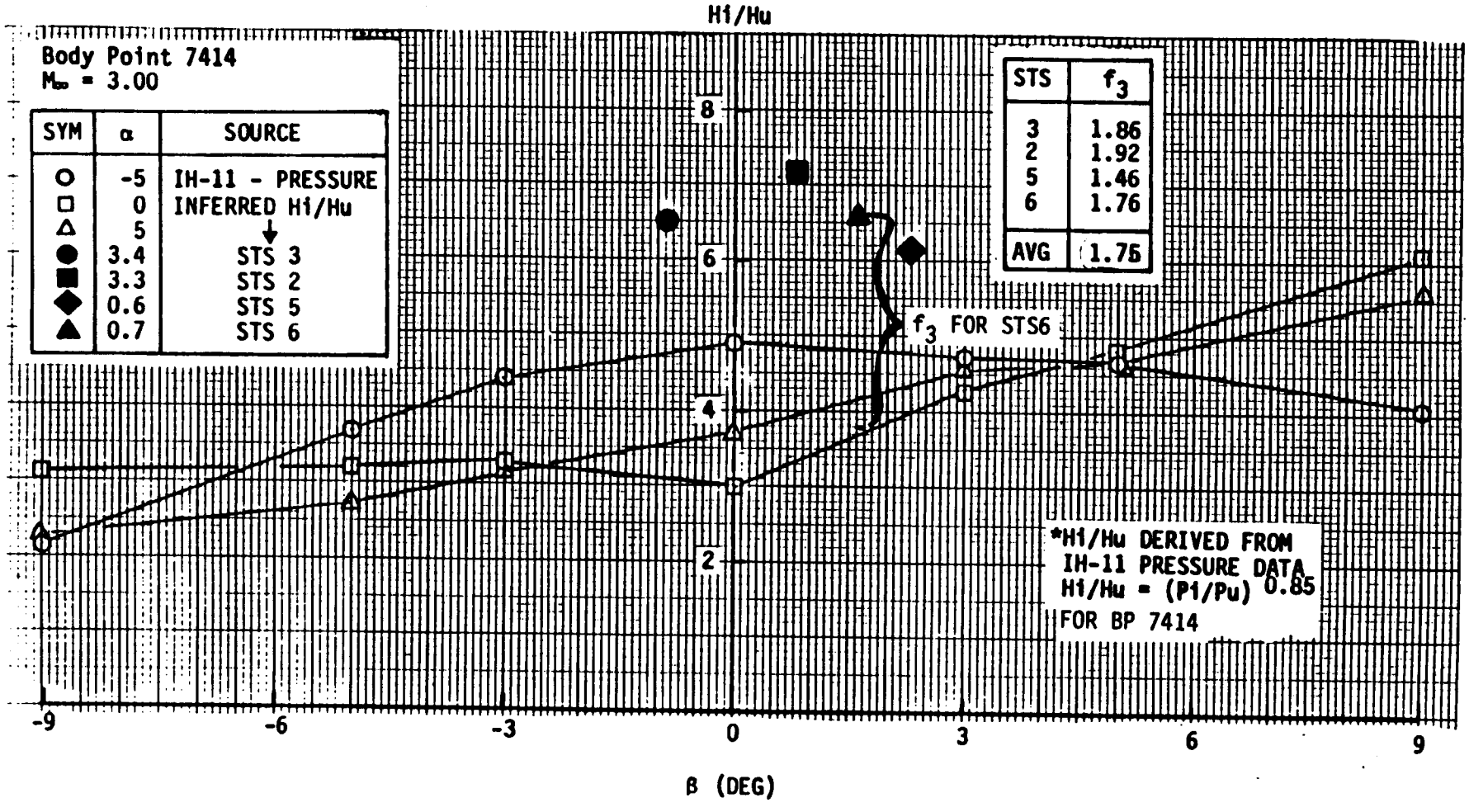

a) M = 3.00

Fig. 19 Wind Tunnel Hi/Hu Data Base and Flight Factor (f_3) Determination for BP 7414

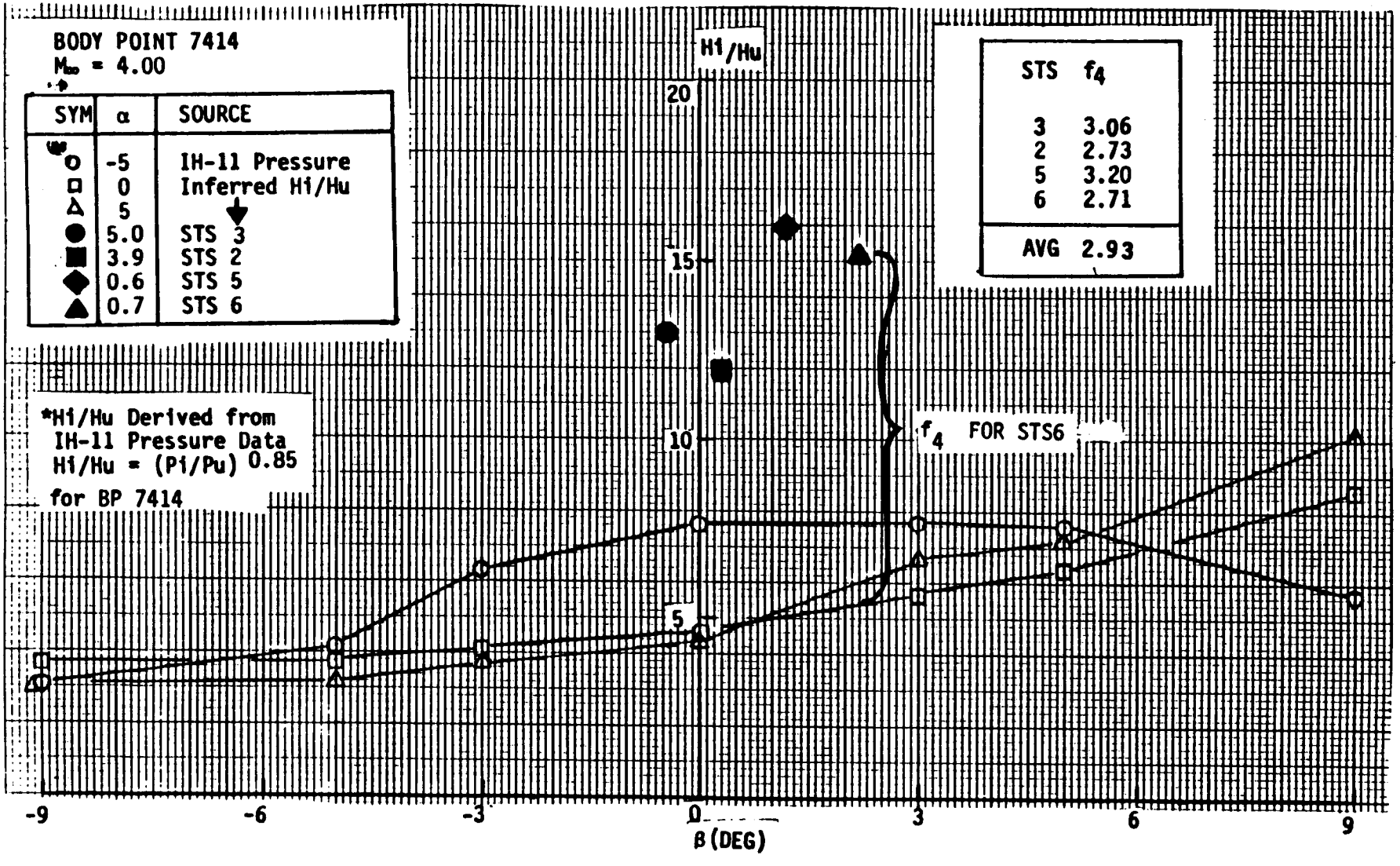

b) M = 4.00

Fig. 19 Wind Tunnel Hi/Hu Data Base and Flight (f_4) Determination for BP 7414

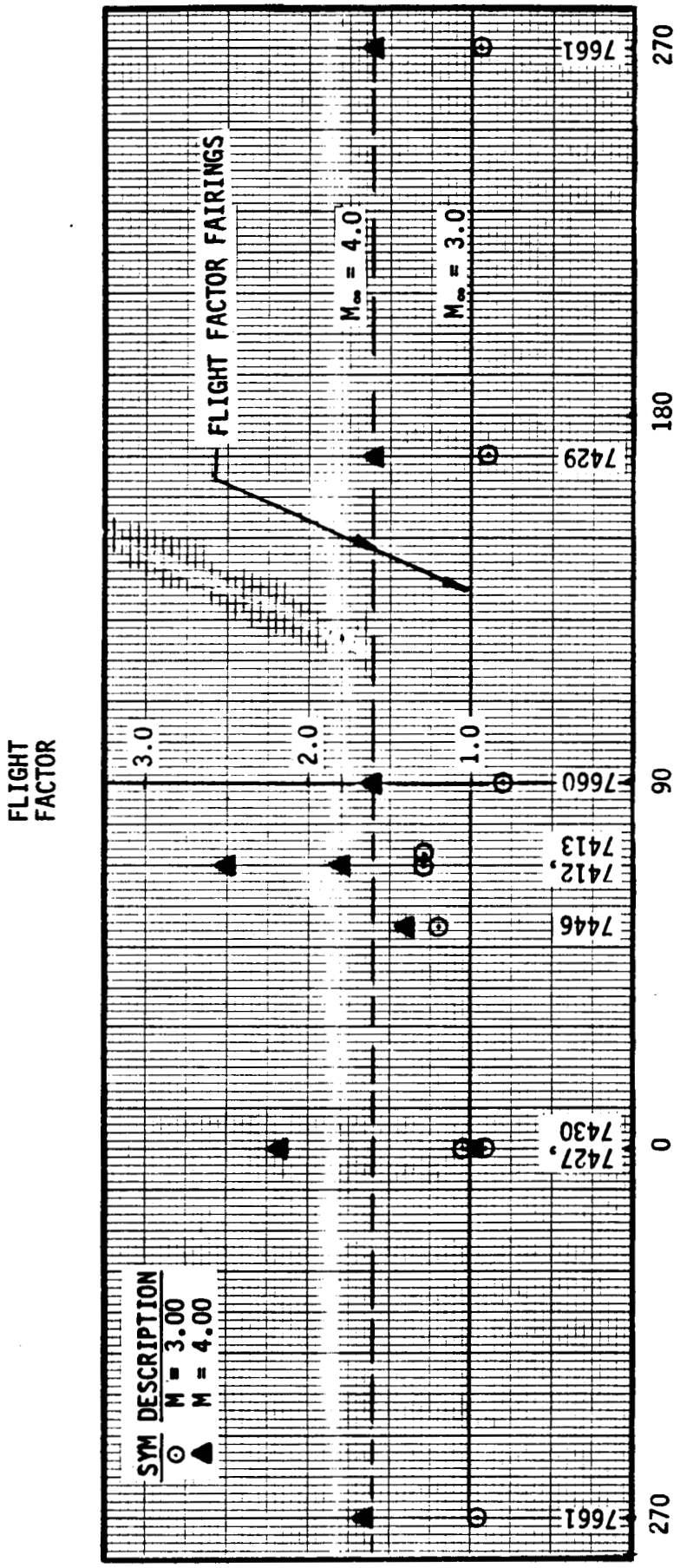

Fig. 20 DFI Flight Factor Summary - SRB Nose Cone (Zone 2)

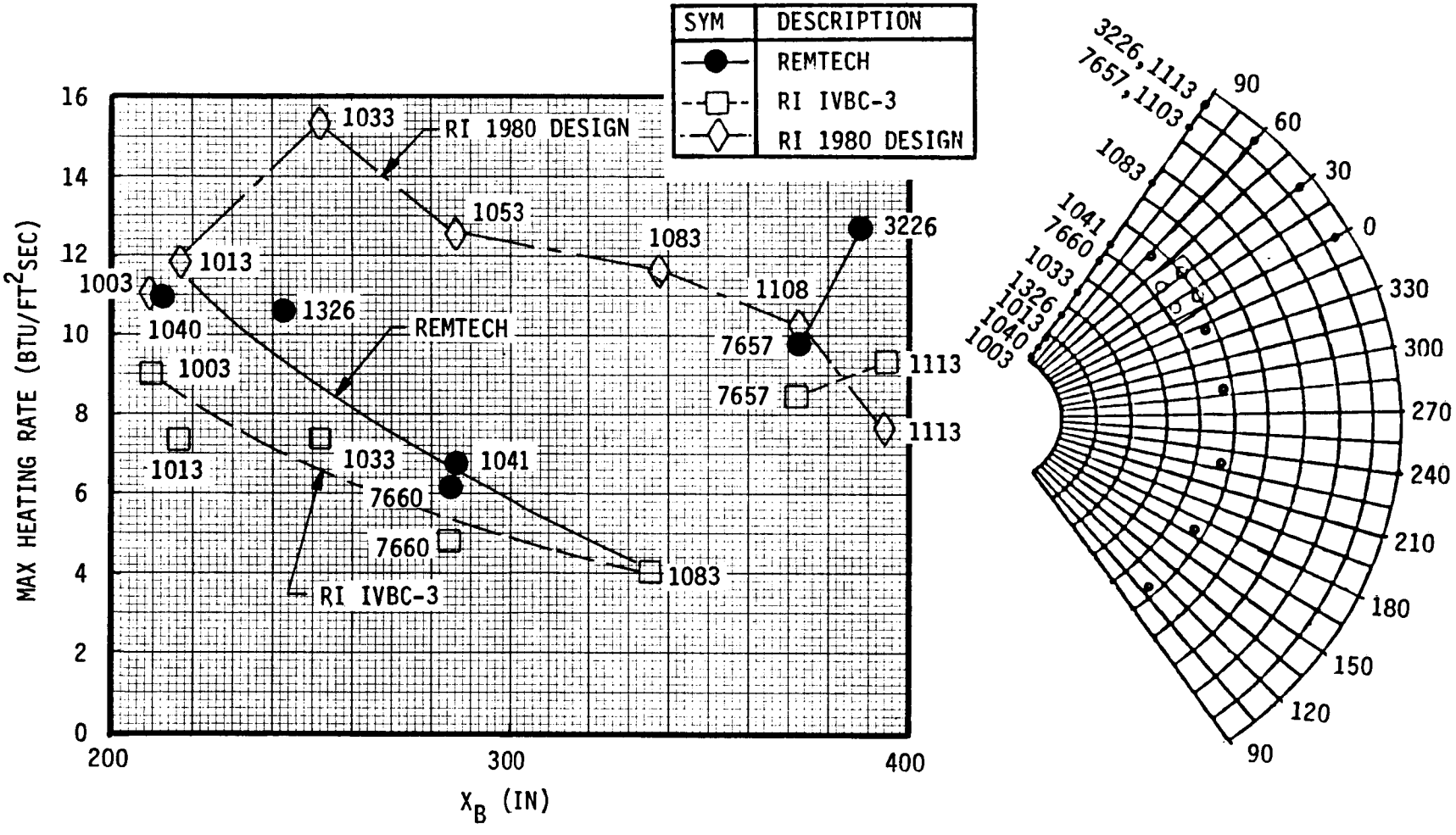

a) Max Heating Rate

Fig. 21 SRB Nose Cone Environemnts (θ_B = 90 Deg. Axial Distribution)

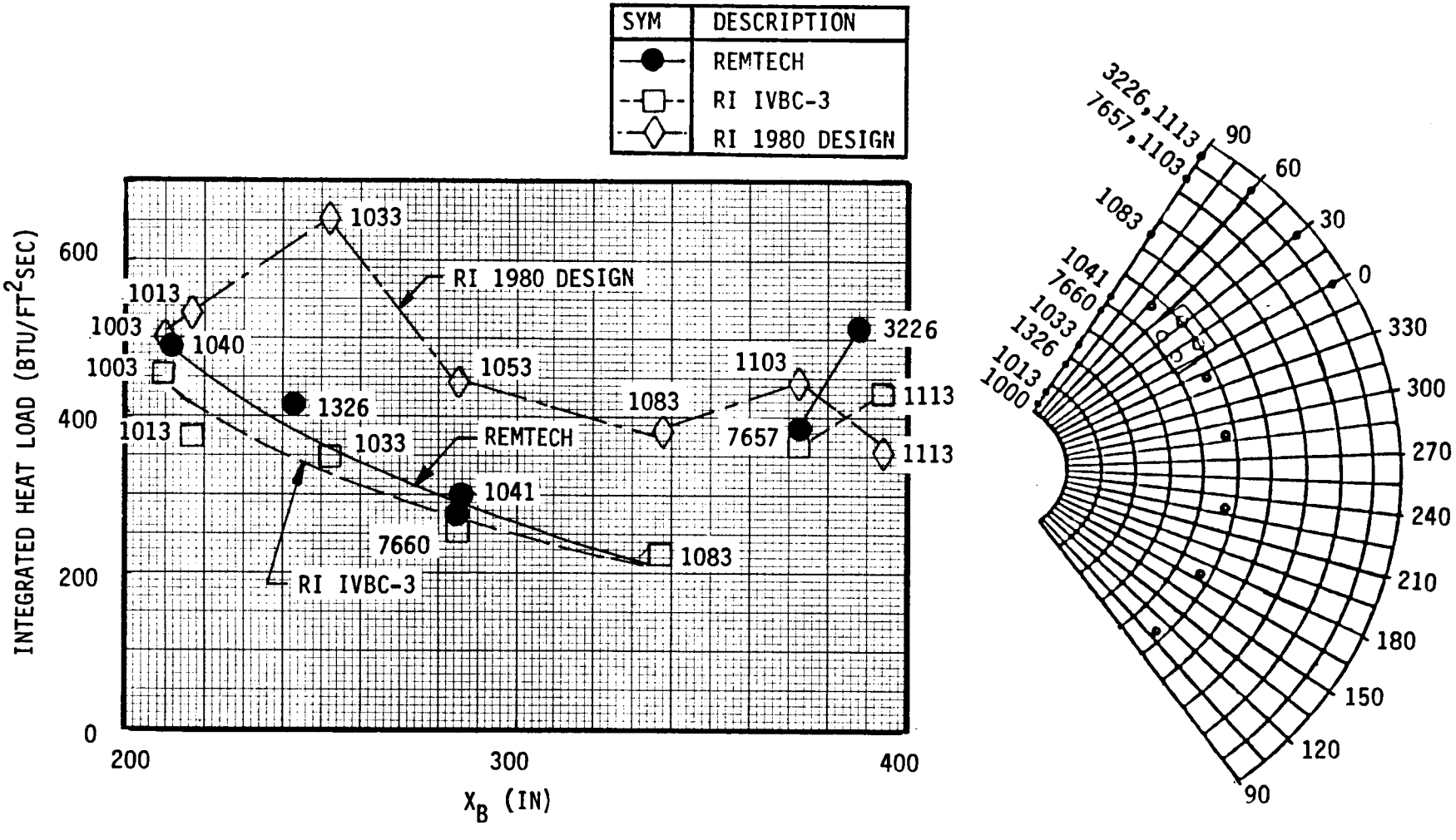

b) Integrated Heat Load

Fig. 21 (Concluded)

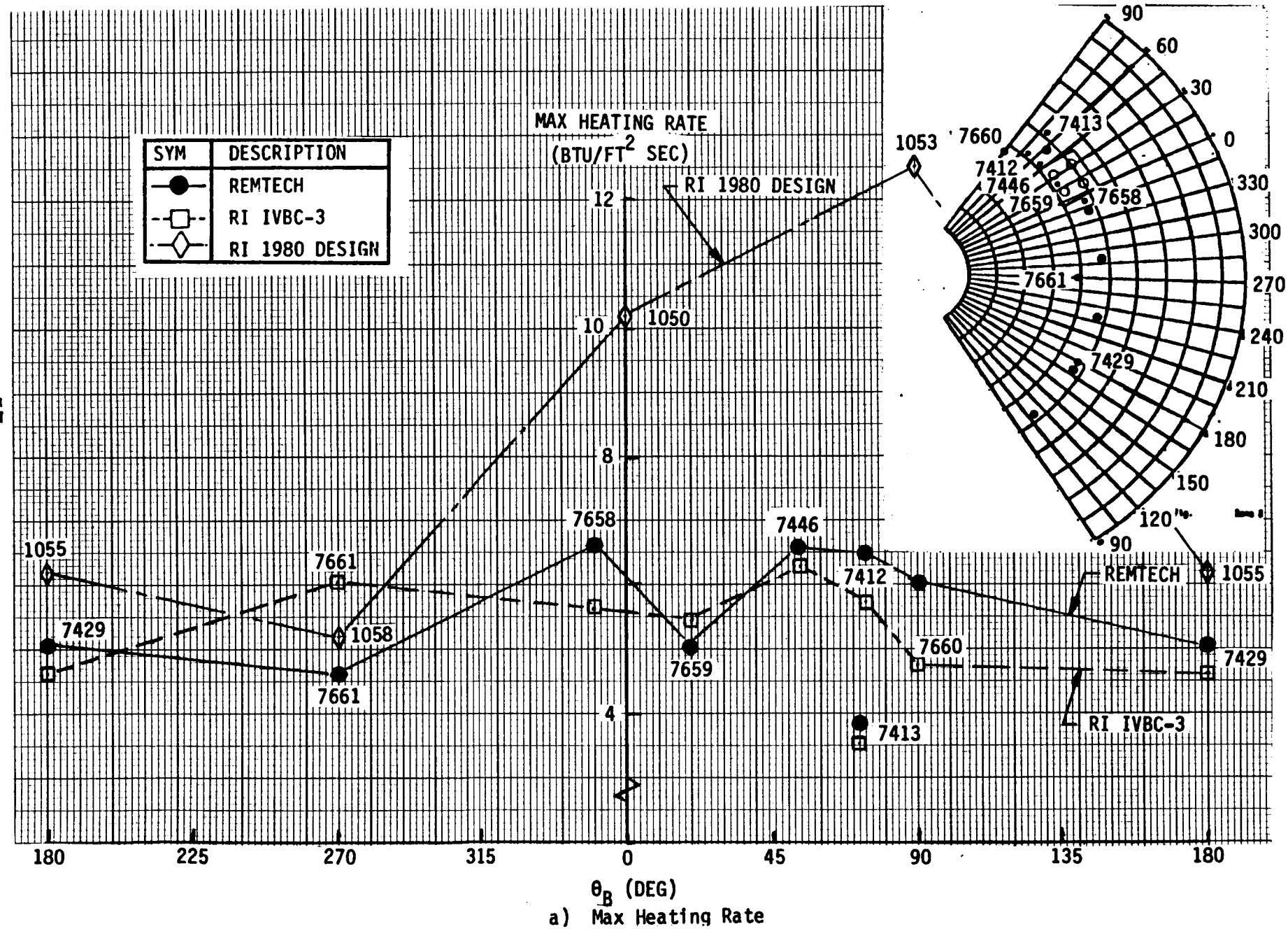

a) Max Heating Rate

Fig. 22 SRB Nose Cone Environment (Circumferential Distribution)

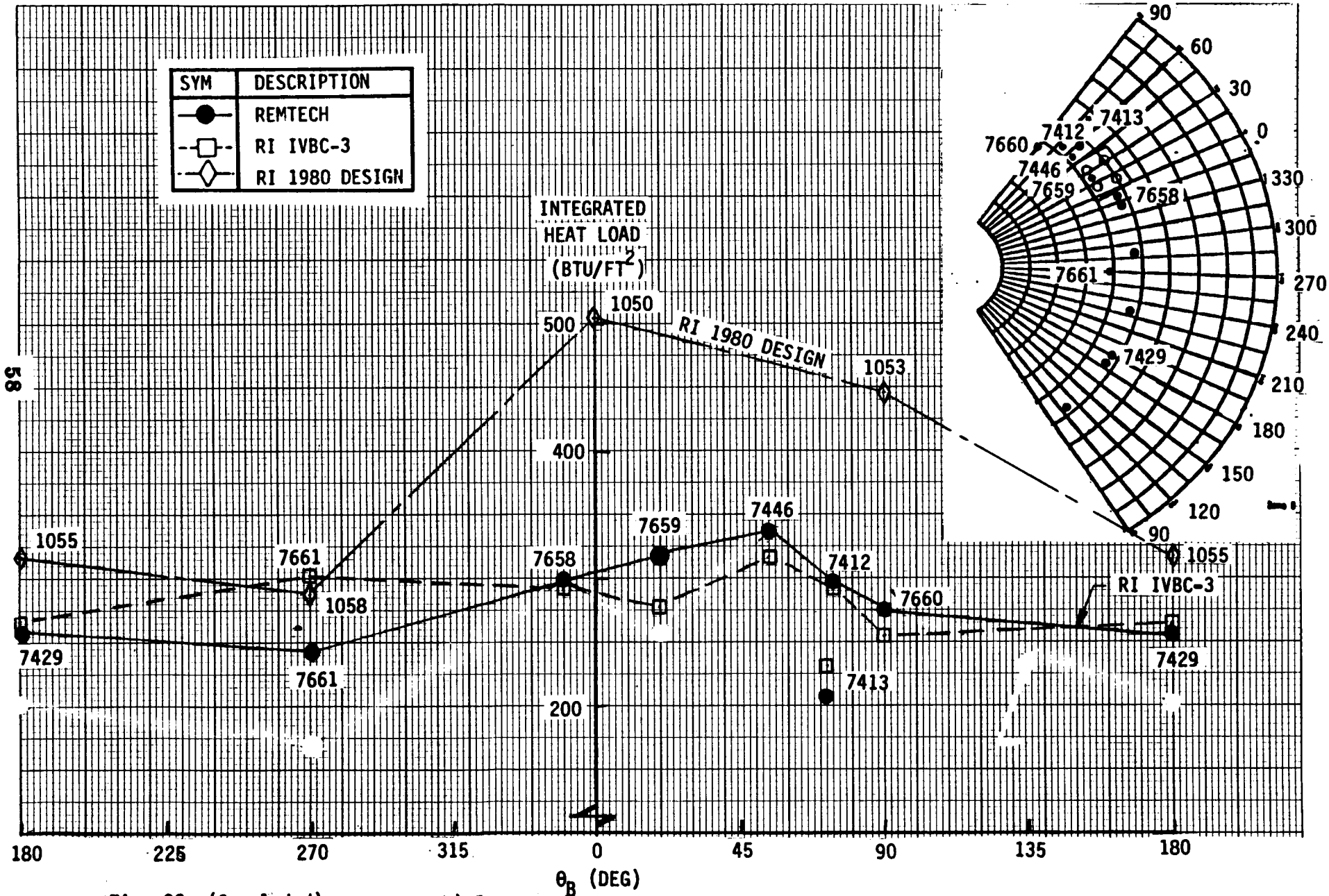

Fig. 22 (Concluded) b) Integrated Heat Load

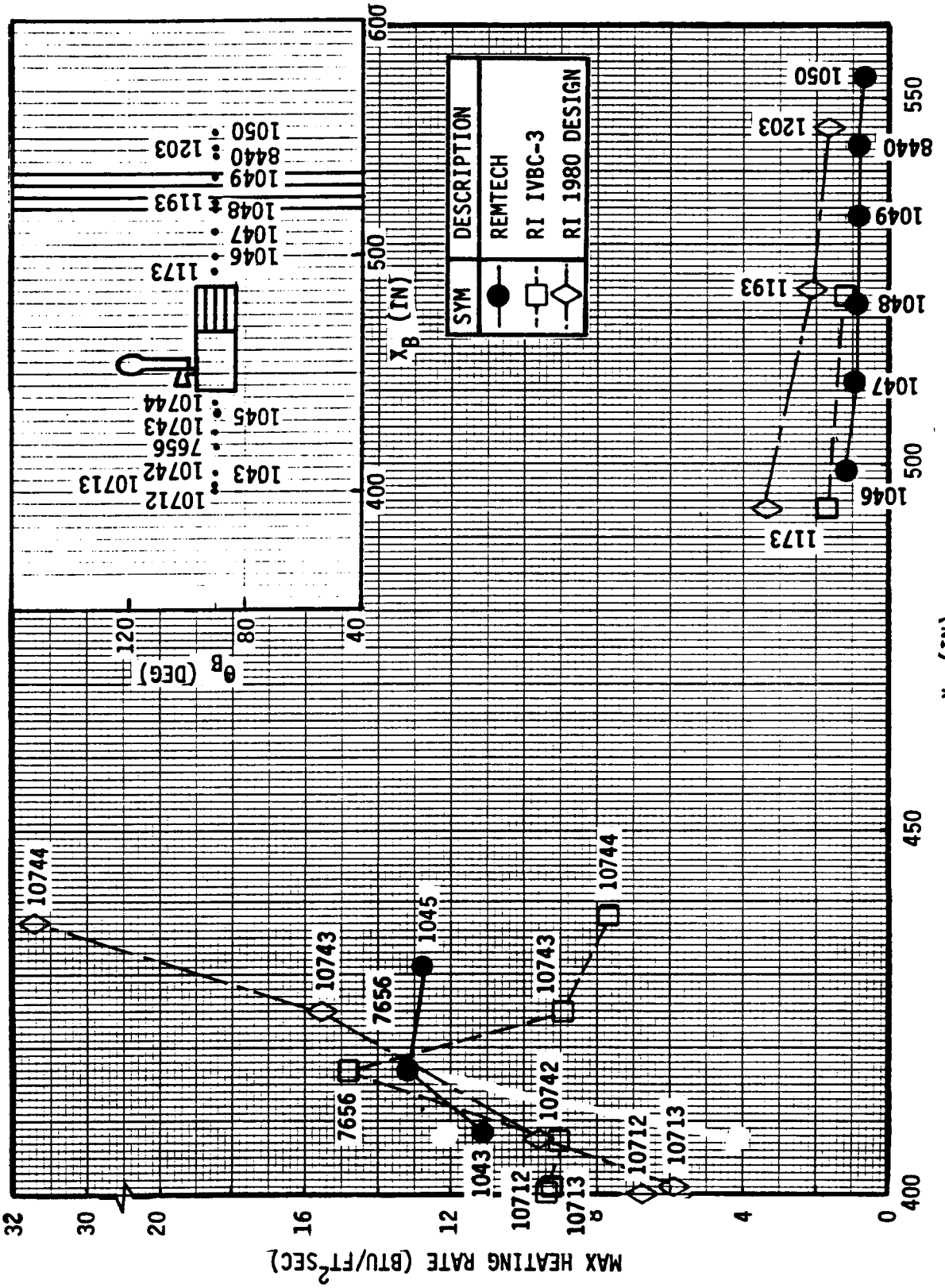

Fig. 23 SRB/ET FWD Attach Area Environments ($\theta_B = 90^0$)
a) Maximum Heating Rate

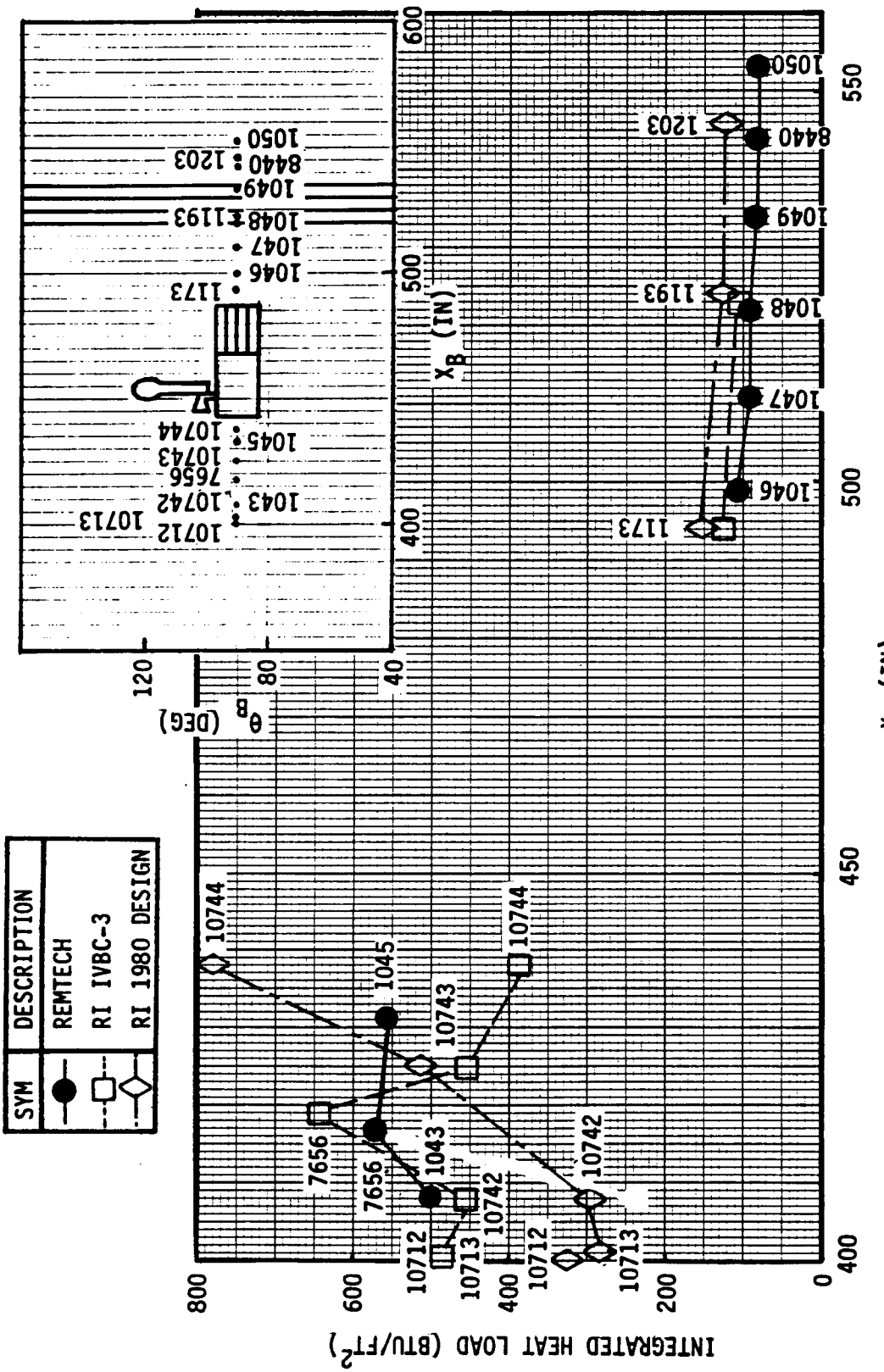

b) Integrated Heat Load

Fig. 23 (Concluded)

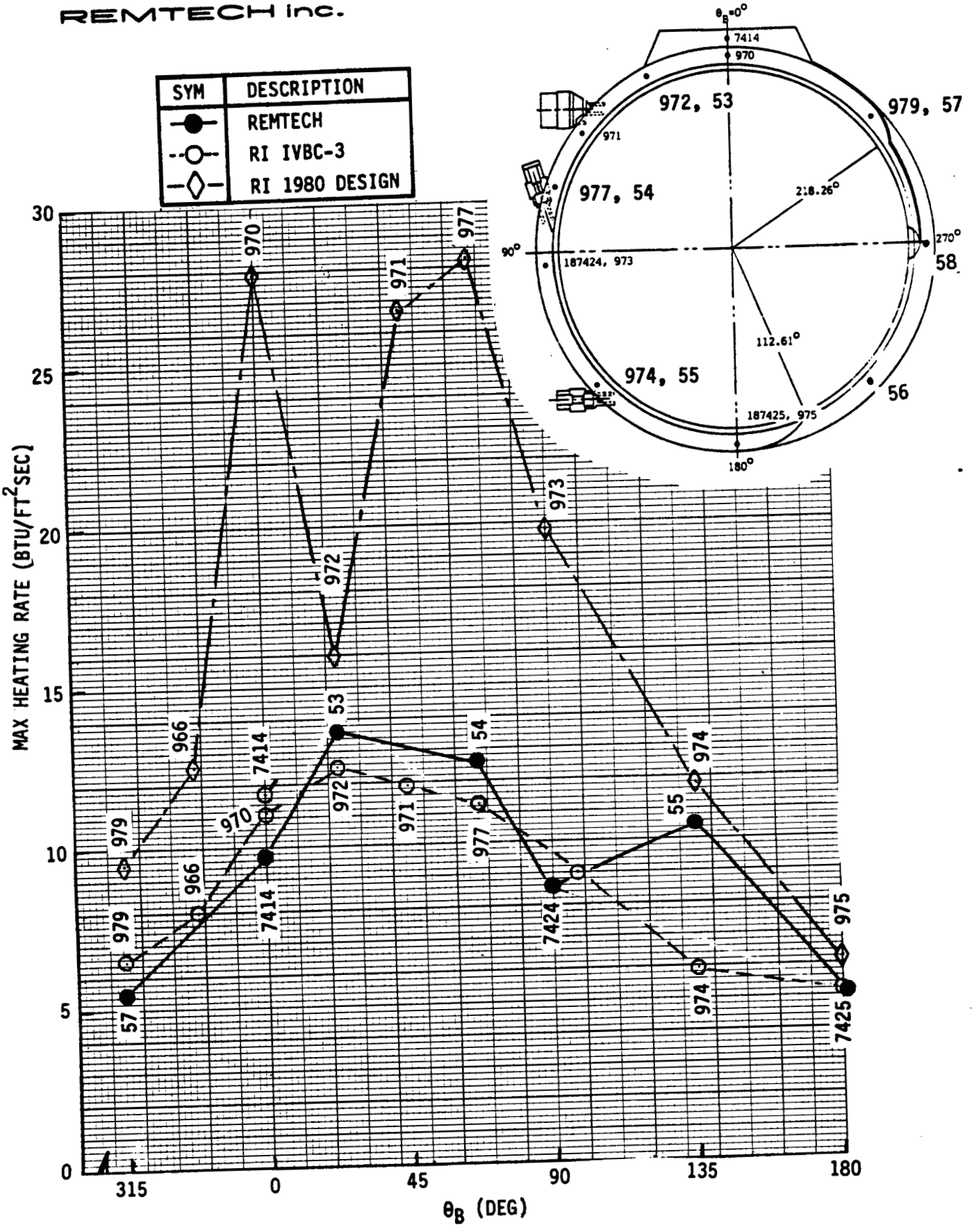

a) Maximum Heating Rate

Fig. 24 Attach Ring Environments (Forward Face)

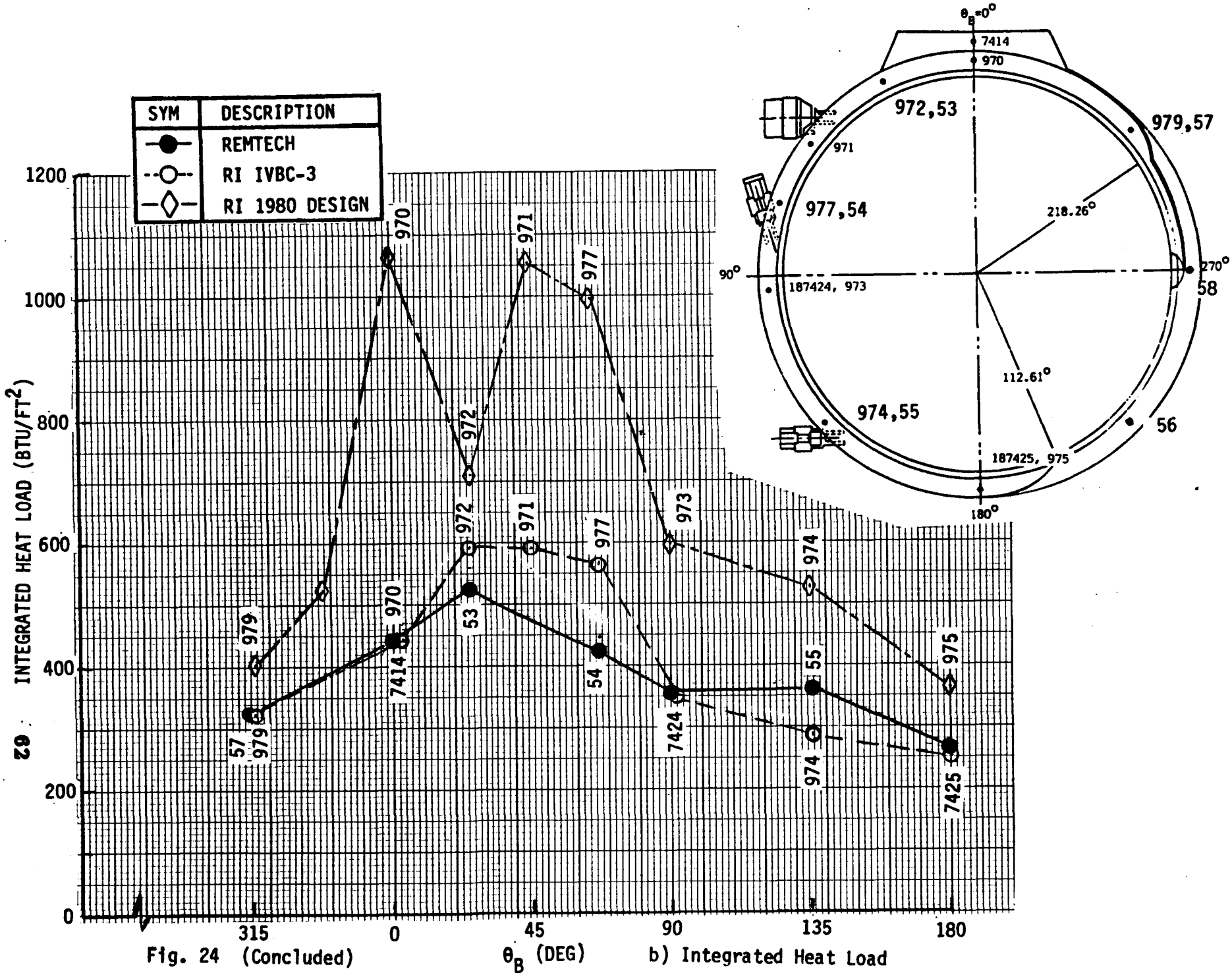

Fig. 24 (Concluded) b) Integrated Heat Load

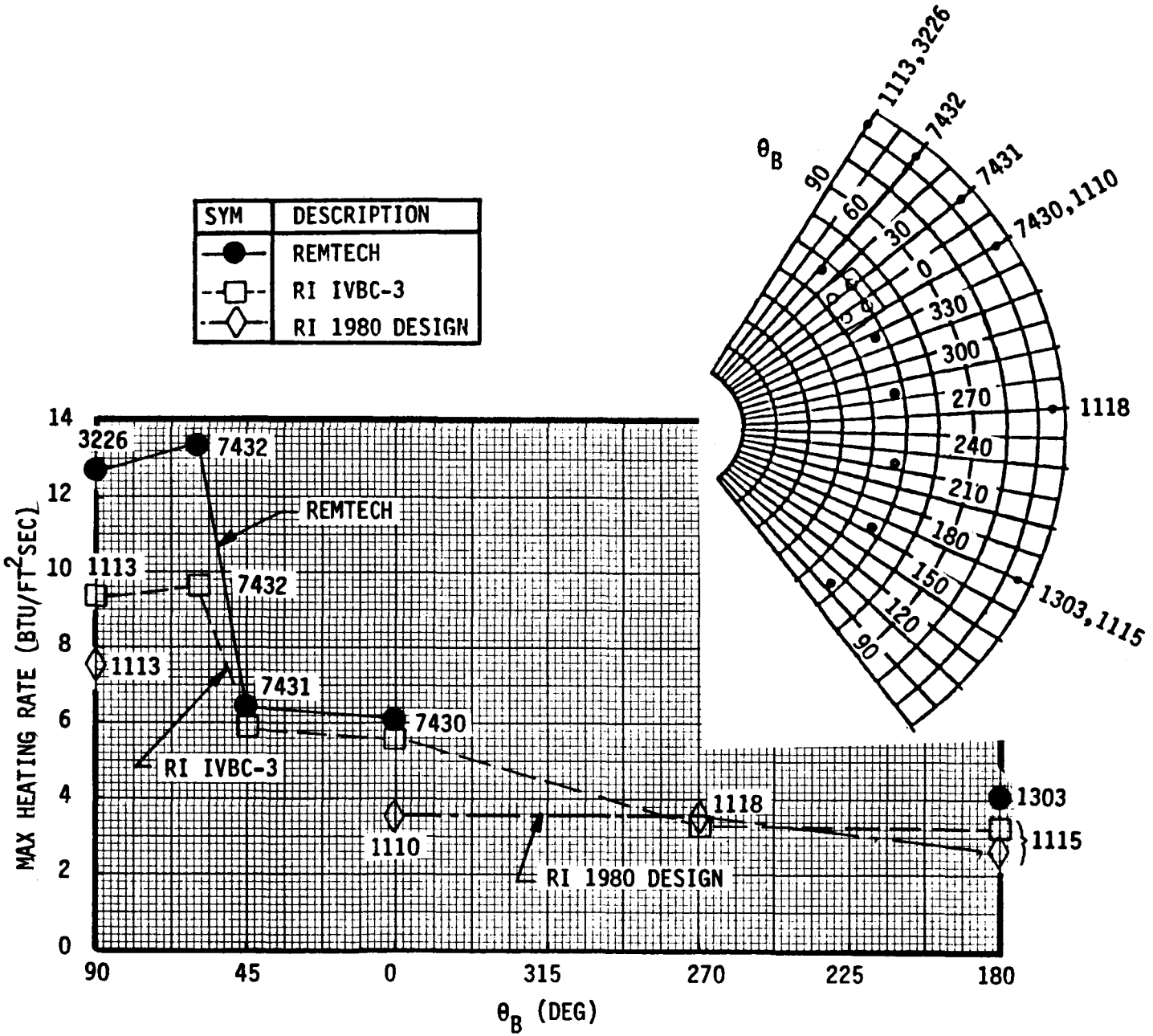

a) Maximum Heating Rate

Fig. 25 SRB Reflected Shock Impingement Area Environments

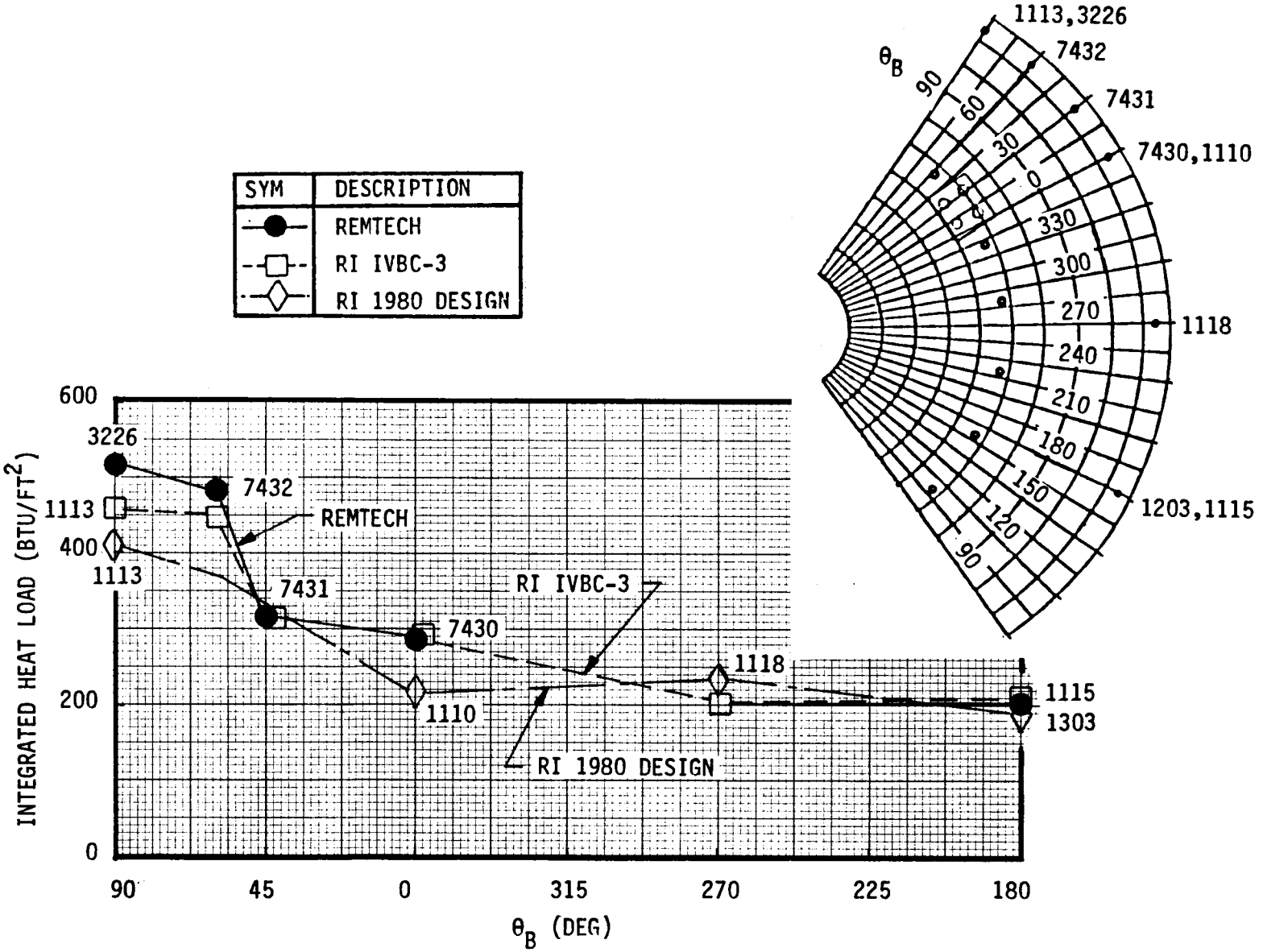

b) Integrated Heat Load

Fig. 25 (Concluded)

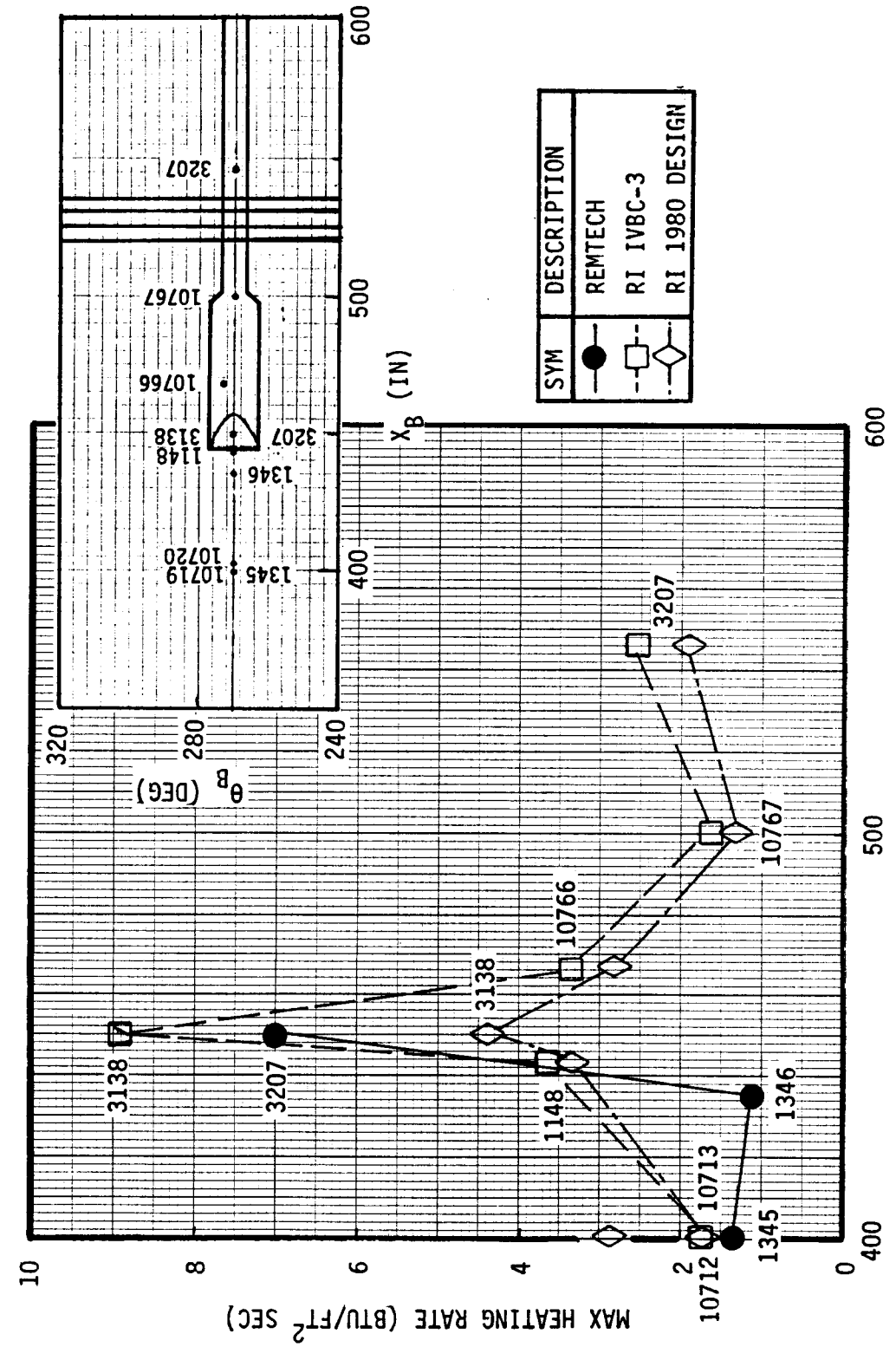

Fig. 26 Systems Tunnel Foreward Face Environments

a) Maximum Heating Rate

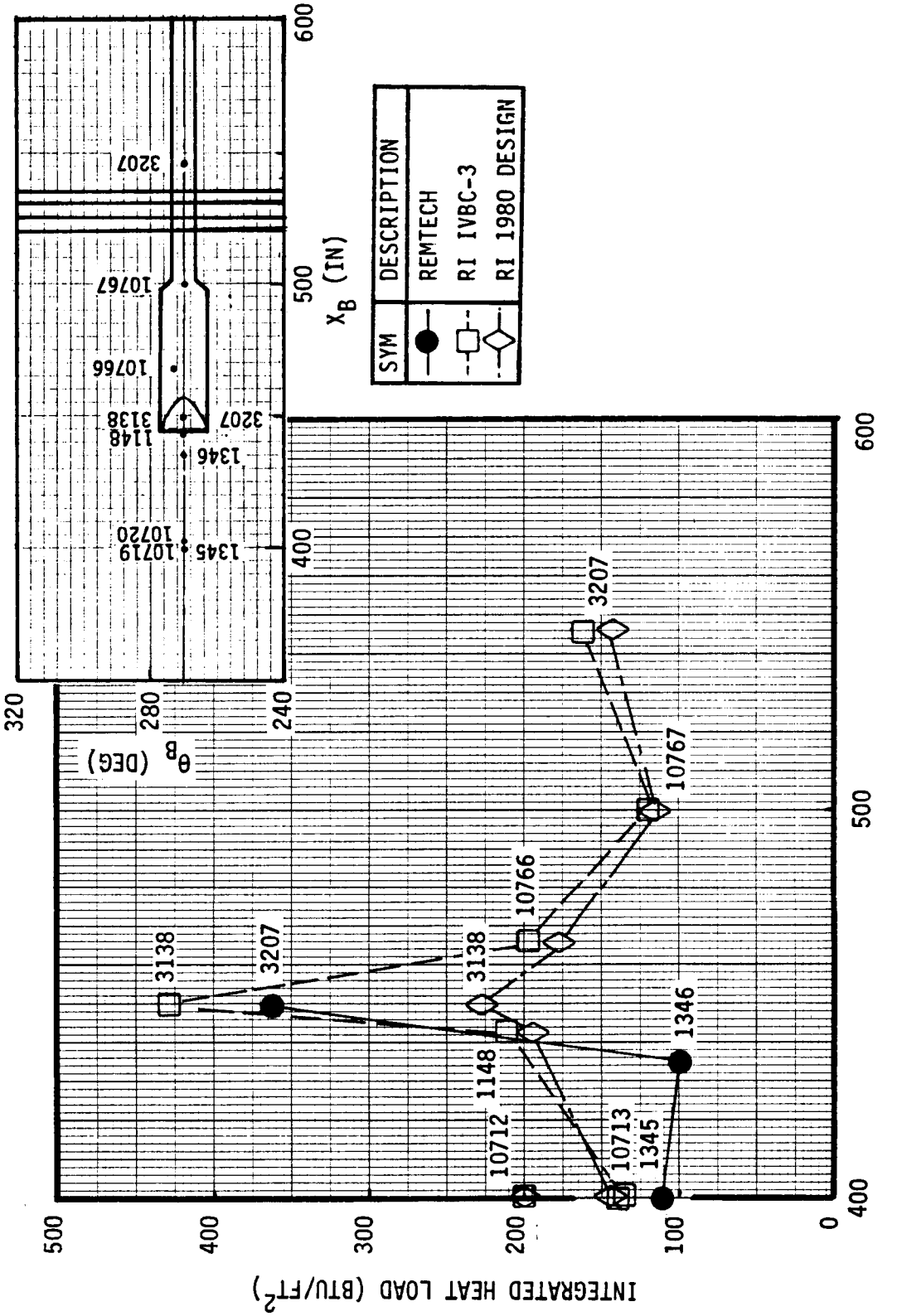

b) Integrated Heat Load

Fig. 26 (Concluded)

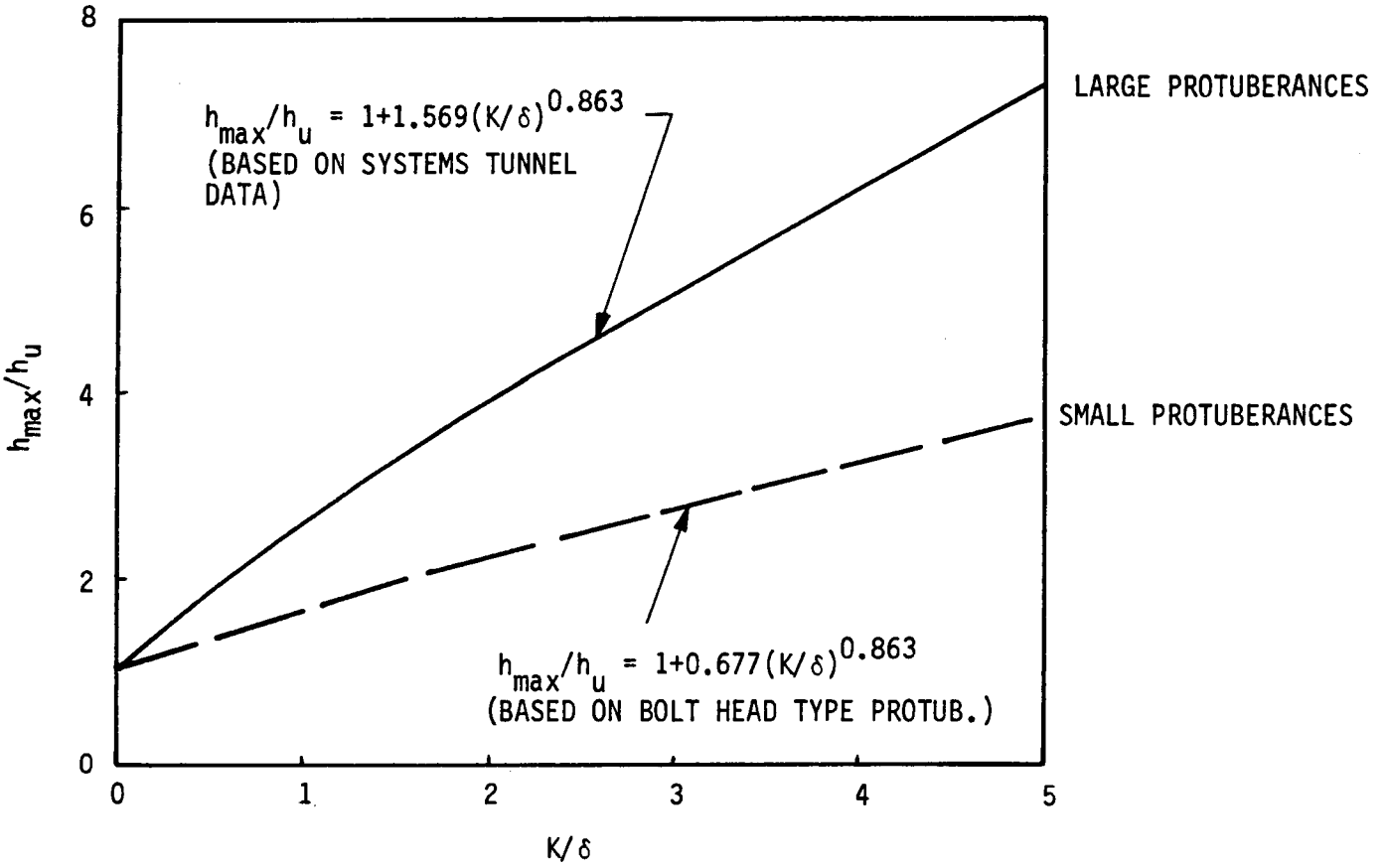

Fig. 27 Protuberance Heating Factor Curves

Table 1 SRB Body Point Definition

REMTECH			ROCKWELL			COMMENT
BODY POINT	X_B (In)	θ_B (Deg)	BODY POINT	X_B (In)	θ_B (Deg)	
1040	213.9	90.0	1003	210.0	90.0	ZONE 2, NOSE CONE
1041	286.5	90.0	187660	284.6	90.0	
1298	213.9	180.0	1015	217.3	180.0	
1300	243.3	180.0	1035	251.9	180.0	
1303	373.1	180.0	1105	373.0	180.0	
1304	213.9	270.0	1018	217.3	270.0	
1307	329.8	270.0	1088	338.4	270.0	
1311	243.3	0.0	1030	251.9	0.0	
1313	329.8	5.0	1080	338.5	0.0	
1326	243.3	90.0	1033	251.9	90.0	
1449	276.1	20.0	1030	251.9	0.0	
1451	292.1	20.0	—	—	—	
1455	292.1	32.0	10706	293.8	34.0	
3226	388.0	90.0	1113	395.0	90.0	
7412	287.0	74.0	187412	287.0	74.0	
7413	313.5	72.0	187413	313.5	72.0	
7426	200.0	90.0	187426	200.0	0.0	
7427	213.9	0.0	187427	214.0	0.0	
7429	300.0	180.0	187429	300.0	180.0	
7430	388.0	0.0	187430	387.0	0.0	
7431	388.0	45.0	187431	387.0	45.0	
7432	388.0	60.0	187432	387.9	60.0	
7446	286.0	54.0	187446	286.0	54.0	
7657	373.1	90.0	187657	373.0	90.0	
7658	300.0	352.0	187658	300.0	355.0	
7659	287.0	20.0	187659	284.5	20.0	
7660	284.6	90.0	187660	284.6	90.0	
7661	283.4	270.0	187661	284.5	270.0	

Table 1 SRB Body Point Definition (continued)

REMTECH			ROCKWELL			COMMENT
BODY POINT	X_B (In)	θ_B (Deg)	BODY POINT	X_B (In)	θ_B (Deg)	
31	451.7	104.0	10784	451.7	105.8	ZONE 3, FORWARD SKIRT
1000	399.0	0.0	1120	401.0	0.0	
1021	447.5	45.0	1157	459.6	30.0	
1022	495.9	45.0	1157	459.6	30.0	
1043	407.7	90.0	10742	407.8	90.0	
1045	431.0	90.0	10743	425.0	90.0	
1046	499.4	90.0	1173	494.2	90.0	
1047	511.5	90.0	1173	494.2	90.0	
1048	521.9	90.0	1193	523.8	90.0	
1049	534.0	90.0	1193	523.8	90.0	
1050	553.4	90.0	1203	547.0	90.0	
1065	399.0	135.0	10715	401.0	135.0	
1290	407.7	76.0	—	—	—	
1291	419.8	76.0	—	—	—	
1292	431.9	76.0	10745	449.5	80.0	
1345	399.0	270.0	10720	401.0	270.0	
1346	435.4	277.0	10720	401.0	270.0	
1404	408.0	104.0	12000	420.0	100.0	
1406	432.0	104.0	12001	438.0	100.0	
1410	480.0	104.0	10792	486.6	100.0	
1496	444.0	140.0	1154	459.6	45.0	
3207	450.0	270.0	3138	450.0	270.0	
3229	490.0	105.0	10792	461.0	100.0	
4214	480.0	110.0	10791	460.9	100.0	
7444	419.0	46.0	187444	417.3	46.0	
7653	459.6	0.0	187653	459.6	0.0	
7654	459.0	104.0	10791	460.9	100.0	
7655	448.0	73.0	10745	449.5	80.0	
7656	419.8	92.0	187656	419.9	90.0	
7682	511.0	270.0	187682	522.9	0.0	
8440	544.0	10.0	188440	544.0	90.0	
8441	544.0	135.0	188441	544.0	135.0	
8442	544.0	180.0	188442	544.0	180.0	

Table 1 SRB Body Point Definition (continued)

REMTECH			ROCKWELL			COMMENT
BODY POINT	X_B (In)	θ_B (Deg)	BODY POINT	X_B (In)	θ_B (Deg)	
41	620.0	270.0	3207	546.1	270.0	ZONE 4, MOTOR CASE
42	876.0	270.0	3367	819.5	270.0	
43	1061.0	270.0	3517	1077.4	270.0	
44	1237.0	270.0	3517	1077.4	270.0	
1004	719.2	0.0	1280	675.9	0.0	
1005	892.3	0.0	1360	819.5	0.0	
1006	1065.3	0.0	1510	1077.4	0.0	
1052	719.2	90.0	1283	675.9	90.0	
1055	1238.4	90.0	1583	1203.8	90.0	
7418	876.0	260.0	187418	876.0	263.0	
7419	1237.0	0.0	187419	1237.0	0.0	
7420	1237.0	99.0	187420	1237.0	97.0	
7421	1237.0	279.0	187421	1237.0	277.0	
7687	620.0	0.0	187687	620.0	0.0	
7688	620.0	90.0	187688	620.0	90.0	
7689	620.0	180.0	187689	620.0	180.0	
7690	620.0	282.0	187690	620.0	282.0	
8437	1061.0	90.0	188437	1061.0	90.0	
8438	1061.0	180.0	188438	1061.0	180.0	

Table 1 SRB Body Point Definition (continued)

REMTECH			ROCKWELL			COMMENT
BODY POINT	X_B (In)	θ_B (Deg)	BODY POINT	X_B (In)	θ_B (Deg)	
51	1411.5	270.0	3737	1463.0	270.0	ZONE 5, MOTOR CASE
52	1498.0	270.0	3757	1498.0	270.0	
53	1504.0	22.5	972	1505.0	22.5	
54	1504.0	67.5	977	1505.0	67.5	
55	1504.0	135.0	974	1505.0	135.0	
56	1504.0	225.0	976	1504.0	225.0	
57	1504.0	315.0	979	1505.0	315.0	
58	1504.0	270.0	10510	1503.0	270.0	
1010	1411.5	0.0	1709	1411.4	315.0	
1011	1498.0	0.0	10512	1498.0	0.0	
1012	1584.5	0.0	1790	1567.2	0.0	
1057	1498.0	90.0	10516	1498.0	90.0	
1058	1584.5	90.0	1793	1567.2	90.0	
1242	1481.5	0.0	1730	1463.0	0.0	
1338	1498.0	263.0	3756	1498.0	269.0	
1369	1498.0	22.5	10513	1498.0	30.0	
1384	1498.0	67.5	10515	1498.0	60.0	
7414	1504.0	0.0	187414	1503.0	0.0	
7424	1504.0	98.0	187424	1505.0	98.0	
7425	1504.0	180.0	187425	1505.0	180.0	
7685	1530.0	225.0	1776	1532.0	225.0	
7686	1520.0	0.0	9001	1519.0	0.0	
8439	1397.0	90.0	188439	1397.0	90.0	

Table 1 SRB Body Point Definition (continued)

REMTECH			ROCKWELL			COMMENT
BODY POINT	X_B (In)	θ_B (Deg)	BODY POINT	X_B (In)	θ_B (Deg)	
61	1637.5	0.0	1830	1638.0	0.0	ZONE 6, MOTOR CASE
62	1714.3	0.0	1860	1694.0	0.0	
63	1733.3	0.0	6302	1734.0	0.0	
64	1733.3	0.0	6301	1732.0	0.0	
65	1733.3	0.0	6305	1734.0	0.0	
66	1838.0	0.0	6502	1838.0	0.0	
67	1637.5	90.0	—	—	—	
68	1714.3	180.0	—	—	—	
69	1838.0	180.0	6552	1838.0	180.0	
1013	1714.3	0.0	1900	1758.0	0.0	
1015	1825.1	0.0	1930	1808.0	0.0	
1059	1714.3	90.0	1833	1633.0	90.0	
1060	1800.8	90.0	1933	1808.0	90.0	
1253	1813.0	180.0	1935	1808.0	180.0	
1260	1825.1	180.0	1955	1837.0	180.0	
1365	1729.9	0.0	6302	1734.0	0.0	
1366	1769.7	0.0	6402	1778.0	0.0	
4220	1637.5	180.0	1835	1633.0	180.0	
7415	1838.0	3.0	6505	1839.9	0.0	
7416	1838.0	303.0	3959	1837.0	271.0	
7417	1838.0	177.0	1955	1837.0	180.0	
7683	1785.0	0.0	6403	1778.0	0.0	
7684	1785.0	180.0	6453	1778.0	180.0	
8447	1839.0	32.0	1957	1837.0	30.0	
8448	1838.0	48.0	1951	1837.0	45.0	

Table 1 SRB Body Point Definition (concluded)

REMTECH			ROCKWELL			COMMENT
BODY POINT	X_B (In)	θ_B (Deg)	BODY POINT	X_B (In)	θ_B (Deg)	
1036	1896.0	50.0	2116	1896.0	45.0	ZONE 7, AFT SKIRT
1061	1849.3	90.0	2131	1842.0	90.0	
1074	1849.3	135.0	2141	1842.0	135.0	
1134	1869.4	315.0	10414	1888.0	315.0	
1135	1894.5	315.0	10414	1888.0	315.0	
1136	1920.3	315.0	2199	1931.0	315.0	
1276	1849.3	198.0	2231	1842.0	210.0	
1277	1849.3	238.0	10152	1841.0	238.0	
1280	1873.5	198.0	—	—	—	
1281	1873.5	238.0	—	—	—	
1284	1896.0	198.0	—	—	—	
1288	1920.3	198.0	—	—	—	
1289	1920.3	238.0	10160	1888.0	250.0	
4221	1877.5	90.0	2133	1861.0	90.0	
4222	1877.5	135.0	2143	1861.0	135.0	
7445	1854.7	18.0	10314	1853.0	16.0	
7651	1854.7	2.0	10302	1852.0	0.0	
8407	1884.9	2.0	10313	1859.0	3.0	
8409	1920.0	52.0	2126	1896.0	60.0	
8434	1910.0	90.0	2136	1896.0	90.0	
8435	1910.0	275.0	10209	1899.0	281.0	
8436	1910.0	135.0	2146	1896.0	135.0	
8443	1910.0	178.0	2156	1896.0	180.0	

Table 2 Light Weight Tank Trajectory

TIME	ALT	$+(\alpha)$	$-(\alpha)$	$+(\beta)$	$-(\beta)$	P_∞	$(\rho)_\infty$	V_∞
10.0	1350.0	0.11	-1.42	0.58	-0.58	0.2027E+04	0.2281E-02	183.1
15.0	2823.0	1.36	-0.47	3.23	-3.23	0.1921E+04	0.2165E-02	306.3
20.0	4296.0	2.61	0.48	5.89	-5.89	0.1821E+04	0.2059E-02	429.5
25.0	6939.0	-0.32	-1.98	4.75	-4.75	0.1653E+04	0.1890E-02	569.5
30.0	9582.0	-3.24	-4.44	3.62	-3.62	0.1498E+04	0.1739E-02	709.4
35.0	13300.0	-3.02	-3.96	2.82	-2.82	0.1302E+04	0.1549E-02	837.3
40.0	17020.0	-2.79	-3.48	2.02	-2.02	0.1127E+04	0.1379E-02	965.3
45.0	21310.0	-2.61	-3.95	1.87	-1.87	0.9490E+03	0.1204E-02	1073.0
50.0	25840.0	-2.76	-4.41	2.02	-2.02	0.7859E+03	0.1040E-02	1183.0
55.0	30590.0	-2.82	-4.15	2.12	-2.12	0.6392E+03	0.8861E-03	1301.0
60.0	35560.0	-2.28	-3.78	2.06	-2.06	0.5095E+03	0.7402E-03	1435.0
62.0	37630.0	-1.85	-3.61	1.90	-1.90	0.4623E+03	0.6809E-03	1497.0
64.0	39750.0	-1.43	-3.57	1.82	-1.82	0.4179E+03	0.6220E-03	1569.0
66.0	41950.0	-1.07	-3.35	1.80	-1.80	0.3760E+03	0.5646E-03	1647.0
68.0	44230.0	-0.68	-3.23	1.78	-1.78	0.3367E+03	0.5094E-03	1729.0
70.0	46580.0	-0.46	-3.01	1.86	-1.86	0.3002E+03	0.4572E-03	1814.0
72.0	49020.0	-0.26	-2.69	1.94	-1.94	0.2663E+03	0.4083E-03	1904.0
74.0	51530.0	0.05	-2.41	2.12	-2.12	0.2352E+03	0.3628E-03	1999.0
76.0	54130.0	0.34	-2.14	2.34	-2.34	0.2068E+03	0.3203E-03	2100.0
78.0	56810.0	0.79	-1.73	2.61	-2.61	0.1811E+03	0.2804E-03	2206.0
80.0	59570.0	0.94	-1.04	3.01	-3.01	0.1579E+03	0.2428E-03	2313.0
82.0	62410.0	0.41	-0.76	3.46	-3.46	0.1377E+03	0.2104E-03	2423.0
84.0	65320.0	-0.34	-0.98	3.98	-3.98	0.1195E+03	0.1813E-03	2539.0
86.0	68310.0	-0.89	-1.27	4.60	-4.60	0.1033E+03	0.1555E-03	2656.0
88.0	71390.0	-1.16	-1.57	5.13	-5.13	0.8905E+02	0.1329E-03	2777.0
90.0	74540.0	-1.13	-1.62	5.10	-5.10	0.7657E+02	0.1134E-03	2901.0
92.0	77770.0	-1.07	-1.64	5.00	-5.00	0.6573E+02	0.9663E-04	3025.0
94.0	81080.0	-0.96	-1.63	4.94	-4.94	0.5634E+02	0.8229E-04	3154.0
96.0	84460.0	-0.98	-1.62	4.87	-4.87	0.4821E+02	0.7000E-04	3286.0
98.0	87910.0	-0.85	-1.59	4.51	-4.51	0.4115E+02	0.5941E-04	3422.0

Table 2 Light Weight Tank Trajectory (Concluded)

TIME	ALT	$+(\alpha)$	$-(\alpha)$	$+(\beta)$	$-(\beta)$	P_∞	$(\rho)_\infty$	V_∞
100.0	91420.0	-0.83	-1.60	4.72	-4.72	0.3498E+02	0.5015E-04	3566.0
102.0	95000.0	-0.82	-1.57	4.52	-4.52	0.2973E+02	0.4220E-04	3705.0
104.0	98640.0	-0.82	-1.61	3.62	-3.62	0.2526E+02	0.3545E-04	3850.0
106.0	102300.0	-0.84	-1.63	3.09	-3.09	0.2143E+02	0.2977E-04	3995.0
108.0	106100.0	-0.89	-1.65	3.03	-3.03	0.1817E+02	0.2499E-04	4143.0
110.0	109900.0	-0.95	-1.70	3.30	-3.30	0.1540E+02	0.2096E-04	4293.0
112.0	113700.0	-0.81	-1.59	5.24	-5.24	0.1305E+02	0.1758E-04	4432.0
114.0	117600.0	-0.51	-1.72	6.99	-6.99	0.1107E+02	0.1475E-04	4535.0
116.0	121400.0	-0.05	-1.89	5.59	-5.59	0.9413E+01	0.1239E-04	4605.0
118.0	125200.0	0.74	-1.58	4.93	-4.93	0.8032E+01	0.1045E-04	4665.0
120.0	129000.0	1.44	-1.50	4.49	-4.49	0.6879E+01	0.8836E-05	4715.0
122.0	132700.0	1.53	-1.80	5.14	-5.14	0.5914E+01	0.7501E-05	4754.0
124.0	136400.0	1.18	-2.46	6.11	-6.11	0.5105E+01	0.6394E-05	4790.0
126.0	140000.0	0.74	-3.00	6.47	-6.47	0.4424E+01	0.5475E-05	4829.0
128.0	140200.0	0.75	-3.03	6.84	-6.84	0.4391E+01	0.5431E-05	4832.0

Table 3 Vandenburg Hot and Reference Day Atmosphere Properties

TIME (sec)	ALTITUDE (ft)	P_∞ (lb/ft^2)		T_∞ (^oF)		$\rho_\infty \times (10^{-4})$ ($slugs/ft^3$)	
		VAN_{REF}	VAN_{HOT}	VAN_{REF}	VAN_{HOT}	VAN_{REF}	VAN_{HOT}
10	1350	2030.00	2020.00	56.35	97.93	22.800	21.100
15	1350	1920.00	1920.00	56.22	92.23	21.700	20.200
20	4296	1820.00	1820.00	54.66	86.53	20.600	19.500
25	4296	1650.00	1660.00	49.32	76.30	18.900	18.100
30	9582	1500.00	1520.00	41.89	66.07	17.400	16.800
40	17023	1130.00	1150.00	16.14	37.26	13.800	13.500
50	25837	786.00	818.00	-19.31	3.14	1.040	10.300
60	35558	510.00	542.00	-58.64	-39.81	7.400	7.500
70	46585	300.00	320.00	-77.19	-92.24	4.570	5.080
80	59569	158.00	162.00	-80.56	-97.37	2.430	2.600
84	65321	119.00	121.00	-75.90	-86.21	1.810	1.880
90	74541	76.60	76.800	-66.11	-68.31	1.130	1.140
96	84458	48.20	48.300	-58.63	-49.05	0.700	0.685
100	91421	35.00	35.300	-53.23	-35.54	0.501	0.486
106	102327	21.40	22.100	-40.33	-15.27	0.298	0.284
110	109863	15.40	16.100	-31.75	-2.38	0.210	0.206
120	129001	6.88	7.570	-6.15	30.36	0.088	0.090
126	140227	4.42	5.000	11.06	49.23	0.055	0.057

Table 4 DFI Flight Factor Summary

ZONE	GAGE	X_B (IN)	θ_B (DEG)	f_3	f_4
2	7412	287.0	74.0	1.12	2.21
Nose Cone	7413	313.5	72.0	1.43	1.88
↓	7426	200.0	90.0	1.00	1.00
	7427	213.9	0.0	0.82	1.05
	7429	300.0	180.0	1.00	1.70
	7430	388.0	0.0	1.21	2.25
	7431	388.0	45.0	1.40	2.77
	7432	388.0	60.0	1.52	3.08
	7446	286.0	54.0	1.33	1.53
	7657	373.1	90.0	1.00	1.63
	7658	300.0	352.0	1.75	2.99
	7659	287.0	20.0	0.73	1.12
	7660	284.6	90.0	1.00	1.63
	7661	283.4	270.0	1.04	1.74
3					
Fwd, Skirt	7444	419.0	46.0	1.00	1.00
↓	7653	459.0	0.0	1.04	1.04
	7654	459.0	104.0	1.30	1.80
	7655	448.0	73.0	1.00	1.40
	7656	419.8	92.0	1.00	1.00
	7682	511.0	270.0	1.87	2.24
	8440	544.0	90.0	1.00	1.00
	8441	544.0	135.0	1.04	1.04
	8442	544.0	180.0	1.04	1.04
4					
Motor Case	7418	876.0	260.0	1.28	1.04
↓	7419	1237.0	0.0	1.48	0.76
	7420	1237.0	99.0	1.66	1.14
	7421	1237.0	279.0	1.43	1.20
	7687	620.7	0.0	0.99	2.45
	7688	620.0	90.0	1.29	1.22
	7689	620.0	180.0	1.04	1.01
	7690	620.0	282.0	1.53	1.60
	8427	1061.0	90.0	1.00	1.00
	8438	1061.0	180.0	0.97	0.86

Table 4 DFI Flight Factor Summary (concluded)

ZONE	GAGE	X_B (IN)	θ_B (DEG)	f_3	f_4
5					
Motor Case	7417	1504.0	0.0	1.69	1.69
Attach Ring	7424	1504.0	90.0	1.36	1.36
↓	7425	1504.0	180.0	1.00	1.00
	7685	1530.0	225.0	1.00	1.00
	7686	1527.0	0.0	1.00	1.00
	8439	1397.0	90.0	2.10	2.10
6					
Aft Motor	7415	1838.0	0.0	1.00	1.00
Case	7416	1838.0	280.0	↓	↓
↓	7417	1838.0	180.0		
	7683	1785.0	0.0		
	7684	1785.0	180.0		
	8447	1839.0	35.0		
	8448	1838.0	48.0		
7					
Aft Skirt	7445	1854.7	18.0	1.00	1.60
↓	7651	1854.7	2.0	1.00	1.60
	8407	1884.9	2.0	1.00	1.60
	8409	1920.0	52.0	1.00	1.60
	8434	1910.0	90.0	1.00	1.60
	8435	1910.0	275.0	1.00	1.00
	8436	1910.0	135.0	1.00	1.60
	8443	1910.0	178.0	1.00	1.60

Table 5 SRB Design Ascent Convective Heating Summary
Zone 2

REMTECH					ROCKWELL						
					RI-IVBC 3 (10/87)					1980 DESIGN	
BODY POINT	X_B (In)	θ_B (Deg)	MAX. HTG. RATE (Btu/ft^2sec)	HEAT LOAD (Btu/ft^2)	BODY POINT	X_B (In)	θ_B (Deg)	MAX. HTG. RATE (Btu/ft^2sec)	HEAT LOAD (Btu/ft^2)	MAX. HTG. RATE (Btu/ft^2sec)	HEAT LOAD (Btu/ft^2)
1040	213.9	90.0	10.99	488.1	1003	210.1	90.0	9.00	453.0	11.94	530.4
*1041	286.5	90.0	6.70	303.0	187660	284.6	90.0	4.76	255.0	—	—
*1298	213.9	180.0	9.87	411.5	1015	217.3	180.0	6.08	348.4	7.33	411.3
1300	243.3	180.0	7.16	326.2	1035	251.9	180.0	5.35	310.9	6.94	359.6
1303	373.1	180.0	4.06	203.5	1105	373.0	180.0	3.23	213.1	3.42	229.2
1304	213.9	270.0	4.96	277.1	1018	217.3	270.0	7.54	395.8	8.08	418.3
1307	329.8	270.0	2.92	175.3	1088	338.4	270.0	3.28	201.0	3.94	238.1
1311	243.3	0.0	7.96	345.2	1030	251.9	0.0	6.25	328.9	7.02	377.1
*1313	329.8	5.0	7.18	287.2	1080	338.5	0.0	4.45	253.1	4.92	278.9
*1326	243.3	90.0	10.63	428.8	1033	251.9	90.0	7.40	350.7	15.36	653.0
*1449	276.1	20.0	8.44	390.8	1030	251.9	0.0	6.25	328.9	7.02	377.1
*1451	292.1	20.0	10.41	452.7	10706	293.8	34.0	7.09	344.7	11.84	506.2
*1455	292.1	32.0	10.44	457.8	10706	293.8	34.0	7.09	344.7	11.84	506.2
*3226	388.0	90.0	12.71	518.6	1113	395.0	90.0	9.31	458.9	7.65	409.9
7412	287.0	74.0	6.50	298.9	187412	287.0	74.0	5.71	291.5	—	—
7413	313.5	72.0	3.56	209.8	187413	313.5	72.0	3.83	230.9	—	—
7426	200.0	90.0	9.32	347.8	187426	200.0	0.0	10.86	394.3	—	—
7427	213.9	0.0	4.18	255.3	187427	214.0	0.0	6.87	364.6	—	—
7429	300.0	180.0	5.09	258.7	187429	300.0	180.0	4.61	265.5	—	—
7430	388.0	0.0	6.10	284.0	187430	387.0	0.0	5.61	290.8	—	—
7431	388.0	45.0	6.42	315.5	187431	387.0	45.0	5.93	312.9	—	—
*7432	388.0	60.0	13.41	483.8	187432	387.9	60.0	9.59	447.5	—	—
7446	286.0	54.0	6.53	337.5	187446	286.0	54.0	6.33	316.8	—	—
7657	373.1	90.0	9.75	377.9	187657	373.0	90.0	8.46	352.6	—	—
7658	300.0	352.0	6.53	299.4	187658	300.0	355.0	5.66	293.1	—	—
7659	287.0	20.0	6.50	318.7	187659	284.5	20.0	5.48	278.5	—	—
7660	284.6	90.0	6.10	276.9	187660	284.6	90.0	4.76	255.6	—	—
7661	283.4	270.0	4.66	246.3	187661	284.5	270.0	6.08	303.8	—	—

Table 5 SRB Design Ascent Convective Heating Summary
Zone 3

REMTECH					ROCKWELL						
					RI-IVBC 3 (10/87)					1980 DESIGN	
BODY POINT	X_B (In)	θ_B (Deg)	MAX. HTG. RATE (Btu/ft^{2}sec)	HEAT LOAD (Btu/ft^2)	BODY POINT	X_B (In)	θ_B (Deg)	MAX. HTG. RATE (Btu/ft^{2}sec)	HEAT LOAD (Btu/ft^2)	MAX. HTG. RATE (Btu/ft^{2}sec)	HEAT LOAD (Btu/ft^2)
31	451.7	104.0	6.05	301.3	10784	451.7	105.8	7.80	397.2	17.79	597.4
1000	399.0	0.0	1.19	102.3	1120	401.0	0.0	1.84	141.5	5.39	318.9
1021	447.5	45.0	2.11	140.3	1157	459.6	30.0	1.78	127.8	2.01	151.1
1022	495.9	45.0	1.78	116.1	1157	459.6	30.0	1.78	127.8	2.01	151.1
1043	407.7	90.0	11.10	499.0	10742	407.8	90.0	9.10	458.9	9.56	298.8
*1045	431.0	90.0	12.80	564.3	10743	425.0	90.0	8.96	454.0	15.58	513.1
1046	499.4	90.0	1.22	100.5	1173	494.2	90.0	1.69	127.3	3.42	151.8
1047	511.5	90.0	1.00	90.8	1173	494.2	90.0	1.69	127.3	3.42	151.8
1048	521.9	90.0	0.99	90.9	1193	523.8	90.0	1.25	105.0	2.14	127.6
1049	534.0	90.0	0.90	85.6	1193	523.8	90.0	1.25	105.0	2.14	127.6
1050	553.4	90.0	0.85	82.6	1203	547.0	90.0	—	—	1.73	121.8
1065	399.0	135.0	1.65	119.4	10715	401.0	135.0	2.53	170.3	3.60	176.4
1290	407.7	76.0	2.99	161.9	—	—	—	—	—	—	—
1291	419.8	76.0	2.68	170.6	—	—	—	—	—	—	—
1292	431.9	76.0	4.19	221.0	10745	449.5	80.0	4.60	244.6	14.03	382.1
1345	399.0	270.0	1.38	112.3	10720	401.0	270.0	1.84	139.3	1.70	146.1
1346	435.4	277.0	1.27	101.1	10720	401.0	270.0	1.84	139.3	1.70	146.1
1404	408.0	104.0	9.05	367.3	12000	420.0	100.0	7.00	347.0	—	—
1406	432.0	104.0	8.53	417.2	12001	438.0	100.0	7.97	389.4	—	—
1410	480.0	104.0	2.64	155.3	10792	486.6	100.0	4.67	240.1	9.15	341.7
1496	444.0	140.0	6.39	325.4	10749	442.0	120.0	5.08	267.3	4.33	249.4
3207	450.0	270.0	7.02	364.9	3138	450.0	270.0	8.92	430.7	4.41	228.5
3229	490.0	105.0	1.68	114.9	10792	461.0	100.0	4.70	243.0	9.15	341.7
4214	480.0	110.0	2.70	159.7	10791	460.9	100.0	4.70	243.0	15.37	487.9
7444	419.0	46.0	2.46	161.7	187444	417.3	46.0	2.77	138.9	—	—
7653	459.6	0.0	1.45	105.6	187653	459.6	0.0	1.67	114.3	—	—
7654	459.0	104.0	3.05	171.1	10791	460.9	100.0	4.70	243.0	15.37	487.9
7655	448.0	73.0	5.08	228.1	10745	449.5	80.0	4.60	244.6	14.03	382.1
7656	419.8	92.0	13.21	574.9	187656	419.9	90.0	14.40	643.7	—	—
7682	511.0	270.0	2.25	150.5	187682	522.9	0.0	2.61	162.4	—	—
8440	544.0	10.0	0.87	82.7	188440	544.0	90.0	0.96	88.5	—	—
8441	544.0	135.0	0.95	90.2	188441	544.0	135.0	1.25	98.2	—	—
8442	544.0	180.0	1.34	96.1	188442	544.0	180.0	1.44	104.6	—	—

Table 5 SRB Design Ascent Convective Heating Summary
Zone 4

REMTECH					ROCKWELL						
					RI-IVBC 3 (10/87)					1980 DESIGN	
BODY POINT	X_B (In)	θ_B (Deg)	MAX. HTG. RATE (Btu/ft^2sec)	HEAT LOAD (Btu/ft^2)	BODY POINT	X_B (In)	θ_B (Deg)	MAX. HTG. RATE (Btu/ft^2sec)	HEAT LOAD (Btu/ft^2)	MAX. HTG. RATE (Btu/ft^2sec)	HEAT LOAD (Btu/ft^2)
41	620.0	270.0	3.06	180.9	3207	546.1	270.0	2.59	161.0	1.95	145.4
42	876.0	270.0	2.30	138.0	3367	819.5	270.0	2.89	170.0	1.93	140.4
43	1061.0	270.0	2.02	130.7	3517	1077.4	270.0	2.65	159.0	1.94	138.5
44	1237.0	270.0	2.61	150.3	3517	1077.4	270.0	2.65	159.0	1.94	138.5
1004	719.2	0.0	1.54	108.7	1280	675.9	0.0	1.49	109.5	1.42	118.3
1005	892.3	0.0	2.23	137.5	1360	819.5	0.0	1.76	116.9	1.48	121.8
1006	1065.3	0.0	2.31	143.9	1510	1077.4	0.0	2.08	131.6	2.06	141.4
1052	719.2	90.0	1.28	101.3	1283	675.9	90.0	1.31	102.7	1.25	110.4
1055	1238.4	90.0	1.58	112.1	1583	1203.8	90.0	2.08	128.7	2.47	140.2
7418	876.0	260.0	1.31	93.4	187418	876.0	263.0	2.03	116.3	—	—
7419	1237.0	0.0	2.59	131.0	187419	1237.0	0.0	2.92	158.6	—	—
7420	1237.0	99.0	1.77	101.9	187420	1237.0	97.0	2.04	114.7	—	—
7421	1237.0	279.0	1.51	100.4	187421	1237.0	277.0	1.69	107.4	—	—
7687	620.0	0.0	1.81	118.3	187687	620.0	0.0	1.53	109.5	—	—
7688	620.0	90.0	0.75	77.4	187688	620.0	90.0	0.92	75.0	—	—
7689	620.0	180.0	1.26	95.8	187689	620.0	180.0	1.28	95.2	—	—
7690	620.0	282.0	1.66	118.5	187690	620.0	282.0	1.81	109.3	—	—
8437	1061.0	90.0	1.11	92.5	188437	1061.0	90.0	1.63	97.6	—	—
8438	1061.0	180.0	1.00	86.4	188438	1061.0	180.0	1.38	103.7	—	—

Table 5 SRB Design Ascent Convective Heating Summary
Zone 5

REMTECH					ROCKWELL						
					RI-IVBC 3 (10/87)					1980 DESIGN	
BODY POINT	X_B (In)	θ_B (Deg)	MAX. HTG. RATE (Btu/ft^{2}sec)	HEAT LOAD (Btu/ft^2)	BODY POINT	X_B (In)	θ_B (Deg)	MAX. HTG. RATE (Btu/ft^{2}sec)	HEAT LOAD (Btu/ft^2)	MAX. HTG. RATE (Btu/ft^{2}sec)	HEAT LOAD (Btu/ft^2)
51	1411.5	270.0	3.85	205.1	3737	1463.0	270.0	2.63	155.0	1.96	137.2
* 52	1498.0	270.0	5.36	275.7	3757	1498.0	270.0	2.89	164.2	1.95	136.7
53	1504.0	22.5	13.58	521.1	972	1505.0	22.5	12.48	592.0	16.06	712.0
54	1504.0	67.5	12.53	422.6	977	1505.0	67.5	11.26	564.0	28.40	997.1
* 55	1504.0	135.0	10.46	362.9	974	1505.0	135.0	5.97	284.0	11.78	527.8
56	1504.0	225.0	5.24	268.7	976	1504.0	225.0	5.83	291.0	2.01	139.3
57	1504.0	315.0	5.42	277.1	979	1505.0	315.0	6.65	327.0	9.52	403.6
58	1504.0	270.0	3.64	184.9	10510	1503.0	270.0	2.89	164.0	2.50	145.6
1010	1411.5	0.0	1.84	120.8	1709	1411.4	315.0	1.39	104.5	1.73	125.9
1011	1498.0	0.0	4.80	220.6	10512	1498.0	0.0	9.25	359.0	11.59	496.2
1012	1584.5	0.0	3.74	123.5	1790	1567.2	0.0	2.83	107.4	2.63	103.8
1057	1498.0	90.0	8.51	353.3	10516	1498.0	90.0	13.09	449.0	8.83	298.9
1058	1584.5	90.0	1.38	70.8	1793	1567.2	90.0	2.25	93.4	2.28	94.1
1242	1481.5	0.0	3.86	196.7	1730	1463.0	0.0	5.59	233.0	2.41	164.0
1338	14980	263.0	1.47	90.6	3756	1498.0	269.0	2.89	164.0	1.95	136.7
1369	1498.0	22.5	9.93	388.7	10513	1498.0	30.0	10.86	433.0	6.34	315.5
1384	1498.0	67.5	12.54	423.3	10515	1498.0	60.0	17.40	574.0	20.67	860.4
7414	1504.0	0.0	9.72	448.4	187414	1503.0	0.0	11.65	491.0	—	—
7424	1504.0	98.0	8.69	358.0	187424	1505.0	98.0	9.19	353.0	—	—
7425	1504.0	180.0	5.24	267.0	187425	1505.0	180.0	5.08	256.0	—	—
7685	1530.0	225.0	1.26	68.3	1776	1532.0	225.0	1.45	74.0	2.29	95.3
7686	1520.0	0.0	1.01	57.6	9001	1519.0	0.0	4.86	128.0	6.39	167.1
8439	1397.0	90.0	2.68	153.1	188439	1397.0	90.0	3.71	158.0	—	—

Table 5 SRB Design Ascent Convective Heating Summary
Zone 6

REMTECH					ROCKWELL						
					RI-IVBC 3 (10/87)					1980 DESIGN	
BODY POINT	X_B (In)	θ_B (Deg)	MAX. HTG. RATE (Btu/ft^2sec)	HEAT LOAD (Btu/ft^2)	BODY POINT	X_B (In)	θ_B (Deg)	MAX. HTG. RATE (Btu/ft^2sec)	HEAT LOAD (Btu/ft^2)	MAX. HTG. RATE (Btu/ft^2sec)	HEAT LOAD (Btu/ft^2)
* 61	1637.5	0.0	3.72	122.9	1830	1638.0	0.0	1.49	75.9	2.33	97.9
62	1714.3	0.0	3.11	111.1	1860	1694.0	0.0	2.19	87.4	2.26	96.3
63	1733.3	0.0	4.33	136.8	6302	1734.0	0.0	6.04	154.1	7.71	185.9
64	1733.3	0.0	8.6	220.2	6301	1732.0	0.0	9.64	240.3	15.41	293.3
65	1733.3	0.0	4.33	136.8	6305	1734.0	0.0	6.04	154.1	7.71	185.9
* 66	1838.0	0.0	6.69	178.6	6502	1838.0	0.0	4.50	121.4	3.71	127.5
67	1637.5	90.0	1.38	70.5	—	—	—	—	—	—	—
68	1714.3	180.0	1.73	69.8	—	—	—	—	—	—	—
69	1838.0	180.0	3.35	88.3	6552	1838.0	180.0	2.01	86.1	3.37	120.1
1013	1714.3	0.0	2.18	90.5	1900	1758.0	0.0	2.79	98.9	2.17	94.6
1015	1825.1	0.0	2.36	88.9	1930	1808.0	0.0	1.76	78.1	2.47	99.9
1059	1714.3	90.0	0.80	54.7	1833	1633.0	90.0	1.48	75.0	1.82	85.4
1060	1800.8	90.0	0.78	54.6	1933	1808.0	90.0	1.12	66.2	1.53	79.1
1253	1813.0	180.0	0.86	57.3	1935	1808.0	180.0	1.12	66.2	1.07	70.3
1260	1825.1	180.0	0.83	56.0	1955	1837.0	180.0	2.03	83.2	2.05	91.7
1365	1729.9	0.0	3.31	109.2	6302	1734.0	0.0	6.04	154.1	7.71	185.9
1366	1769.7	0.0	2.68	95.2	6402	1778.0	0.0	6.02	153.6	5.97	158.9
4220	1637.5	180.0	1.75	70.3	1835	1633.0	180.0	1.45	74.0	1.70	85.4
*7415	1838.0	3.0	6.69	178.6	6505	1839.9	0.0	4.50	121.5	4.55	141.8
7416	1838.0	303.0	3.15	106.6	3959	1837.0	271.0	3.92	119.9	3.88	120.8
7417	1838.0	177.0	2.57	86.3	1955	1837.0	180.0	2.03	83.2	2.05	91.7
7683	1785.0	0.0	1.40	69.6	6403	1778.0	0.0	1.20	68.1	1.79	86.6
7684	1785.0	180.0	0.86	57.4	6453	1778.0	180.0	1.13	66.4	1.77	86.3
8447	1839.0	32.0	2.24	90.7	1957	1837.0	30.0	2.25	87.8	4.07	126.3
8448	1838.0	48.0	1.64	76.3	1951	1837.0	45.0	2.25	87.6	1.10	70.0

Table 5 SRB Design Ascent Convective Heating Summary
Zone 7

REMTECH					ROCKWELL						
					RI-IVBC 3 (10/87)					1980 DESIGN	
BODY POINT	X_B (In)	θ_B (Deg)	MAX. HTG. RATE (Btu/ft^{2}sec)	HEAT LOAD (Btu/ft^2)	BODY POINT	X_B (In)	θ_B (Deg)	MAX. HTG. RATE (Btu/ft^{2}sec)	HEAT LOAD (Btu/ft^2)	MAX. HTG. RATE (Btu/ft^{2}sec)	HEAT LOAD (Btu/ft^2)
1036	1896.0	50.0	1.60	75.2	2116	1896.0	45.0	2.37	100.7	3.65	125.0
1061	1849.3	90.0	0.99	58.9	2131	1842.0	90.0	1.21	76.6	2.41	102.1
1074	1849.3	135.0	1.26	66.7	2141	1842.0	135.0	1.18	74.8	2.30	100.3
1134	1869.4	315.0	2.27	88.6	10414	1888.0	315.0	3.36	116.7	4.75	143.2
1135	1894.5	315.0	2.17	86.4	10414	1888.0	315.0	3.36	116.7	4.75	143.2
1136	1920.3	315.0	1.66	74.5	2199	1931.0	315.0	2.23	96.8	4.64	141.5
1276	1849.3	198.0	1.81	75.6	2231	1842.0	210.0	1.46	80.8	2.24	99.3
1277	1849.3	238.0	1.84	72.7	10152	1841.0	238.0	1.36	76.8	2.35	101.0
1280	1873.5	198.0	2.01	74.4	—	—	—	—	—	—	—
1281	1873.5	238.0	2.34	81.4	—	—	—	—	—	—	—
1284	1896.0	198.0	1.92	72.1	—	—	—	—	—	—	—
1288	1920.3	198.0	1.67	66.0	—	—	—	—	—	—	—
1289	1920.3	238.0	1.99	80.3	10160	1888.0	250.0	2.12	95.6	2.37	101.2
4221	1877.5	90.0	0.98	59.0	2133	1861.0	90.0	1.19	74.6	2.41	102.0
4222	1877.5	135.0	1.47	66.4	2143	1861.0	135.0	1.20	75.5	2.30	100.1
7445	1854.7	18.0	3.29	106.2	10314	1853.0	16.0	7.53	205.6	8.06	195.7
7651	1854.7	2.0	2.82	98.5	10302	1852.0	0.0	3.80	125.1	5.03	150.2
8407	1884.9	2.0	2.37	87.3	10313	1859.0	3.0	3.64	127.6	3.20	118.8
8409	1920.0	52.0	1.63	77.0	2126	1896.0	60.0	1.77	89.7	2.44	103.2
8434	1910.0	90.0	1.38	67.7	2136	1896.0	90.0	1.77	88.0	2.40	101.8
8435	1910.0	275.0	1.68	76.5	10209	1899.0	281.0	3.37	118.0	2.43	102.4
8436	1910.0	135.0	1.07	60.0	2146	1896.0	135.0	1.12	72.5	2.29	99.9
8443	1910.0	178.0	1.44	67.3	2156	1896.0	180.0	1.53	80.8	2.08	96.8

END
DATE
AUG 17, 1989